

*Characterization of amygdalar Fkbp5
role in stress-induced anxiety-like
behaviour*

Thesis submitted for the degree of

Doctor of Philosophy

at the University of Leicester



by

Satyam Patel

Department of Cell Physiology and Pharmacology

University of Leicester

April 2012

Abstract

The physiological response to excessively strong aversive stimuli – the stress response – is relatively maladaptive and leads to various psychopathologies such as anxiety disorders only in a minority of individuals. Our lab has previously shown that severe acute restraint stress heightens anxiety-like behaviour in wild-type but not in the extracellular serine protease, neuropsin, deficient mice. Dissecting molecular changes underlying genotypic differences, our microarray and qRT-PCR approaches revealed that the stress-induced upregulation of glucocorticoid receptor (GR) co-chaperone, Fkbp5, expression in the amygdala is significantly attenuated in neuropsin^{-/-} mice compared to the wild-type mice and attenuated expression can be restored by bilateral intra-amygdala injection of recombinant neuropsin. Further, blocking neuropsin cleavage of EphB2 with anti-EphB2 antibody suppressed only neuropsin-mediated but not corticosterone-driven upregulation of Fkbp5 expression in primary amygdala cultures unraveling novel neuropsin-dependent mechanism acting in synergy with the well characterized corticosterone pathway to mediate the robust stress-effect on Fkbp5 expression. Importantly, wild-type mice lacking amygdala specific Fkbp5 exhibit stress protective phenotype in unconditioned anxiety tests and unimpaired learning and memory in fear conditioning paradigm. Proteomic analysis using subcellular fractionation revealed that stress triggers nuclear translocation of constitutively cytoplasmic FKBP51 in the amygdala. Nuclear FKBP51, in dexamethasone treated N2a cells, co-purifies with linker histone H1 implying at possible FKBP51 involvement in posttranslational modification of histone H1 to control gene expression necessary for maladaptive neuronal plasticity underlying altered behavioural outcomes. Therefore, this study characterizes and concludes an indispensable role of amygdalar Fkbp5 in stressful episodes developing into anxiety disorders.

Acknowledgement

I bow my head with great reverence to Him who is omnipresent, omnipotent and omniscient and the cause behind every effort.

I would like to express my indebtedness and veneration to Dr. Robert Pawlak for giving me an opportunity to work in the exciting area of behavioural neuroscience and providing his meticulous guidance and indelible inspiration throughout my research.

My special thanks to Mr. Benjamin Attwood, Dr. Julie Bourgoignon, Dr. Emanuele Schiavon, Dr. Anna Skrzypiec and Dr. Mariusz Mucha for teaching me and helping me through various lab techniques.

I would also like to thank everyone in Cell Physiology & Pharmacology department at University of Leicester. Thanks to Dr. L. Miguel Martins and Dr. Nicoleta Moiso for providing and guiding me with N2a cell line for my study. I take this opportunity to extend my thanks to the staff (Debbie, Sally, Alison, Jacqui and Peter) of Division of Biomedical Services for helping me with the animal work and members of PNAACL (Dr. Andrew Bottrill and Dr. Sharad Mistry) for their valuable advice with the proteomics work.

I am thankful to all my friends Tom, Caitlyn, BB, Hedge, Tim and Ruth for feeding me and making my day-to-day life enjoyable during the course of my research.

I would like to thank Marie Curie Commission for their financial support.

Words would never be able to fathom the depth of feelings for my reverend parents, Mrs Bakula Patel and Mr Gunvant Patel, an indelible inspiration, and affection during my research. A special thank you is owed to Richa (my wife) for her kind words of encouragement and support during my regular moments of stress and for having faith in me that I could do it. Thank you for taking over my part of responsibility for the house and allowing me to focus on my study. Without you, this thesis would never have been possible.

Table of Contents

Abstract	2
Acknowledgement.....	3
Table of contents	4
List of figures & tables.....	7
List of abbreviations.....	10
Chapter 1 Introduction.....	12
1.1 Anxiety disorders	13
1.2 Fear locus in the brain - The amygdala.....	14
1.3 Stress response	16
1.4 Stress-induced anxiety behaviour	18
1.5 Glucocorticoid receptor co-chaperone: FKBP51.....	21
1.6 Regulation of Fkbp5 expression	29
1.7 Fkbp5 in stress-related psychiatric disorders.....	32
1.8 Aims and Objectives	38
Chapter 2 Materials and Methods	40
2.1 Animals.....	41
2.2 Neuropsin-/- mice genotyping	41
2.3 Restraint stress.....	43
2.4 Dissection & pooling of amygdala tissue	43
2.5 Primer design and validation	45
2.6 Quantitative reverse-transcription polymerase chain reaction.....	49
2.7 Stereotaxic injections	50
2.8 Plasma corticosterone levels	51

2.9 Amygdala neuronal cultures	51
2.10 Western blotting.....	53
2.11 Immunohistochemistry.....	55
2.12 Subcellular fractionation.....	56
2.13 Fkbp5-GFP cloning.....	57
2.14 Mouse neuroblastoma N2a cell cultures & transfection	60
2.15 FKBP51 <i>in vitro</i> translocation experiment	62
2.16 Chromatin immunoprecipitation.....	63
2.17 FKBP51 pull down assay	66
2.18 Lentiviral Fkbp5 gene silencing.....	68
2.19 Elevated-plus maze.....	73
2.20 Open field.....	73
2.21 Fear conditioning	74
2.22 miRNA microarray study	76
2.23 miRNA overexpression construct	77
2.24 Statistical analysis.....	80
Chapter 3 Stress regulation of Fkbp5 in amygdala	81
3.1 Introduction	82
3.1.1 Neuropsin in synaptic plasticity	82
3.1.2 EphB2 - NMDA clustering	83
3.1.3 Stress molecule Fkbp5	86
3.2 Results	87
3.3 Discussion	96
Chapter 4 Stress regulation of FKBP51 in amygdala	99
4.1 Introduction	100
4.2 Results	101
4.3 Discussion	117
Chapter 5 Amygdalar Fkbp5 in stress-induced anxiety	124
5.1 Introduction	125

5.1.1 Measuring anxiety behaviour.....	125
5.1.2 Assessing learning and memory.....	128
5.1.3 Fkbp5 in behaviour	131
5.2 Results.....	134
5.3 Discussion	145
Chapter 6 Stress-regulated amygdala miRNAs	149
6.1 Introduction	150
6.1.1 miRNA physiology.....	150
6.1.2 miRNA, stress and synaptic plasticity	152
6.2 Results.....	155
6.3 Discussion	167
Chapter 7 Concluding remarks & Future avenues	169
Appendix I.....	176
Bibliography	177

List of figures & tables

Figure 1.1	Functional domains of human FKBP51 & FKBP52.....	23
Figure 1.2	Schematic model of GR signalling.....	26
Figure 2.1	Agarose gel electrophoresis of genotyping PCR products.....	42
Figure 2.2	Graphical presentation of amygdala dissection.....	44
Figure 2.3	Primer efficiency calculation curve and agarose gel electrophoresis of qRT-PCR products.....	46
Figure 2.4	Representative melting curve analysis.....	47
Table 2.1	List of qRT-PCR primers.....	49
Figure 2.5	Cloning of Fkbp5 into pEGFP-N1 vector.....	58
Figure 2.6	Validation of Fkbp5-GFP constructs.....	61
Figure 2.7	Shearing genomic DNA.....	65
Figure 2.8	Representative landmarks of mouse skull.....	65
Table 2.2	List of Fkbp5 targeting SMART vector lentiviral shRNA constructs.....	69
Figure 2.9	Verification of stereotaxic lentivirus injection into the basolateral complex of amygdala.....	70
Figure 2.10	Lentivirus-mediated Fkbp5 gene silencing in amygdala.....	71
Figure 2.11	Stereotaxically injected lentivirus knockdowns FKBP51 in amygdala.....	72
Figure 2.12	Schematic diagram of the fear conditioning experimental protocol.....	75
Figure 2.13	Validation of miRNA precursor expressing constructs.....	79
Figure 3.1	Stress-induced Fkbp5 upregulation is attenuated in neuropsin ^{-/-} mice.....	88
Figure 3.2	Intra-amygdala neuropsin injection rescues attenuated Fkbp5 upregulation in neuropsin ^{-/-} mice.....	89

Figure 3.3	Differential Fkbp5 upregulation in neuropsin ^{+/+} and neuropsin ^{-/-} mice is independent of corticosterone.....	91
Table 3.1	Plasma corticosterone levels: Tukey's post-hoc results.....	92
Figure 3.4	Anti-EphB2 antibody blocks and NMDA receptor agonist mimics neuropsin-dependent Fkbp5 upregulation.....	94
Table 3.2	Fkbp5 expression in amygdala neurons: Tukey's post-hoc results.....	95
Figure 4.1	FKBP51 is stress-upregulated in neuropsin ^{+/+} mice but not in neuropsin ^{-/-} mice.....	102
Figure 4.2	FKBP51 displays cytoplasmic and nuclear distribution in the amygdala neurons.....	103
Figure 4.3	Stress triggers FKBP51 nuclear translocation in amygdala.....	105
Table 4.1	FKBP51 nuclear translocation in amygdala: Tukey's post-hoc results.....	106
Figure 4.4	Dexamethasone promotes nuclear accumulation of FKBP51....	108
Table 4.2	FKBP51 nuclear translocation in N2a cells: Tukey's post-hoc results.....	109
Figure 4.5	FKBP51 does not interact directly with DNA.....	110
Figure 4.6	Stress does not affect Akt phosphorylation at serine 473 in amygdala.....	112
Figure 4.7	Proteomic analysis of cytoplasmic and nuclear FKBP51 interactome.....	114
Table 4.3	Mass spectrometric identification of proteins co-purified with cytosolic and nuclear FKBP51.....	115
Figure 5.1	Amygdala-specific Fkbp5 silencing protects wild type mice from stress-induced anxiety in elevated plus maze.....	135
Figure 5.2	Silencing amygdalar Fkbp5 expression protects wild type mice from stress-induced suppression of exploratory behaviour in the open field.....	137
Table 5.1	Number of centre zone entries: Tukey's post-hoc results.....	138
Table 5.2	Distance travelled in centre zone: Tukey's post-hoc results....	138

Table 5.3	Time spent in centre zone: Tukey's post-hoc results.....	138
Figure 5.3	Representative track plots of animal's exploration pattern in the open field.....	140
Table 5.4	Contextual memory: Tukey's post-hoc results.....	141
Figure 5.4	Deleting Fkbp5 gene in amygdala does not impair hippocampus-dependent memory in wild type mice.....	142
Figure 5.5	Amygdalar Fkbp5 is not involved in conditioned fear.....	143
Table 5.5	Cued memory: Tukey's post-hoc results.....	144
Figure 6.1	Schematic model of miRNA biogenesis and mechanism of action.....	151
Figure 6.2	Spatial distribution of (A) raw and (B) local background corrected data.....	156
Figure 6.3	Variance stabilizing normalization.....	157
Figure 6.4	Correlation analysis.....	159
Figure 6.5	Principle component analysis.....	160
Table 6.1	List of 20 amygdala miRNAs most deregulated by stress.....	162
Figure 6.6	Volcano plot of test vs. control expression analysis.....	163
Figure 6.7	Heatmap of hierarchically clustered miRNA probes.....	164
Figure 6.8	Overexpression of stress-upregulated miRNAs has no impact on Fkbp5 expression <i>in vitro</i>	165
Figure 7.1	Stress regulation of amygdalar FKBP51.....	171
Figure I.1	Graphical presentation of relationship between protein and peptide probabilities.....	176

List of abbreviations

AMPA	α -amino-3-hydroxy-5-methyl-4-isoxazolepropionic acid receptor
ANOVA	Analysis of variance
AR	Androgen receptor
BDNF	Brain-derived neurotrophic factor
BLA	Basolateral complex of amygdala
BNST	Bed nucleus of the stria terminalis
BSA	Bovine serum albumin
CeA	Central nucleus of amygdala
CREB	cAMP response element binding protein
CS	Conditioned stimulus
Cyp40	Cyclophilin 40
DIV	Days <i>in vitro</i>
EPM	Elevated plus-maze
FC	Fear conditioning
GAPDH	Glyceraldehyde-3-phosphate dehydrogenase
GC	Glucocorticoid
GFP	Green fluorescent protein
GR	Glucocorticoid receptor
GRC	Glucocorticoid receptor complex
GRE	Glucocorticoid response element
HPA	Hypothalamic-pituitary-adrenal
Hsp90	Heat shock protein 90
LBD	Ligand binding domain
LTP	Long-term potentiation

MeCP2	Methylated CpG binding protein 2
miRISC	miRNA-induced silencing complex
MR	Mineralocorticoid receptor
NMDA	N-methyl-D-aspartic acid
pAkt(S473)	Akt phosphorylated at serine 473
PBS	Phosphate buffered saline
PBS + PI	Phosphate buffered saline containing protease inhibitors
PBS-T	Phosphate buffered saline containing tween-20
PCR	Polymerase chain reaction
PFA	Paraformaldehyde
PFC	Prefrontal cortex
PP5	Protein phosphatase 5
PPIase	Peptidylprolyl isomerase
PR	Progesterone receptor
PTSD	Post-traumatic stress disorder
PVN	Paraventricular hypothalamic nucleus
qRT-PCR	Quantitative reverse transcriptase PCR
RT	Room temperature
SNP	Single nucleotide polymorphism
TPR	Tetratricopeptide repeat
US	Unconditioned stimulus
UTR	Untranslated region

Chapter 1

Introduction

1.1 Anxiety disorders

Normal anxious apprehension is marked as pathological anxiety when unpredictable, exaggerated and uncontrollable fear responsivity to inappropriate objects or events in absence of true danger interfere with optimal daily living (Rosen, 1998). According to the ICD-10 and DSM-IV-TR, various forms of clinical anxiety disorders include: generalised anxiety disorder, acute stress disorder, post-traumatic stress disorder (PTSD), panic disorder, agoraphobia, specific phobia, social phobia and obsessive-compulsive disorder (American Psychiatric Association, 2000; World Health Organisation, 1992). Anxiety disorders are one of the most prevalent and disabling neuropsychiatric disorders (Kessler, 2005). Despite of their heterogeneity, anxiety disorders share a common state of exaggerated arousal and exhibit substantially overlapping symptoms (Klein, 1989).

In addition to understanding how anxiety disorders develop, what mediates the transition of a natural adaptive reaction, anxiety, to its pathological form only in some people and not in others with similar experiences also needs to be focused on to develop preventive programs. Rosen and Schulkin has defined three interacting sets of predisposing factors that may contribute to the development of anxiety disorders: 1) biological factors, primarily of genetic nature; 2) developmental factors, resulting from early life experiences during critical stages in development for example infant-mother separation and childhood

abuse; and 3) physical or psychological traumatic factors, focused on traumatic events or circumstances at any age (Hammen, 1992; Rosen, 1998). According to the diatheses-stress theory, interaction between these, either innate or acquired, precipitating factors in synergy confers an individual, greater vulnerability to psychopathology. For instance exposure to psychosocial stress more likely triggers anxiety in individuals carrying genetic vulnerability (Barlow, 1998; Barlow, 2000). Even though psychosocial stress is a major risk factor for the entire group of anxiety disorders, diagnostically prior exposure to extreme stressor or traumatic event is an essential criterion for only two stress-related anxiety disorders: acute stress disorder and PTSD (Yehuda, 2002). Hence understanding stress-mediated molecular changes leading to pathological anxiety is of great importance.

1.2 Fear locus in the brain - The amygdala

Fear is a reflex emotion belonging to the defensive system that helps to predict a danger when it is distal and survive when it is proximal. Rosen and Schulkin proposed that hyperexcitability of fear circuitry underlie chronic hypervigilance towards threatening stimuli in anxiety patients although it remains controversial (Rosen, 1998). Nevertheless neuro-imaging studies do support abnormal activity patterns of fear structures, for instance heightened amygdala activation, in anxious subjects (Shin, 2010). Earlier approaches included lesion studies to understand the involvement of brain regions in fear circuitry. Two

pioneering studies reported a collection of emotional disturbances, loss of fear emotion in particular, in rhesus monkeys with bilateral surgical lesion to the temporal cortex (Brown, 1888; Kluver, 1937). Although it was Weiskrantz who pointed out that lesion to a group of heterogeneous nuclei called amygdala, underlying the temporal cortex, was responsible for the loss of fear to the dominant monkeys (Weiskrantz, 1956). Amygdala is at the centre of neuro-anatomical circuitry of both innate and learned fear responses. Named after almond in Greek, bilaterally situated in the medial temporal lobe the amygdala can be divided into two distinct subdivisions: 1) basolateral region consisting of lateral, basal or basolateral and accessory basal or basomedial nuclei, and 2) central region involving central, medial and cortical nuclei (Swanson, 1998; LeDoux, 2007).

Basolateral complex of the amygdala (BLA) is critical to acquisition, consolidation, recall and expression of fear memory (Maren, 2004). Sensory gateway to the amygdala, lateral nuclei, receives and integrates synaptic information from various sensory structures such as thalamic nuclei (auditory and somatosensory), perirhinal cortex (visual) and piriform cortex (olfactory) and subsequently projects to most of the subnuclear regions within the amygdala (LeDoux, 2000). Spatial and contextual information related to conditioning is conveyed by the hippocampus to both lateral as well as basal nuclei (Maren, 1999). Indeed, lesions aimed at the lateral nucleus of amygdala impair acquisition and expression of conditioned fear only to the discrete

sensory cues (Nader, 2001). Excitotoxic lesions of BLA, in contrast, blocked both hippocampus-independent sensory and hippocampus-dependent contextual fear conditioning in rats (Maren, 1996). Importantly, excitotoxic lesions to BLA blocked fear-potentiated startle regardless of whether they were made after 6 or 30 days of training indicating BLA as neural locus for storage of fear memories (Lee, 1996).

Processed information from different nuclei of BLA is either relayed back to the afferent structures or converges into the two major output regions the central nucleus of the amygdala and the bed nucleus of the stria terminalis (BNST) or commonly known as the extended amygdala, which have parallel projections to multiple brainstem regions, hypothalamus and higher cortical areas that mediate behavioral and physiological signs of fear and anxiety (Davis, 2000). Bilateral lesions of the central amygdala blocked potentiation of startle response in presence of fear-eliciting aversive stimuli (Hitchcock, 1986). Hence, two subsystems of amygdala contribute to sensory convergence (BLA) and response divergence (central amygdala) of fear conditioning.

1.3 Stress response

First conceptualized as generalized adaptation syndrome by Hans Selye in 1936, stress can be thought of as the organism's response to threatening environmental stimuli that bring the physiological equilibrium out of balance

(Selye, 1955). Stressor-triggered “flight or fight” response leads to activation of autonomic nervous system and HPA-axis releasing fast-acting adrenaline and slow-acting glucocorticoid (GC), respectively (de Kloet, 2005). Transient elevation in stress hormones levels helps the organism escape from the stressor and promotes adaptation to a new equilibrated state. This process of reinstating homeostasis through change is called “allostasis” (McEwen, 2004). Released GCs exert classical negative feedback effect on the HPA-axis, to shut down the stress response, at multiple levels: hypothalamus, pituitary and hippocampus among other brain regions (Lopez, 1999). Effective coping characterized by rapid onset on exposure to stressor and efficient termination afterwards forms an important part of the defense mechanism (McEwen, 2000). Insufficient coping events, in contrast, leading to prolonged and sustained stress responses can cause wear and tear on the body and brain homeostasis, resulting in “allostatic load” or “overload” (McEwen, 2004).

Stressors can be categorized as: systemic or physiologic stressors that pose a direct challenge to homeostasis and psychosocial stressors, of either innate or learned nature, that reflect an anticipation of a looming challenge to homeostasis (Sapolsky, 2003). Both stressors are potent activators of the HPA-axis and autonomic nervous system via two distinct pathways (McEwen BS, 2002). Real homeostatic challenges require little sensory processing and relays information directly from the brainstem to the paraventricular hypothalamic nucleus (PVN) and hence the responses are reflexive and fast (Herman, 2003).

In contrast, limbic brain areas such as the amygdala, hippocampus, and medial prefrontal cortex (PFC), supplemented by other connected brain structures, control and evaluate the emotional significance of the anticipatory fear-related adaptive stress responses to avoid unnecessary allostatic load (McEwen, 2000; Herman, 2003). Having little direct anatomical interactions with the PVN, limbic structures heavily rely on intermediary neurons to relay their influence on HPA-axis activation. The hippocampus and medial PFC appears to inhibit HPA-axis response to psychogenic stress whereas HPA-axis activation by anxiogenic stressors involves contributions from the basolateral, central and medial amygdalar nuclei (Herman, 2005). Given the well-documented neural regulation of HPA-axis by higher limbic brain structures it is often described as Limbic-HPA-axis system in the literature (Lopez, 1999).

1.4 Stress-induced anxiety behaviour

Single traumatic episode or repeated psychosocial stress exposure can leave maladaptive footprints leading to long-term behavioural disturbances, most likely resulting from GCs hypersecretion (Roozendaal, 2009). Importantly, severe acute or chronic stress exposure leads to neural dysregulation of the HPA-axis response: habituation to familiar stressor and sensitization to novel stressor. After 14 days of ferret odour exposure, rats exhibited habituation by decreased levels of corticosterone and c-fos expression in the PVN. However, exposure to restraint stress displayed sensitization by elevated corticosterone

and c-fos expression in the PVN (Weinberg, 2009). Similarly, women with a history of childhood trauma, due to sensitization, had augmented HPA-axis response to mild psychosocial stress (Heim, 2001). In addition, Sandstrom and colleagues reported that rats subjected to six hours of isolation stress during postnatal developmental stage had persistently elevated baseline corticosterone levels during adulthood compared to non-stressed group (Sandstrom, 2005). Postnatally stressed rats, with long-term higher basal corticosterone levels, displayed impairment in hippocampus-dependent working memory when tested on radial arm maze (Sandstrom, 2005). Thus, stress-induced dysregulation of the HPA-axis, sensitization and increased basal GC levels, play an important role in determining animal's coping behaviour and physiological outcomes.

Various acute and chronic stress paradigms have been extensively studied in the rodents to dissect the molecular mechanisms underlying traumatic experience-related modulation in the behaviour. An important although often overlooked aspect is the overlap of neural circuitry mediating stress response and emotional memory at the level of the amygdala (LeDoux, 1994; Herman, 1997). Supporting evidence confirms that, along with the hippocampus and the PFC, the amygdala itself undergoes functional and structural plastic changes to create stressful experience-related maladaptive behavioural responses (Roozendaal, 2009). Dendritic remodeling, a form of structural plasticity,

represents longer lasting cellular traces of stress-induced adaptive plasticity (Lamprecht, 2004).

Pioneering research by Dr. Sumantra Chattarji's group has shown that acute and chronic stress-induced anxiety like behaviour correlates with the neuronal remodeling in the BLA. Interestingly, acute immobilization stress (single 2 hours session), although failed to affect morphology and behaviour one day post-stress, elicited gradual increase in spine density on principle BLA neurons and delayed enhancement in anxiety-like behaviour on the elevated plus-maze (EPM) when measured after 10 days (Mitra, 2005). Robust dendritic hypertrophy is observed in the BLA following 10 and 21 days of chronic immobilisation stress (Vyas, 2002; Mitra, 2005; Vyas, 2006). Higher spine density alongside dendritic elongation in pyramidal and stellate neurons of BLA accompanied the increased anxiety-like behaviour in chronically stressed rats. Surprisingly, unlike chronic immobilization stress, 10 days of chronic unpredictable stress neither elicited hypertrophy in the BLA nor induced anxiogenic behaviour in the rats (Vyas, 2002). Hence, it is noteworthy that disparate physiological and behavioural findings may be attributable to differences in the type and severity of stressor. Findings also indicate that stress paradigms eliciting, either delayed or rapid, neuronal remodeling always exhibit concomitant anxiogenic behaviour, and vice versa (Mitra, 2005). A remarkable aspect of stressful experience-mediated maladaptive changes in the BLA is the unfortunate irreversibility even after termination of the stress (Vyas,

2004). Temporal persistence of BLA neuronal remodeling and heightened anxiety-like behaviour even after 21 days of stress-free recovery may perhaps underlie slowly diminishing symptoms of stress-related anxiety disorders (Yehuda, 2002). Consistent with abundant expression of GR in the BLA, exploration of molecular mechanisms revealed that single or 10 daily subcutaneous doses of corticosterone, equivalent to physiological stress levels, mimicked the BLA dendritic elongation and enhanced anxiety-like behaviour elicited by chronic immobilization stress (Gray, 1996; Mitra, 2008). Therefore, emphasizing on corticosterone and GR position at the forefront of mechanism behind stress-induced structural plasticity and anxiety behavior. Taken together, the above findings contribute to the emerging framework between stress-induced structural plasticity in the amygdala and pathogenesis of anxiety disorders and further, outlines the importance of deciphering the linking cellular and molecular correlates.

1.5 Glucocorticoid receptor co-chaperone: FKBP51

Main HPA axis effectors, glucocorticoids (GC), bind to steroid-activated transcription factors: mineralocorticoid receptor (MR) and glucocorticoid receptor (GR). High-affinity MR is occupied by GC under basal conditions, whereas low-affinity GR requires elevated GC levels for activation, explaining their crucial involvement in the stress system (de Kloet ER, 2005). Constitutively steroid-free GR reside in both the cytoplasm and nucleus in the form of a

complex with chaperones and co-chaperones. These molecules also regulate GR actions such as folding, maturation, translocation and transcriptional activation (Grad, 2007).

In the mature GR complex, single GR molecule associates with heat shock protein 90 (Hsp90) dimer, one of tetratricopeptide repeat (TPR) domain-containing proteins and p23 molecule. Only four TPR domain-containing proteins have been co-purified so far with steroid receptors: FKBP51, FKBP52, protein phosphatase 5 (PP5) and cyclophilin-40 (CyP40) (Pratt, 1997). FKBP51, encoded by *Fkbp5* gene, belongs to the immunosuppressive drugs binding immunophilin protein family. Smith and colleagues were the first to purify FKBP51, known as p54 and FKBP54 two decades ago, as a component of an unactivated progesterone receptor complex (Smith, 1990). However, Wiederrecht et al. coined the term FKBP51 for a novel 51 kDa FK506 binding protein in JURKAT cells, homologous to another member of the same family, FKBP52 (Wiederrecht, 1992). FKBP51 and FKBP52 proteins share 75% sequence similarity and 60% identity.

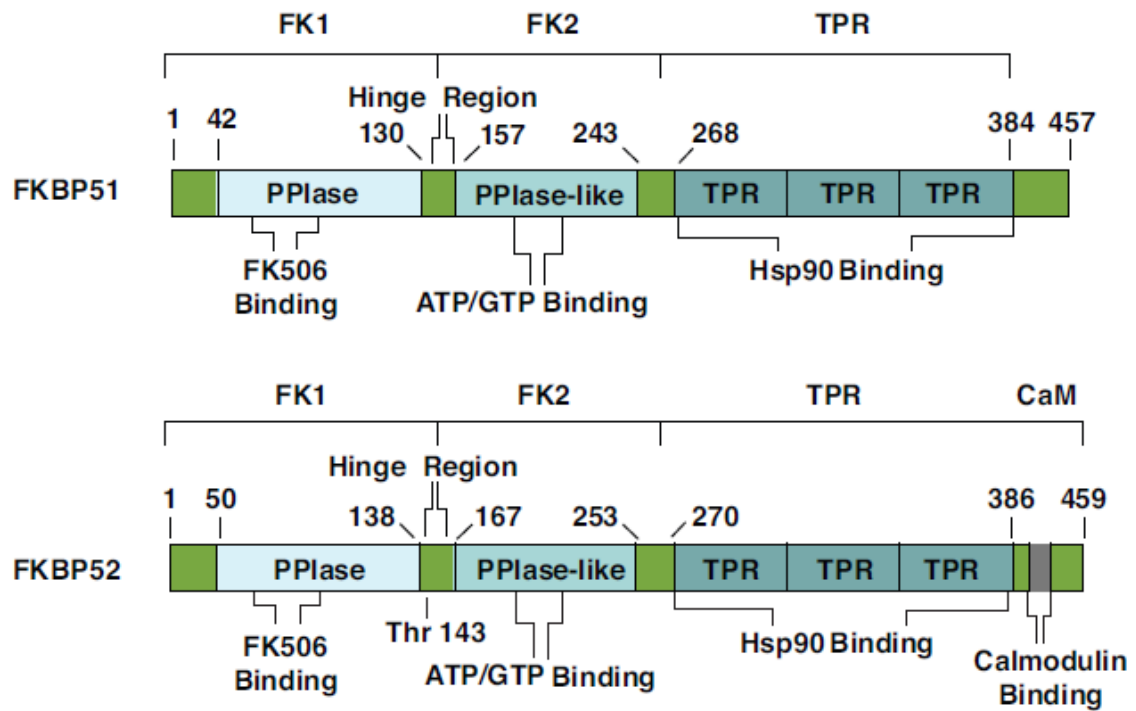


Figure 1.1 Functional domains of human FKBP51 & FKBP52. PPlase, peptidyl-prolyl cis-trans isomerase; TPR, tetratricopeptide repeat; FK1, FKBP-like 1; FK2, FKBP-like 2; CaM, calmodulin. Adapted from Stechschulte et al. 2011.

FKBP51 contains two FKBP-like domains (FK1 & FK2) and a C-terminal TPR domain together with other functional domains, as shown in **Figure 1.1**. Similar to other immunophilins, FKBP51 catalyses cis-trans conversion of prolyl-peptide bonds also known as peptidylprolyl isomerase (PPIase) activity. Immunosuppressive drugs, such as FK506 and rapamycin, bind to the N-terminal FK1 domain to inhibit FKBP51-mediated chymotryptic cleavage of small substrates (Niar, 1997). Conservation of responsible residues confers measurable PPIase activity between FKBP51 and FKBP52 (Sinars, 2003). Amino acid differences in proline rich loop overhanging FK1 PPIase pockets are proposed to affect interaction with other large proteins (Riggs, 2007). FK2 domain, unlike FK1, lacks the PPIase activity and does not bind to FK506 due to differences in several amino acids (Sinars, 2003).

FKBP52 is phosphorylated by casein kinase II at threonine 143 in the hinge region connecting FK1 and FK2 domain inhibiting Hsp90 binding, whereas FKBP51 lacks TEEED phosphorylation site (Miyata, 1997). C-terminal TPR domain of FKBP51 comprises of three repeats of a consensus 34-amino acid motif. All four TPR domain-containing Hsp90 co-chaperones compete for a common TPR-binding site MEEVD generated in the extreme C-terminal region of Hsp90 dimer (Scheufler, 2000). Interestingly mutants lacking C-terminal region outside TPR domain do not associate with Hsp90 and progesterone receptor (PR; Barent, 1998). Final 30 C-terminal FKBP51 amino acids enhance its Hsp90 binding compared to FKBP52 (Cheung-Flynn, 2003). These structural

differences between largely homologous FKBP51 and FKBP52 might explain the preferential association of FKBP51 over FKBP52 with steroid receptors.

Large TPR immunophilins, FKBP51 and FKBP52, differentially regulate GR hormone responsiveness and localisation. Constitutive FKBP51 binding to the glucocorticoid receptor complex (GRC) reduces the receptor affinity for GC. Adding FKBP51-rich squirrel monkey lymphocyte cytosol to the cytosol of L929 cells, FKBP51 increasingly suppresses GC binding to the GRC (Reynolds, 1998). Mutating squirrel monkey FKBP51 TPR domain at Lys352Ala and Arg356Ala disrupts Hsp90 binding and results in a loss of inhibitory effect on GR transactivation in COS-7 cells. Deletion of either FK1 or FK2 also failed to inhibit GR transactivation despite intact Hsp90 binding. Loss of PPIase activity, on the other hand, allowed inhibition of GR transactivation equivalent to wild type FKBP51 in COS-7 cells (Denny, 2005). To sum up, FKBP51 binding to Hsp90 and both FK1 and FK2 domains are crucial for GR regulation, while PPIase activity is dispensable for this effect.

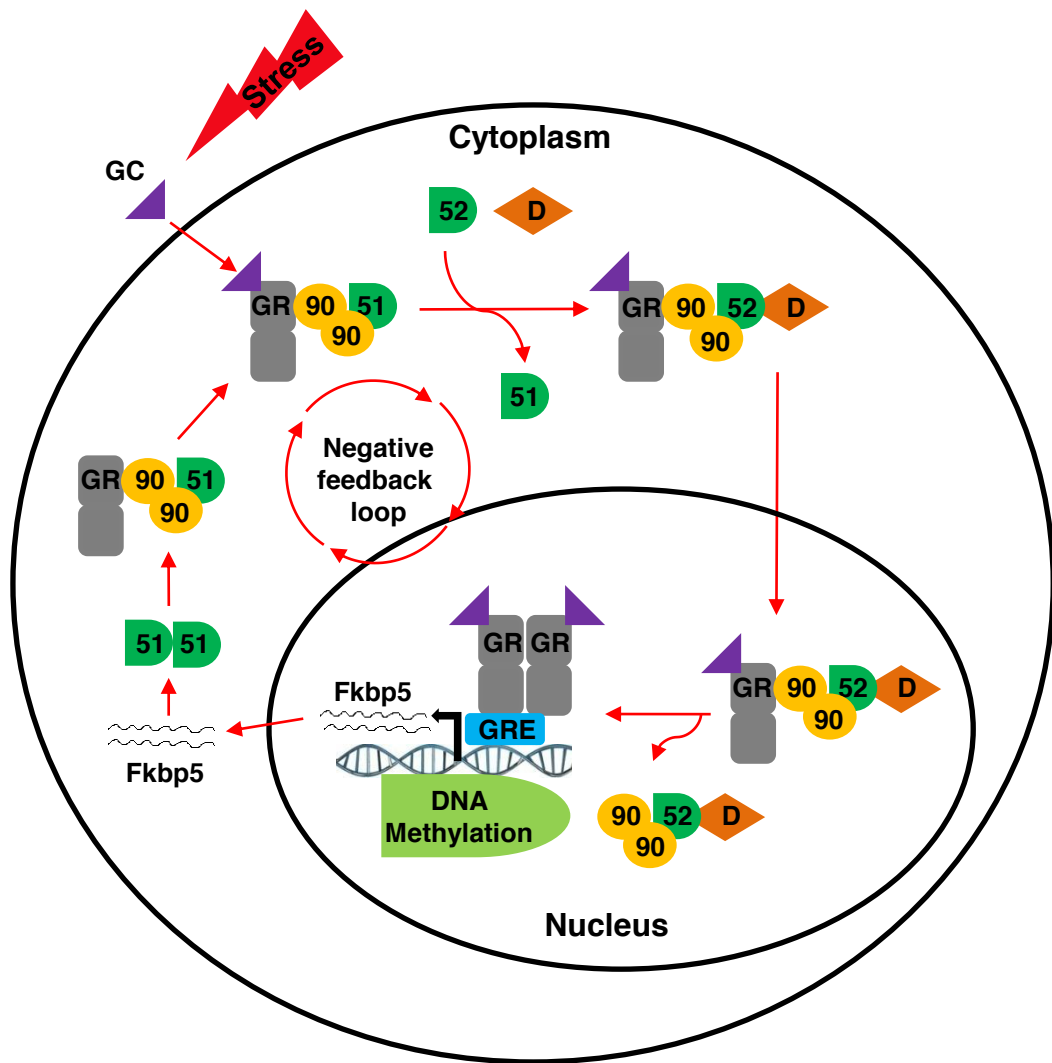


Figure 1.2 Schematic model of GR signalling. FKBP51 is constitutively bound to mature GRC through Hsp90 rendering the complex in cytoplasm. GC binding induces switching of FKBP51 by FKBP52. FKBP52 recruits dynein triggering nuclear translocation of the complex. In the nucleus, GC dimer interacts with GRE to regulate target gene transcription. GC, glucocorticoid; GR, glucocorticoid receptor; 51, FKBP51; 52, FKBP52; 90, Hsp90; D, dynein; GRE, glucocorticoid response element.

Glucocorticoid binding results in FKBP51 replacement by homologous FKBP52 in GR complex (**Figure 1.2**). More FKBP51 than FKBP52 immunoprecipitated with GR from control L929 cell cytosol, while this proportion reversed following dexamethasone treatment. The levels of GR-associated Hsp90 were not altered by dexamethasone treatment, in line with both FKBP proteins competing for the common Hsp90 binding site. Dexamethasone-induced FKBP52 incorporation into GRC also resulted in simultaneous recruitment of motor protein dynein triggering GR translocation to the nucleus. Indeed cellular fractionation confirmed that FKBP51-bound GR is recovered from cytoplasm (but not the nucleus) in vehicle treated cells whereas FKBP52-bound GR is predominantly recovered from the nuclear pellet after dexamethasone treatment (Davies, 2002).

FKBP51 holds hormone-free GRC in the cytosol, owing to its poor interaction with the transporter protein dynein (**Figure 1.2**). Upon steroid binding, FKBP52 replaces FKBP51 and interacts with dynein triggering GRC nuclear translocation. Increasing concentration of FKBP52 mitigates FKBP51-mediated inhibition of GR transcription in neuroblastoma cells (Wochnik, 2005). Tatro et al. replicated the FKBP51 and FKBP52 regulation of GR localisation in neurons. FKBP51 silencing increased basal nuclear localisation of GR and FKBP52 knockdown impaired cortisol-triggered GR nuclear translocation in SH-SY5Y cells (Tatro, 2009).

In the yeast model FKBP52 potentiation of GR signalling is blocked by co-expression of only FKBP51 and not PP5. Hence, competition for common TPR binding site on Hsp90 does not seem to be the precise mechanism for this mutual antagonism between FKBP5s (Riggs, 2003). Studies attempting to find correlations between the domain structures, its binding partners and subcellular protein localization shed some light on the above mechanisms. Ligand-binding domain (LBD) of GR determines its cellular localisation (Wan, 2001). Wild type GR primarily localises in the cytoplasm and associates with FKBP51, whereas nuclear progesterone receptor (PR) purifies with FKBP52 with in COS-1 cells. However replacing LBD in GR with LBD of PR shifts the localization of the chimera to the nucleus where it immunoprecipitates with FKBP52 (Banerjee, 2008). In addition FKBP51 chimeras with two point mutations (Leu119Pro & Ala116Val) in the hinge region overhanging PPIase pocket show potentiation of transcriptional activity of androgen receptor (AR) equivalent to wild-type FKBP52 in yeast and mouse cells (Riggs, 2007). This suggests the FK1 domain and the hinge region interacting partners determine the divergent effects of FKBP51 and FKBP52.

Based on the above findings a model has been proposed in which FKBP51 and FKBP52 bind to GR indirectly through their interaction with Hsp90 mediated by their TPR domains. This facilitates FK1 domain interaction with the LBD of GR to directly influence hormone binding while the linker region serves as the interaction surface. Hence the amino acid differences between FK1 domain and

the proline rich loop determine the divergent regulation of GR by FKBP51 and FKBP52.

1.6 Fkbp5 gene expression and regulation

First human and mouse Fkbp5 genes mapping to chromosome 6 (6p21.31) and 17 (17A3.3), respectively, were cloned about a decade ago. With 13 exons human Fkbp5 spans ~150 kb of genomic DNA. Mouse Fkbp5 on the other hand has 11 exons covering ~90 kb genomic DNA. The first two non-coding human Fkbp5 exons are absent in mouse Fkbp5. Expression of Fkbp5 is not restricted to thymus as proposed initially as it is expressed in numerous tissues including various brain regions (Scharf, 2011). Among all the GR co-chaperones, regulation of Fkbp5 gene expression remains most widely studied. Partially because Fkbp5 was identified as a GC transcriptional target showing abundant expression after 1 μ M dexamethasone treatment for 4 hours in murine WEHI-7TG thymoma cells and human C7TK.4 leukemic T cells (Baughman, 1991 & 1997). GC-induced increase in Fkbp5 mRNA levels is dose-dependent and mediated directly through GC receptor since the upregulation is suppressed only by co-incubation with 1 μ M GC receptor antagonist ORG 34116 and not by the protein synthesis inhibitor, 100 μ M cycloheximide, in human lymphocyte IM-9 cells (Vermeer, 2003). Interestingly asthma patients treated with fluticasone had almost 6-fold higher Fkbp5 expression in airway epithelial cells compared to placebo group. Basal Fkbp5 expression and fluticasone treatment

response negatively correlated in these asthma patients (Woodruff, 2007). Together these findings disclosed a novel intracellular ultra-short negative feedback regulatory loop for GR that hints towards Fkbp5 regulating GR sensitivity.

Finding the molecular mechanism of regulation of Fkbp5 expression involved screening its locus for potential presence of glucocorticoid response element (GRE). In human leukemic cells, construct containing intron 2 GREs but not the Fkbp5 promoter responded to GC in luciferase assay (U, 2004). Similar to GC, progestin and androgen also directly induce Fkbp5 gene expression by binding to a promiscuous and highly conserved distal hormone response element located in intron 5 region (Hubler, 2004; Magee, 2006). How GR and AR binding to Fkbp5 distal intronic element could induce transcription was explained using chromatin immunoprecipitation analysis in two different studies. Epigenetic marks such as histone trimethylation at K4 and K36, previously associated with active transcription, confirmed open conformation for transcription by steroid. In addition recruitment of SW1/SNF chromatin remodelling complexes to the Fkbp5 locus upon steroid binding further opened the chromatin for enhanced transcription. Deletion of BRM subunit of the SW1/SNF complex abolishes steroid induced Fkbp5 transcription (Makkonen, 2009; Paakinaho, 2010). Hence, steroid-induced long-range activation essentially involves looping between distal steroid elements and transcription machinery to activate poised Fkbp5 expression.

Influence of genetic and epigenetic elements on *Fkbp5* gene expression is also rapidly emerging. Several single nucleotide polymorphisms (SNP) in *Fkbp5* gene are associated with higher FKBP51 protein levels. They have been extensively studied owing to their crucial role as a determinant of GR sensitivity in psychiatric patients (Binder, 2009). As the name suggests Methyl-CpG-binding protein 2 (MeCP2) binds to the methylated CpGs and modify chromatin to suppress the target gene expression. MeCP2 knockout mice, a mouse model of Rett syndrome, show higher basal *Fkbp5* expression compared to wild-type mice in the absence of transcriptional repressor providing evidence of *Fkbp5* epigenetic regulation (Urduingio, 2008). *Fkbp5* elevation is glucocorticoid-independent since no notable differences in basal glucocorticoid levels between wild-type and MeCP2 deficient mice were seen and corticosterone implants did not alter MeCP2 binding to methylated CpGs in *Fkbp5* genomic regions (Nuber, 2005). More studies are needed to clarify the above in light of recent experiments demonstrating that plasma corticosterone levels exhibit positive correlation with *Fkbp5* gene expression and negative correlation with the % DNA methylation at two *Fkbp5* intron 1 CpG sites in blood (Lee, 2011). Corticosterone-induced decrease in *Fkbp5* DNA methylation was robust in blood and modest in hippocampus and hypothalamus brain regions identifying distinct effects on different tissues (Lee, 2010). While still unclear, these findings certainly emphasize the complexity of *Fkbp5* regulation.

1.7 Fkbp5 in stress-related psychiatric disorders

First insights into FKBP51 regulation of GR sensitivity came from New World monkeys. Despite of their 50-100 times higher circulating cortisol levels compared to humans, these primates lack signs of hypercortisolemia and display GR resistance. Molecular studies found that 13-fold higher expression of GR co-chaperone, FKBP51, in lymphocytes account for the observed GR resistance in these primates. Squirrel monkey FKBP51 expressed in COS-7 cells potently inhibited GR raising the median dexamethasone effective concentration (EC_{50}) for GR transactivation by 17-fold (Reynolds, 1999; Denny, 2000; Westberry, 2006). In addition, FKBP51 levels determine how a healthy individual copes with the Trier Social Stress Test-induced psychosocial stress. Higher FKBP51 in homozygous minor allele carriers of all three Fkbp5 SNPs (rs4713916, rs1360780 and rs3800737) showed elevated cortisol levels during recovery period and delayed reduction in self-reported anxiety (Ising, 2008). It is tempting to speculate that higher FKBP51 reduced GR-mediated effects (through the intracellular ultra-short negative feedback loop) and thus impaired GR-mediated feedback inhibition of HPA axis in both humans and non-human primates. The resulting prolonged hypercortisolemia makes individuals vulnerable to stress-related diseases.

Post-traumatic stress disorder is the only psychiatric disorder within DSM-IV classification requiring prior trauma experience as a diagnostic criterion.

Importantly, not everyone exposed to trauma develops PTSD, suggesting interplay between environmental and genetic factors determines one's susceptibility. GR transcriptional target *Fkbp5* hypothetically sits in a strategic position where *Fkbp5* genotype can interact with the environment to determine GR regulation of HPA axis. Indeed strong clinical data have emerged correlating *Fkbp5* genotype with altered GR sensitivity in psychiatric patients (Binder, 2009). A study reported significantly lower fasting blood *Fkbp5* and *STAT5B* (a GR inhibitor) expression in World Trade Centre survivors later diagnosed with PTSD (Yehuda, 2009). Commonly observed GR hypersensitivity is consistent with reduced FKBP51 levels in affected individuals. Authors hinted towards *Fkbp5* as a state marker of PTSD with differential expression between control and PTSD subjects determined by risk-related *Fkbp5* polymorphism (Sarapas, 2011). Surprisingly peripheral blood mononuclear cell gene expression profiling in trauma survivors at onset and 4 months later, identified differential *Fkbp5* upregulation following trauma correlated with the development of PTSD (Segman, 2005). Also children carrying high induction alleles of *Fkbp5* polymorphs rs1360780 and rs3800373 showed higher peritraumatic dissociation, a PTSD predictor in adults, following medical injury (Koenen, 2005). Similarly, 4 out of 8 *Fkbp5* polymorphisms tested in around 800 African-American subjects, interacted with severity of childhood abuse to predict the PTSD symptoms in adult life. Genotype alone did not correlate with the PTSD emphasizing the interaction between high *Fkbp5* induction allele and childhood trauma predicted the PTSD (Binder, 2008). Molecular analysis

revealed 183 transcripts differentially regulated by PTSD symptom severity, and genotype \times PTSD interaction resulted in addition of 32 more PTSD associated transcripts with *Fkbp5* being one of the most significant genes. Hence, *Fkbp5* genotype-driven differential gene expression pattern can also predict the biological subtype of PTSD (Mehta, 2011). Xie et al. partially replicated this by reporting that African-American high induction TT homozygotes of rs9470080 SNP with a history of childhood adversity are at a greater risk of developing PTSD compared to individuals with no childhood adversity and European-American ethnicity (Xie, 2010). These studies strongly point towards *Fkbp5* as a genetic marker of PTSD in African-American ethnicity at least.

Fkbp5 genotype has also been implicated in mood disorders associated with altered HPA axis activity. Genome-wide analysis to identify SNPs in HPA axis-related genes associated with depressive symptoms in two different European cohorts revealed positive correlation of minor alleles of four *Fkbp5* polymorphisms (rs9470080, rs9394309, rs7748266 and rs1360780) with lower saliva cortisol levels and depressive symptoms (Velders, 2011). In 317 nuclear families with bipolar pedigree, overrepresentation of *Fkbp5* SNP rs4713902 major allele was significantly associated with the hereditary bipolar depression in 554 affected offspring. Association of four SNPs (rs1043805, rs3800373, rs9296158 and rs1360780) depended on covariates such as suicide attempts and number of depressive episodes (Willour, 2009). Similarly, depressed patients of

German ethnicity homozygous for TT genotype at rs1360780 polymorph had suffered significantly more depressive episodes compared to other genotypes (Binder, 2004). In contrast, another study found overrepresentation of rs1360780 TT genotype positively associated with the disease status but not the number of depressive episodes in the non-Hispanic white patients (Lekman, 2008). These findings were replicated with gender specific effects in Swedish (Lavebratt, 2010) and German population (Zobel, 2010). Interaction of the above genotype with environmental factors results in a high number of pronounced behavioural and biochemical effects. An additive effect of T allele of rs1360780 SNP on insecure-resistant attachment relationship with mother was observed in Dutch infants. One or two T allele resulted in higher cortisol reactivity and increased stress reactivity in infants (Luijk, 2010). Similarly, German individual carrying TT genotype with a history of childhood maltreatment was more vulnerable to major depression (Apple, 2011). More homozygous minor allele carriers with severe trauma suffered major depression episodes over 10 years compared to other genotypes. In particular, CC genotype at rs3800373 and AA genotype at rs4713916 significantly lowered the onset of depressive episode in interaction with severe trauma. Interestingly rare alleles of Fkbp5 polymorphs have also been associated with depressive symptoms in kidney transplant (Shinozaki, 2011) and HIV patients (Tatro, 2010).

Moreover Fkbp5 make up predicts not just the mood disorder status but also the responsiveness to the antidepressant treatment. Among the 8 HPA axis-

regulating genes studied for polymorphisms, only Fkbp5 SNPs rs1360780, rs3800373 and rs4713916 showed significant association with response to the anti-depressant treatment at 2 and 5 weeks in two independent samples of depressed patients. Despite the lack of differences in basal Fkbp5 mRNA levels between all three genotypes of rs1360780, higher FKBP51 protein levels in high induction allele TT homozygote accounted for faster treatment response irrespective of the treatment class compared to CT heterozygote and CC homozygote (Binder, 2004). Other studies also reported the Fkbp5 genotype as treatment outcome predictors, although only in Caucasian patients (Lekman, 2008; Kirchheiner, 2008). However, no such correlation between polymorphism and response to treatment was observed in Spanish, Chinese and old-age German patients suggesting detailed research needs to be done to identify Fkbp5 as a predictor for personalised antidepressant treatment (Papiol, 2007; Tsai, 2007; Brent, 2010; Sarginson, 2010). Metaanalysis found only rs1360780 associated with the treatment response instead of rs3800373 and rs4713916 (Zou, 2010). Interestingly, the interaction of GG homozygote of GRIK4 (a kainate receptor subtype) at rs12800734 and TT homozygote of Fkbp5 at rs1360780 can predict the remission to antidepressant treatment (Horstmann, 2010).

A major concern about psychiatric disorders is suicidal tendencies in affected individuals. In a European cohort, treatment-related suicidal events were associated with 1360780TT and rs3800373GG variants of Fkbp5 (Brent, 2010).

Similar associations were replicated in Japanese patients (Supriyanto, 2011), African-American population (Roy, 2010) and outpatients treated with various antidepressants (Perroud, 2011). Further, two different studies showed that Fkbp5 genotype in interaction with childhood trauma increases the risk of suicide attempts in African-Americans subjects (Roy, 2010; Roy, 2012).

Hence, strong evidence supports Fkbp5 role in altered GR sensitivity determined by gene x environment interaction. The association of high induction risk Fkbp5 allele with disease status, responsiveness to antidepressant treatment or suicidal tendencies is rather intriguing since psychiatric conditions such as PTSD associate with enhanced GR sensitivity (Yehuda, 1991 & 2004b) whilst theoretically higher FKBP51 should lead to GR resistance. Indeed, Binder and colleagues, using dexamethasone suppression test, confirmed higher FKBP51 levels associated with increased GR resistance in high-induction allele carrying healthy individuals and with higher GR sensitivity in PTSD patients carrying high-induction risk allele. Taking into account that the Fkbp5 genotype alone did not by itself predict the susceptibility to PTSD, the authors proposed that Fkbp5 genotype-dependent association with GR sensitivity is state-dependent (Binder, 2008). In another study, contrary to author's hypothesis, elevated Fkbp5 transcript and protein levels were observed in post-mortem brain tissue of major depressive disorder in HIV-infected patients (Tatro, 2009). Consistent with this, aged mice lacking Fkbp5 showed resilience to age-related depressive symptoms in tail suspension

test and Porsolt forced swim test (O'Leary III, 2011). Fkbp5^{-/-} mice had attenuated elevation in cortisol levels in response to pharmacological and physiological stress stimuli and lower levels persisted even during recovery period compared to wild-type stressed mice (O'Leary III, 2011; Touma, 2011; Hartmann, 2011). Hence, mice devoid of Fkbp5 display higher GR sensitivity, altered HPA axis activity, active coping behaviour to stress and more "protective" phenotype. Although detailed research is inevitable, the preliminary findings portray Fkbp5 as a promising therapeutic target for psychiatric disorders.

1.8 Aims and Objectives

In situ hybridization revealed serendipitous, abundant expression of extracellular serine protease, neuropsin, mRNA in the neurons of limbic regions (Chen, 1995) raising curiosity to explore its involvement in the plasticity mechanisms underlying stress effects. Indeed, conventional neuropsin^{-/-} mice exhibited resistance to stress-induced anxiety in the elevated plus maze and the open field tests (Attwood, 2011). Encouraged to investigate the molecular mechanisms underlying their anxiolytic phenotype, we compared the expression of the amygdalar genes in wild-type and neuropsin^{-/-} mice using whole-genome RNA microarrays. Microarray analysis revealed 19 amygdala transcripts differentially regulated between naïve wild-type and neuropsin^{-/-} mice. Fkbp5 was among them, showing higher basal expression in neuropsin^{-/-}

compared to wild-type mice (Attwood, 2011). Further, Fkbp5 also emerged as an amygdalar gene most highly upregulated after 6 hours of stress in wild-type mice but less dramatically upregulated in neuropsin-/- mice subjected to stress (unpublished observation). Therefore, this study was designed to investigate if and how differential magnitude of amygdalar Fkbp5 gene and FKBP51 protein expression determines behavioural alterations to stressful events.

Chapter 2

Materials and methods

2.1 Animals

Experiments were performed on three month old male wild-type (C57/BL6J) and neuropsin^{-/-} mice. Animals were housed three to five per cage in a colony room with a 12 hr light/dark cycle (lights on at 7 AM) with *ad libitum* access to commercial chow and tap water. The use of mice for our experiments was approved by the Home Office and by the University of Leicester Ethical Committee.

2.2 Neuropsin^{-/-} mice genotyping

Neuropsin^{-/-} mice were generated and generously gifted by Professor Sadao Shiosaka (Nara Institute of Science & Technology; Japan). Briefly global neuropsin^{-/-} mice have exons 1-3 of neuropsin gene, containing the protease active site, replaced by a neomycin resistance cassette. Mice have been tested positively for the lack of full-length neuropsin transcript and proteolytic activity (Hirata, 2001). Imported neuropsin^{-/-} mice were backcrossed to in-house wild-type mice for 12 generations to avoid genetic background variations. Genomic DNA extraction for genotyping involved incubating ear samples in 100 µl lysis buffer (30 mM NaOH + 2 mM EDTA) for 25 minutes at 75 °C followed by subsequent neutralization with 100 µl neutralisation buffer (40 mM Tris-HCl pH 4.5). Extracted DNA from all the offspring was analyzed by PCR using Mangomix (Bioline) and following primers: wild-type sense (GCCTTTCCTGACCACTCTAA), antisense (GCACCGTGACCTTCAAA) and neo-sense (GGCTTCTCTGAGGCGGAAAGAA).

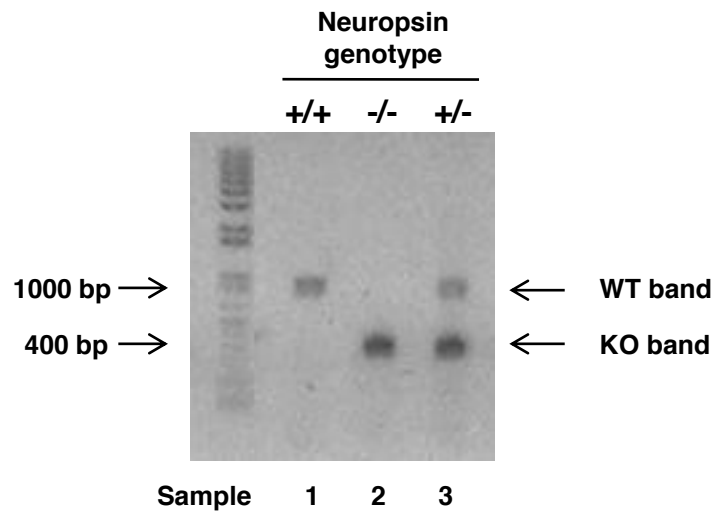


Figure 2.1 Agarose gel electrophoresis of genotyping PCR products. PCR analysis of genomic DNA was performed with specific primers. Neuropsin^{-/-} mice (sample 2, -/-) resulted in a 400 bp PCR product and wild types (sample 1, +/+) generated a 1000 bp product while both bands were clearly evident in heterozygotes (sample 3, +/-). WT, wild type; KO, knockout.

PCR cycles were the following: 96° for 5 min; 96° C for 30 s, 55°C for 30 s, 72°C for 3 min, for 35 cycles; final extension at 72°C for 1 min. The size of amplified PCR products on 1% agarose gel indicated the genotype as shows in **Figure 2.1**.

2.3 Restraint stress

Mice were kept undisturbed for at least one week in their home cage prior to the experiment to avoid unfamiliar environment stress. Restraint stress was induced by immobilizing mice in wire mesh tubes, with the diameter of about the animal's body size, secured at the head and the tail end with clips in their home cages. Restraint stress was conducted during the light period of the circadian cycle. For recovery, mice were removed from the restrainers and put back in their home cages.

2.4 Dissection & pooling of amygdala tissue

Amygdala was dissected from a thick coronal slice, -0.94 to -2.18 mm relative to Bregma, obtained using the brain matrix (Stoelting), as shown in **Figure 2.2**. Right and left amygdala from each animal was pooled together and studied as a single animal (n) throughout the project.

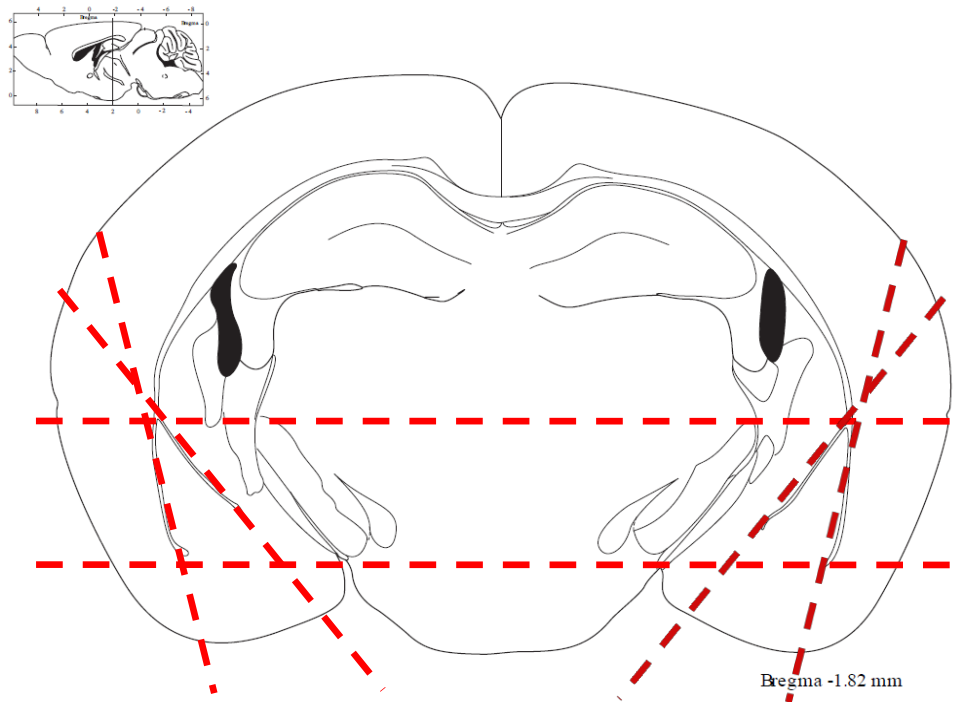


Figure 2.2 Graphical presentation of amygdala dissection. Coronal view of mouse brain at 1.8 mm posterior to Bregma (Adapted from Mouse Brain atlas by Paxinos & Franklin). Red lines indicate cuts made to dissect the amygdala.

2.5 Primer design and validation

Fkbp5 exon sequences were obtained from the ENSEMBLE database. Primers were designed using Primer3 software with following specific parameters: the length of the product between 70 and 120 bp, the melting temperature between 58 °C and 60 °C, the GC content between 45% and 58%, a maximum self-complementarity of 4 and a CG clamp of 1 (Kubista, 2006). Each primer was then plotted against itself and against the second primer using Operon software to identify any potential hairpin or primer-dimers formation, respectively.

Hairpins were defined as two sets of four consecutive bases complementary on same primer and primer-dimers as four consecutive complementary bases on two primers. Fkbp5 primers (**Table 2.1 below**) were then blasted against the mouse genome using nucleotide-nucleotide blast (NCBI Blast) to analyse their specificity for Fkbp5 gene. Custom-made oligos were purchased from Invitrogen.

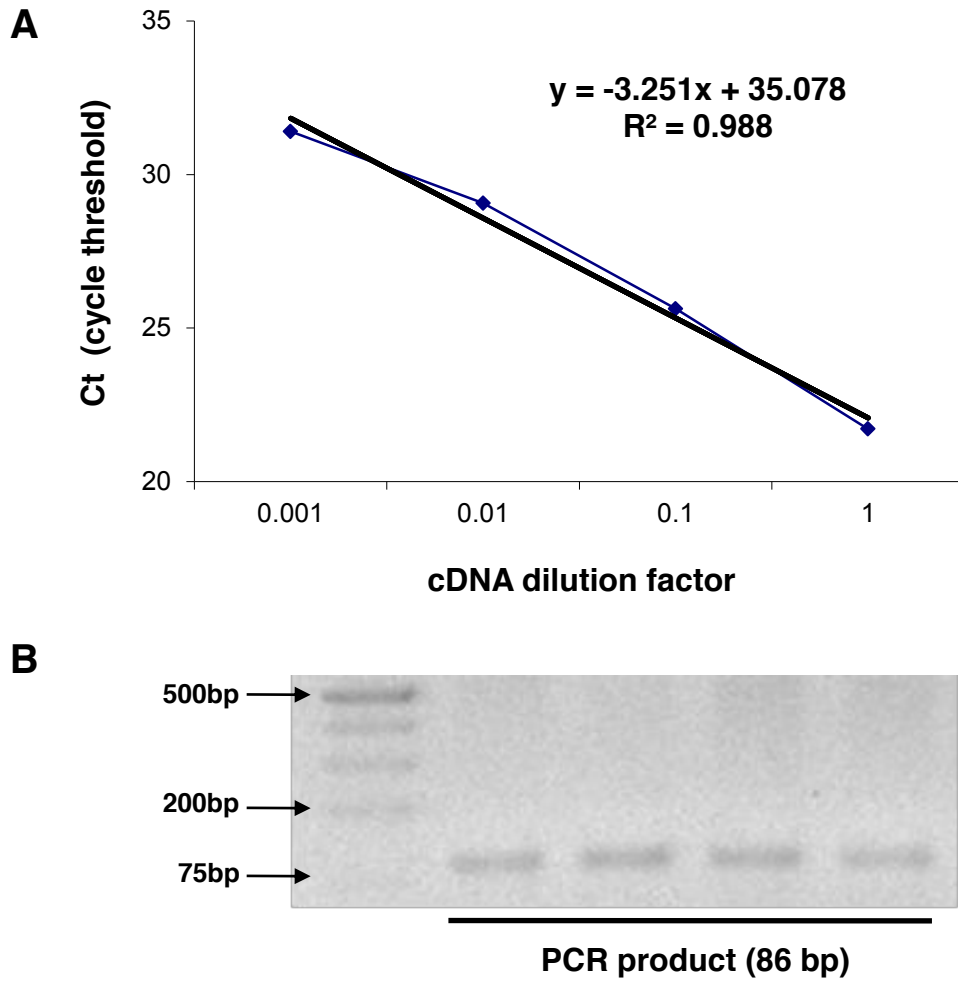


Figure 2.3 Primer efficiency calculation curve and agarose gel electrophoresis of qRT-PCR products. A qRT-PCR reaction was set up using serial dilutions of cDNA as the reaction template and primer pair designed to amplify exon 9 region of Fkbp5 molecule. (A) Ct values are plotted against the logarithm of the serial cDNA dilutions. Slope of the curve's trendline is determined to calculate the primer efficiency using formula (Kubista, 2006).

$$\text{Efficiency} = 10^{-1/\text{slope}}$$

For this set of primers, the slope is -3.251 and therefore the efficiency is 2.0305 (or 103.05%). (B) qRT-PCR products were electrophoresed on 1% agarose gel. Single band of the predicted size for each reaction confirmed that primers specifically amplify the targeted Fkbp5 exon 9 region.

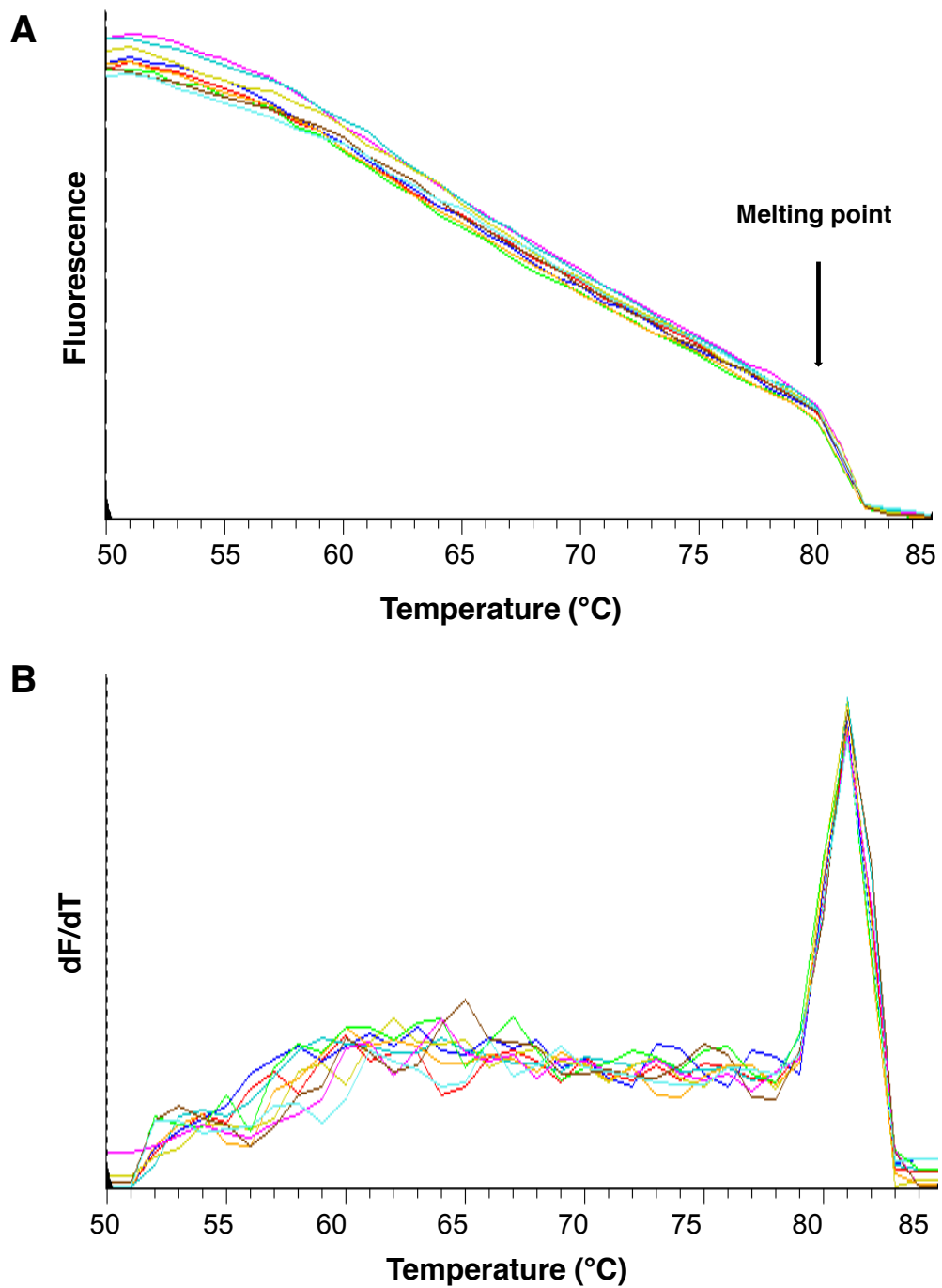


Figure 2.4 Representative melting curve analysis. To confirm absence of undesired DNA products, primer-dimer artefacts and residual DNA contamination (A) fluorescence intensity against temperature and (B) negative first derivative of fluorescence against temperature were plotted.

In order to calculate the efficiency of the designed Fkbp5 primer pair a qRT-PCR reaction was set up using serially diluted cDNA samples as templates. Ct values were plotted against the logarithm of dilution factors to generate a standard curve as shown in **Figure 2.3A**. For Fkbp5 primers, slope of the curve amounted to -3.251, equivalent to the reaction efficiency of 103.05%. Additionally, qRT-PCR products were electrophoresed on agarose gel to ensure the specificity of the primers. To rule out a possibility of unspecific and undesired gene amplification taking place in the “stress” samples, qRT-PCR products from stressed mice were analysed. A single band of the expected \approx 86bp size in the gel image (**Figure 2.3B**) confirms primers specifically amplify exon 9 region of the Fkbp5 molecule.

Fluorescent dye SYBR green was used in our qRT-PCR reactions to measure signal intensity. The dye binds to the double stranded DNA and dissociates as the melting temperature is approached resulting in a rapid drop of fluorescence (**Figure 2.4A**). The dye also binds to any undesired primer-dimer products and may lead to erroneous findings (Kubista, 2006). Each product has a unique melting point and hence the number of peaks on negative first derivative of fluorescence against temperature plot reflects the number of qRT-PCR products. A single peak (**Figure 2.4B**) confirmed absence of any primer-dimer and residual DNA in the reactions.

2.6 Quantitative reverse-transcription polymerase chain reaction (qRT-PCR)

Control and stressed mice were anaesthetized intraperitoneally using sodium pentobarbital and transcardially perfused with ice-cold phosphate buffered saline (PBS). Dissected amygdala tissues were stored in RNA later at -20 °C until further processing. Total RNA was extracted using RNeasy Lipid Tissue Mini kit (QIAGEN) according to the manufacturer's instruction. RNA was treated with RNase-free DNase to remove any genomic DNA contamination. RNA quantity and quality ($A_{260/280} > 1.80$) were measured using NanoDrop ND-1000 Spectrophotometer (Nanodrop Technologies). Following the manufacturer's instructions, 1 µg of total RNA from each extraction was used as the template for reverse-transcription with Superscript III (Invitrogen) using oligo (dT) primers in a total reaction volume of 20 µl. Each cDNA sample was assayed in triplicate wells containing 10 µl of SYBR Green Master Mix (Bio-Rad), 2 µl of cDNA, 250 nM of each Fkbp5 primers (see table below) and nuclease free water to a volume of 20 µl per reaction.

Table 2.1 List of qRT-PCR primers

Primer	Sequence
Fkbp5 forward	ATTTGATTGCCGAGATGTG
Fkbp5 reverse	TCTTCACCAGGGCTTTGTC
β-actin forward	GATTACTGCTCTGGCTCCTAGCA
β-actin reverse	GCCACCGATCCACACAGAGT
GAPDH forward	GCACAGTCAAGGCCGAGAAT
GAPDH reverse	GCCTTCTCCATGGTGGTGAA

The PCR was performed using Chromo4/PTC-200 thermal cycler (MJ Research) under the following cycles: 95° for 15 min; 94° C for 15 s, 55°C for 30 s, 72°C for 30 s, for 40 cycles; final extension at 72°C for 1 min. A melting curve analysis was performed to assess the specificity of the reaction as described above. Control reaction was performed without DNA template and also with non-reverse transcribed RNA as the template. The expression of the gene of interest was normalized against the Ct value for β -actin.

2.7 Stereotaxic injections

Neuropsin-/- mice were intraperitoneally anaesthetized with ketamine/xylazine (100 and 10mg/kg, respectively), placed in stereotaxic apparatus and bilaterally implanted with stainless steel guide cannulae (26 gauge; Plastics One) aimed above the basolateral complex of the amygdala (1.5mm posterior to Bregma, 3.5mm lateral and 4.0mm ventral). The cannulae were secured in place with dental cement. Dummy cannulae were inserted into all implanted cannulae to maintain patency. After a week dummy cannulae were replaced with the injection cannulae (projecting 0.75mm from the tip of the guide cannulae to reach the basolateral complex of the amygdala) and the mice were injected with either 1 μ l of 50 nM recombinant neuropsin (R&D) or vehicle followed by six hours of restraint stress in transparent plexiglass tubes. RNA was extracted from the amygdala, reverse transcribed and Fkbp5 transcript levels measured using qRT-PCR as described in 2.5. Accuracy of the

injection site and the cannulae placement has been histologically visualised after a small volume of bromophenol blue injection (Attwood, 2011).

2.8 Plasma corticosterone levels

Wild type and neuropsin-/- mice were subjected to 30 mins of stress followed by 0 min, 90 mins, 6 hours and 12 hours of recovery period. Animals were euthanized by cervical dislocation and after rapid decapitation, the trunk blood was collected in anti-coagulant (acid-citrate-dextrose) coated tubes. Whole blood was centrifuged for 15 minutes at 4°C and 3500 rpm to isolate plasma for corticosterone level measurement in triplicates using Corticosterone EIA kit (Cayman) according to the manufacturer's instruction.

2.9 Amygdala neuronal cultures

Primary amygdala neuronal cultures were prepared from one day old postnatal C57/BL6 J wild type pulps. Following decapitation, removed brains were placed ventral side up and a coronal slice was prepared by cutting anterior and posterior to the diencephalon. A diagonal cut was then made along the lateral fissure, a horizontal cut was made just below the fimbria of the hippocampus and the amygdala was dissected out by peeling away the cortex and placed into a petri-dish containing sterile HIB buffer (120 mM NaCl, 5 mM KCl, 25 mM HEPES, 9.1 mM Glucose, pH7.4) for preparation of primary amygdala cultures (Kasckow, 1997). Tissue was chopped using a sterilised scalpel blade into 2mm sections, transferred into 30ml container and excess of HIB buffer was aspirated. Next, 5mg of protease (Type XIV; Sigma) and 5mg of thermolysin

(Type X; Sigma) were added to 10ml HIB buffer in a 30ml tube (digestion mixture). Chopped amygdala pieces were incubated in digestion mixture for 30 minutes at room temperature (RT). Digestion solution was replaced by 3ml of Hank's buffered salt solution (HBSS; Gibco) containing 40 µg/ml DNase. The mixture was triturated using a glass pipette, centrifuged at 250g for 3 minutes and then resuspended in 3 ml of plating medium [Neurobasal A medium, 10% fetal bovine serum, 2mM glutamax, 2% B-27 supplement and 5 ml Penicillin-Streptomycin (Gibco)] and centrifuged again at 250 g for 3 minutes. Subsequently the pellet was resuspended in a small volume of plating medium and 20-30 µl droplets containing approximately 2×10^5 cells, obtained from two to three pups, were added to the centre of poly-D-lysine (Sigma) coated 30mm glass coverslips in 6 wells plate. An hour later further 2 ml of plating medium was gently added to each coverslip. Cells were maintained at 37 °C in a humidified atmosphere of 5% CO₂/95% air. After 24 hours, plating medium was replaced with 5 µM cytosine B-D-arabinofuranoside (Ara-C; Sigma) supplemented plating medium to preferentially inhibit proliferation of non-neuronal cells. Morphological and histological characterisation revealed neuronal phenotype of around 85% of cells and glial phenotype of the remaining cells in Ara-C treated cultures (Greene, 1977; Shemer, 1987). Another 24 hours later, medium was changed with maintenance medium [serum-free Neurobasal A medium supplemented with B27 (Gibco)]. Cells were maintained in the maintenance medium for 11-16 days *in vitro* (DIV) with half of the medium being changed with fresh medium every 3-4 days. Neurons were

treated with vehicle, corticosterone, corticosterone + neuropsin, corticosterone + anti-EphB2 antibody, corticosterone + neuropsin + anti-EphB2 antibody or NMDA + glycine for six hours before being harvested and used as a source of mRNA. Final concentration of each drug in 1 ml volume is as follow: corticosterone 10 nM (Cayman); neuropsin 50 nM (R&D); anti-EphB2 antibody 2 µg/ml (R&D); NMDA 100µM (Sigma); glycine 10 µM (Sigma). To block EphB2, neurons were treated with anti-EphB2 antibody 10 min before the experiment. RNA was extracted using RNeasy micro kit (Qiagen), reverse transcribed and Fkbp5 mRNA levels quantified using qRT-PCR as mentioned in 2.6.

2.10 Western blotting

Mice were anaesthetized with sodium pentobarbital and transcardially perfused with ice-cold phosphate buffered saline containing protease inhibitors (PBS + PI). The amygdalae from approximately 2 mm thick slice were dissected using a brain matrix (Stoelting). Tissue samples were homogenized in RIPA buffer (150mM NaCl, 1% NP-40, 0.5% sodium deoxycholate, 0.1% SDS, 50mM Tris, 10mM sodium fluoride, 1mM sodium orthovanadate, complete Roche protease inhibitors, pH 8). Protein concentration was measured using the Bradford method (Pierce kit) and adjusted to 2 mg/ml. Samples were mixed with an equal volume of 2x standard loading buffer (20% glycerol, 4% SDS, 0.004% bromophenol blue & 10% 2-mercaptoethanol) and denatured at 100°C for 5 min. 40 µg (20 µl) of sample proteins per lane was separated by sodium

dodecyl sulphate-polyacrylamide gel electrophoresis (SDS-PAGE; 8% gel, 120V for 90 min) and then transferred (100V for 60 min) onto a Hybond ECL nitrocellulose membrane (Amersham Biosciences). A dual-colour protein ladder (7 μ l per lane; Bio-Rad) was used adjacent to sample lanes to check protein transfer onto the nitrocellulose membrane and later for determining molecular weight of detected bands. Membranes were blocked for 1h at RT using 5% dry skimmed milk in Tris-buffered saline (10mM Tris, 100mM NaCl) with 0.1% Tween-20 (TBS-T; pH 7.6). After washing 3x 10 min in TBS-T, membranes were incubated overnight at 4°C with primary antibody diluted in TBS-T containing either 5% dry skimmed milk (for FKBP51, calpain, vimentin and EphA4) or 2% BSA (Sigma) (for CREB, phospho-Akt(S473) and total Akt). Primary antibodies used (and dilutions) were rabbit anti-FKBP51 (1:250; Abcam), rabbit anti-calpain (1:2000; Abcam), goat anti-mouse vimentin (1:2000; Abcam), mouse anti-EphA4 receptor (1:1000; Zymed), rabbit anti-CREB (1:1000; Cell Signalling), rabbit anti-phospho-Akt(S473) (1:1000; Cell Signalling) and rabbit anti-total Akt (1:500; Cell Signalling). Next morning membranes were washed 3x 10 min in TBS-T and incubated with appropriate horseradish peroxidase (HRP)-conjugated anti-rabbit, anti-goat or anti-mouse secondary antibody (1:1000; Vector labs) in TBS-T with 5% dry skimmed milk for an hour at RT. Followed by washing for 8 x 15 min and signal development using Western Blotting Luminol Reagent (Santa Cruz). Membranes were stripped using Restore™ Western Blot Stripping Buffer (Pierce) and re-blotted using mouse anti- β -actin antibody (1:2500; Sigma; 1h, RT) followed by an anti-mouse HRP conjugated

antibody (1:1000; Vector labs; 1h, RT) to normalize the results. Phospho-Akt(S473) immunostained membranes were stripped and re-blotted for total Akt to normalise the results. Scion Image (Scion Corporation) software was used to measure the relative signal intensities of the bands on western blots.

2.11 Immunohistochemistry

Wild-type C57/BL6J mice were anaesthetized by injecting sodium pentobarbital intraperitoneally and perfused transcardially with ice-cold 4% PBS + PI followed by ice-cold 4% paraformaldehyde (PFA; Sigma). The brains were removed whole and fixed in 4% PFA overnight at 4°C and then transferred to PBS for 5 hours before sectioning. Free-floating 70 µm thick coronal brain sections were cut in cold PBS, on a Campden Instruments Vibroslice HA752 manual vibrating blade microtome. The sections were washed in PBS and pre-incubated for 4 hours at room temperature with normal goat serum (1:500, company) in PBS-T (PBS, 0.5% bovine serum albumin and 0.02% Triton X-100). All primary and secondary antisera were diluted in PBS-T buffer. Sections were then incubated overnight at 4°C with primary rabbit anti-FKBP51 (1:200, Abcam) and mouse monoclonal anti-neuronal nuclei (NeuN; 1:200, Chemicon) antibodies. Next day, sections were washed for 7-8 hours in PBS-T and then incubated overnight at 4°C with goat anti-rabbit AlexaFluor 488 (green; 1:500, Molecular Probes) and donkey anti-mouse AlexaFluor 594 (red; 1:500, Molecular Probes) secondary antibodies. Sections were then washed 4x 10min

in PBS-T followed by 1x 30min in PBS, then mounted onto glass slides using Vectamount medium (Vector Laboratories). Sections in which primary antibodies were omitted served as controls. The sections were examined with a Zeiss LSM 5 Exciter laser scanning confocal microscope and magnified (4x and 64x) images taken using Zeiss Axiovision software.

2.12 Subcellular fractionation

Mice were anaesthetized with sodium pentobarbital and transcardially perfused with ice-cold phosphate buffered saline containing protease inhibitors (PBS + PI). Amygdalae dissected from both the control and stressed wild-type mice were fractionated using Cellular Protein Fractionation Kit (Perkin Elmer) according to the manufacturer's instructions. Protein concentration in each fraction was measured using the Bradford method (Pierce kit) and adjusted to 2 mg/ml. Fractionation purity was verified by western blot analysis of cytosol, membrane/organelle, nuclear and cytoskeletal proteins for their selective markers calpain, EphA4, CREB and vimentin, respectively. Equal amounts (2 mg) of cytosol, membrane/organelle and cytoskeletal fractions together comprised and were treated as cytoplasmic fraction. Cytoplasmic and nuclear FKBP51 levels were measured using western blot technique as described above. To normalize subcellular FKBP51 expression, cytoplasmic and nuclear membranes were stripped and re-blotted with an antibody against markers calpain and CREB, respectively. Scion Image software was used to measure the intensity of the bands.

2.13 Fkbp5-GFP cloning

Fkbp5 cDNA, originally cloned into pCMV-SPORT6 vector (Open Biosystems), was PCR amplified using Velocity DNA polymerase (Bioline). Amplification primers (Forward primer: ACGTGAATTCGGGCGACAGGTCTTCTACTTA and Reverse primer ACGTGGATCCGTGGCGCAGCGCGATACATGG) were designed such that the amplified Fkbp5 cDNA had stop codon mutated to non-functional state and restriction sites EcoRI and BamHI inserted at 5' and 3' end, respectively, for subcloning into pEGFP-N1 plasmid (Clontech) (**Figure 2.5A**).

PCR cycles were the following: 98° for 2 min; 98° C for 30 s, 57°C for 30 s, 72°C for 45 s, for 35 cycles; final extension at 72°C for 5 min. PCR product was separated on 1% agarose gel and visualized using SYBR Safe dye (Invitrogen) and the Safe Imager blue light transilluminator system (Invitrogen). The band corresponding to the desired product size was cut from the gel and cleaned using the Gel Extraction kit (Qiagen). Fkbp5 insert was then cut with BamHI and EcoRI enzymes (New England Biolabs) for 2 hours at 37°C using the following restriction reaction: 10 µl of each purified PCR product; 3 µl of 10x EcoRI restriction buffer; 3 µl of 1 mg/mL BSA; 10 U of each restriction enzyme and nuclease free water to yield a final reaction volume of 30 µl (**Figure 2.5B**). pEGFP-N1 vector was also cut in the same manner but with the addition of 5 U of CIP (Calf Intestinal Alkaline Phosphatase, New England Biolabs) to avoid vector recircularization. Following incubation, the products were separated on a 1% agarose gel and the bands corresponding to the Fkbp5 insert and the

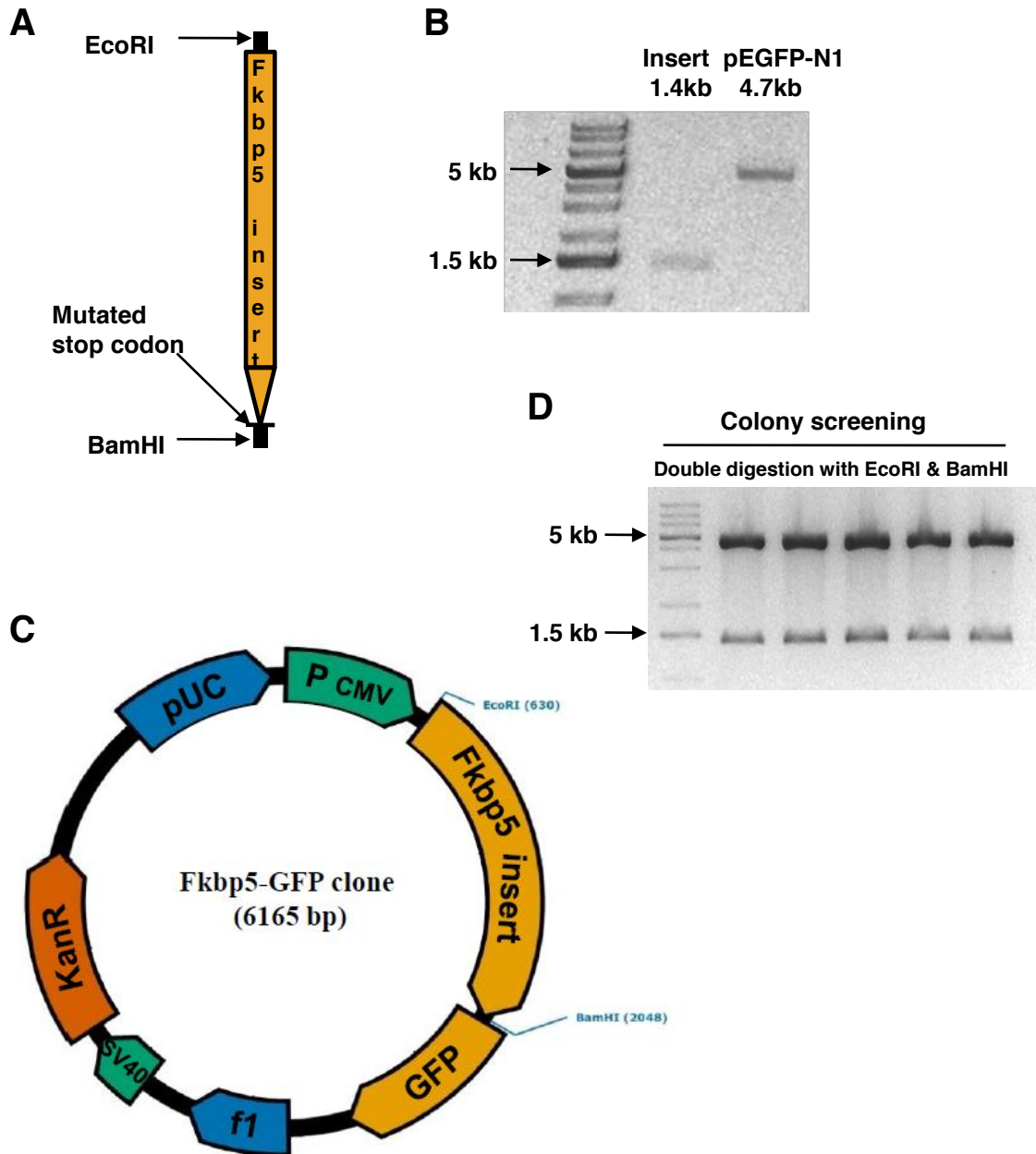


Figure 2.5 Cloning of Fkbp5 into pEGFP-N1 vector. Fkbp5 cDNA was cloned into mammalian GFP expression vector pEGFP-N1 to express GFP-tagged FKBP51. (A) Primers designed to PCR amplify Fkbp5 cDNA mutated stop codon to non-functional state and inserted EcoRI site at 5' end and BamHI site at 3' end. (B) Amplified Fkbp5 insert (lane 1, 1432bp) and pEGFP-N1 vector (lane 2, 4733bp) were double digested with EcoRI and BamHI to generate sticky ends and digested products were agarose gel purified for ligation. (C) Schematic map of Fkbp5 cDNA cloned into the pEGFP-N1 vector. (D) Randomly picked bacterial colonies were tested for the correct insertion of Fkbp5 cDNA into the vector. Plasmids were double digested with BamHI and EcoRI enzymes and electrophoresed on 1% agarose gel.

linearized vector were gel purified. Ligation of insert (PCR product) with the vector (pcDNA3) was performed using the Rapid DNA Ligation Kit (Fermentas) and using a vector: insert ratio of 1:5 for 30 min at 16°C. The ligation reaction mixture contained 50 ng of linearized vector; 5 fold molar excess of DNA insert; 4 µl Rapid ligation buffer; 4 U T4 DNA ligase and nuclease free water to yield a final reaction volume of 20 µl.

Ligation products (**Figure 2.5C**) were transformed using XL10-Gold Ultracompetent Cells (Stratagene). Briefly 5 µl of ligation reaction was added to a 50 µl aliquot of competent cells thawed on ice for 10 minutes and incubated on ice for a further 30 minutes. The mixture was heat-shocked for 30 seconds at 42°C and then placed on ice for 2 min. The mixture was then incubated at 37°C in 0.5 ml of super optimal broth medium with catabolite repression (SOC; Invitrogen) for an hour with shaking at 250 rpm. 100 µl of transformed cells were plated on lysogeny broth (LB) agar Petri dishes supplemented with 100 µg/ml kanamycin and left in a 37 °C incubator overnight. Colonies grown on Petri dishes were picked with sterile tips and grown in tubes containing 6 ml LB Broth and 100 µg/ml kanamycin overnight on a 37 °C shaker at 250 rpm. The plasmid DNA then extracted using Plasmid Mini Prep Columns (Qiagen) was screened for the presence of the Fkbp5 insert by BamHI & EcoRI double digestion, as described above. Positive constructs containing Fkbp5 cDNA displayed two bands on 1% agarose gel: Fkbp5 insert band (1.4kb) and pEGFP-N1 vector band (4.7kb) (**Figure 2.5D**). All the positive constructs were sequenced at the Protein Nucleic Acid Chemistry Laboratory, Leicester.

Sequencing traces were compared with the reference sequence using FinchTV (PerkinElmer) and error free clones were chosen for expression.

2.14 Mouse neuroblastoma N2a cell cultures and transfection

Mouse neuroblastoma N2a cells (generously gifted by Dr. L. Miguel Martins; MRC Toxicology Unit, Leicester) were cultured in Dulbecco's modified eagle medium (DMEM; with L-glutamine; Gibco) supplemented with 10% fetal bovine serum (FBS; Gibco), 50 units/ml penicillin (Invitrogen) and 50 µg/ml streptomycin (Invitrogen) and maintained at 37°C in a humidified atmosphere of 5% CO₂/ 95% air.

Lipofectamine 2000 (Invitrogen) was used to transiently transfect N2a cells according to the manufacturer's instructions at around 85-90% confluence. For each 1 ml of medium in the culture vessel, 1.6 µg Fkbp5-GFP construct DNA and 4 µl Lipofectamine at an optimized 1:2.5 ratio of DNA:Lipofectamine was used to achieve maximum transfection efficiency and minimum cytotoxicity. During transfection, plating DMEM medium was changed with serum- and antibiotics-free DMEM medium. Working culture volume determined DNA and Lipofectamine were each diluted in 50 µl of Opti-MEM® Reduced Serum Medium (Gibco) and incubated for 5 min at RT before being combined, gently mixed and incubated for a further 20 min at RT. The complexed mixture (100 µl) was then added to a single well for 4-6 hours, after which the medium was replaced with plating DMEM medium.

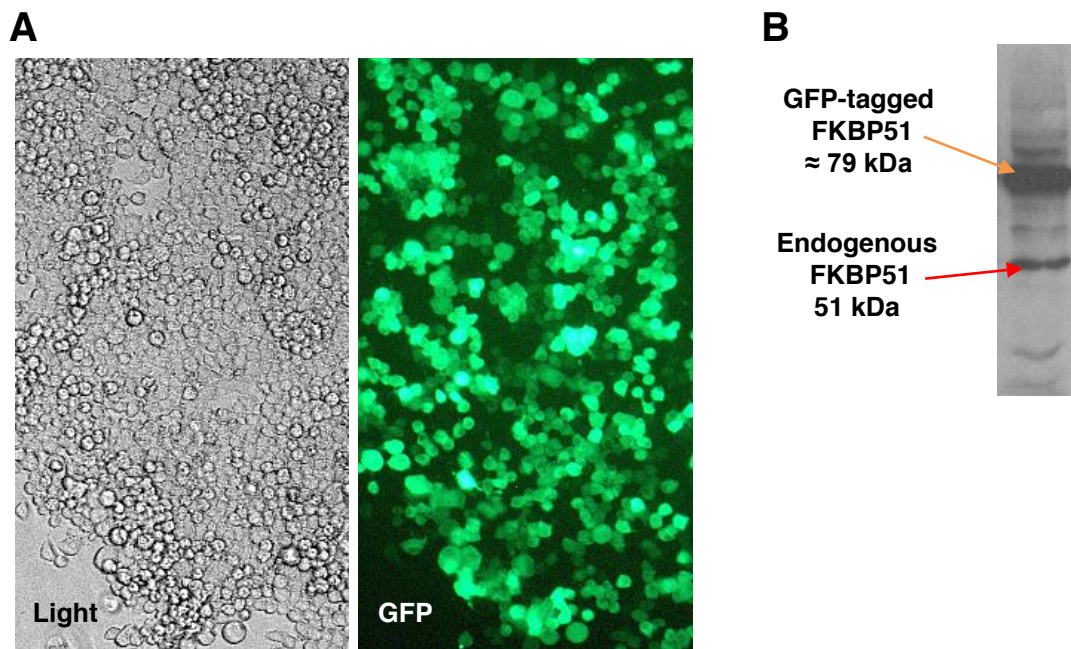


Figure 2.6 Validation of Fkbp5-GFP construct. Mouse neuroblastoma N2a cells were transfected with Fkbp5-GFP construct using Lipofectamine 2000 at around 85-90% confluence. (A) Cells were imaged 48 hours later and ratio of GFP positive cells/total cells was calculated to estimate transfection efficiency. Representative 4 times magnified transmitted light and GFP images are depicted. (B) Whole cell RIPA lysate was blotted for FKBP51 to confirm expression of GFP-tagged FKBP51.

N2a cells cultured on polystyrene Petri-dish (Nunclone, 56.7 cm²) in 10 ml medium were transiently transfected with 16 µg Fkbp5-GFP construct and 40 µl Lipofectamine as above. Transmitted light and GFP images (**Figure 2.6A**; 4x magnification) of cells 48 hours post transfection taken using Nikon TE2000 inverted fluorescence microscope shows more than 80% transfection efficiency. Transfected cells were trypsinized, pelleted and solubilized in ice-cold RIPA buffer (150mM NaCl, 1% NP-40, 0.5% sodium deoxycholate, 0.1% SDS, 50mM Tris, 10mM sodium fluoride, 1mM sodium orthovanadate, complete Roche protease inhibitors, pH 8), sonicated (5 × 10 seconds at full power) briefly on ice and extracts cleared by centrifuging at 3,500 rpm for 10 min at 4°C. Western blot analysis, using rabbit anti-FKBP51 (1:250; Abcam) antibody, of whole cell lysates confirmed presence of two separate bands at 51 kDa and ≈79 kDa corresponding to native and GFP-tagged FKBP51 proteins, respectively (**Figure 2.6B**).

2.15 FKBP51 *in vitro* translocation experiment

N2a cells at high confluence grow to form several layers. Therefore transfecting N2a cells at around 85% confluence although results in higher transfection efficiency, makes it difficult to image individual transfected cells. To overcome this problem, cells cultured on uncoated glass coverslips (30 mm; Menzel) in 6 well multidishes (Nunc), were transiently transfected at 50–70% confluence in 2 ml medium with 3.2 µg Fkbp5-GFP construct and 8 µl Lipofectamine 2000 as mentioned in 2.13. Transfected cells, 48 hours later, were imaged to study FKBP51 cellular distribution, untreated or after 6 hours of treatment with 1 µM

dexamethasone in the medium or next morning after 18 hours of recovery during which 1 μ M dexamethasone containing medium was replaced after 6 hours with steroid free fresh medium. During all the treatment and imaging procedures cells were maintained at 37°C in a humidified atmosphere of 5% CO₂/ 95% air. GFP signal in live cells, indicating localization of tagged FKBP51, was visualised in a Zeiss LSM 5 Exciter laser scanning confocal microscope and images taken using Zeiss Axiovision software. Cytoplasmic and nuclear GFP signal intensity for each cell was measured using ImageJ software. Data were collected from 4 different coverslips and approximate 150 individual cells representing different regions of each coverslip.

2.16 Chromatin immunoprecipitation

Mice were anaesthetized with sodium pentobarbital and transcardially perfused with ice-cold phosphate buffered saline containing protease inhibitors (PBS + PI). Wild type control and stressed mice amygdala tissue was chopped using razor blades and cross linked in 1% PFA at RT for 15 minutes followed by wash with 0.125M glycine to stop the cross linking reaction. Tissue samples were centrifuged at 720 rpm, 4°C for 5 minutes and wash buffer discarded. Pre-chilled Dounce homogenizer was used to homogenize the tissue, around 25 strokes per sample, in lysis buffer (10mM Tris-HCL pH 7.5, 10mM NaCl, 3mM MgCl₂ & 0.5% NP-40) followed by 10 minutes incubation on ice. Homogenates were then centrifuged at 4°C, 3000 rpm for 10 minutes and the resulting nuclear pellet was resuspended in FA lysis buffer (50mM HEPES-KOH pH7.5, 140mM NaCl, 1mM EDTA pH8, 1% Triton X-100, 0.1% sodium deoxycholate, 0.1% SDS

and protease inhibitors). Released chromatin in FA lysates was sonicated for 9 x 30 sec pulses at 60% of maximum power using Branson Digital Sonifier to get an average fragment size of < 500bp (**Figure 2.7**). Throughout the sonication process samples were maintained on ice and samples were let to cool down for a minute between each pulse to avoid degradation of chromatin by heat generated during sonication pulse. Sonicated samples were centrifuged for 30 seconds at 4°C, 8000g to pellet cell debris and DNA concentration in the clear supernatant was measured using Nanodrop-1000. Approximately 25 µg of sonicated chromatin was incubated with 40 µl of protein G sepharose beads (pre-cleared with single stranded 75 ng/µl herring sperm DNA and 0.1 µg/µl BSA for 30 minutes at RT on orbital shaker, GE healthcare) and 2 µg of immunoprecipitating antibody, overnight with rotation at 4°C.

Each sample was immunoprecipitated with antibodies against FKBP51 (Abcam), negative control rabbit IgG (Sigma) and positive control CREB (Cell Signalling). Next morning the beads were washed three times with 1 ml wash buffer (0.1% SDS, 1% Triton X-100, 2mM EDTA pH8, 150mM NaCl & 20mM Tris-HCl pH 8) and once with 1 ml final wash buffer (0.1% SDS, 1% Triton X-100, 2mM EDTA pH 8, 150mM NaCl, 20mM Tris-HCl pH 8). Washed beads were twice eluted with 150 µl of elution buffer (1% SDS, 100mM NaHCO₃) for 15 minutes at 30°C on rotator. Following addition of 10 µl of 5M NaCl, combined eluates were reverse cross-linked at 65°C for 5 hours with shaking. Next, proteins in eluates were digested with 20 µg Proteinase K for 1 hr at 55°C and presence of any DNA fragments was examined on 1% agarose gel.

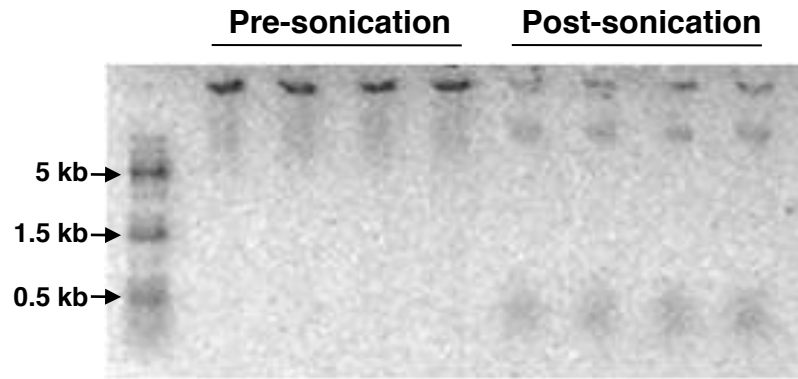


Figure 2.7 Shearing genomic DNA. Sonication of paraformaldehyde cross-linked chromatin in amygdala homogenates yielded DNA fragments of average <500bp on agarose gel.

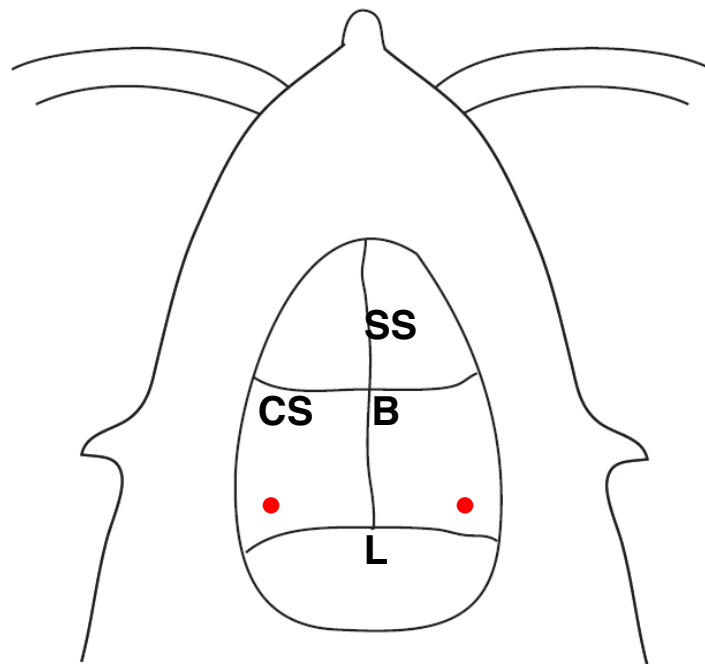


Figure 2.8 Representative landmarks of mouse skull. Red dots indicate the injection site (coordinates: 1.7 mm posterior to bregma and 3.5 mm lateral from the midline) referred from Mouse Brain atlas by Paxinos & Franklin. B, Bregma; L, Lambda; SS, Sagittal suture; CS, Coronal suture.

2.17 FKBP51 pull down assay

N2a cells grown in polystyrene T175 flasks (Nunclone, 175 cm²) in 30 ml medium were transiently transfected at 85-90% confluence with 48 µg Fkbp5-GFP construct and 120 µl Lipofectamine 2000. Cells were treated for 6 hours with either vehicle (sterile PBS) or 1 µM dexamethasone, 48 hours after transfection. To prepare cytoplasmic and nuclear fractions, cells were trypsinized, pelleted, resuspended in ice-cold swelling buffer (10mM HEPES pH 7.9, 1.5mM MgCl₂, 10mM KCl, 0.5mM DTT and protease inhibitors) for 5 minutes and nuclei released using a pre-chilled Dounce homogenizer (20 strokes with a tight pestle). Dounced cells were centrifuged at 228 g for 5 minutes at 4°C to pellet nuclei. The supernatant was cleared (2800 g for 10 minutes at 4°C to pellet any solids) and retained as the cytoplasmic fraction. The nuclear pellet was resuspended in low sucrose buffer (0.25M sucrose & 10mM MgCl₂) and layered over a cushion of high sucrose buffer (0.88M sucrose & 0.5mM MgCl₂) and centrifuged at 2800 g for 10 minutes at 4°C. The resulting cleaner nuclear pellet was resuspended in RIPA buffer, briefly sonicated (5 × 10 seconds at full power) and cleared (2800 g for 10 minutes at 4°C to pellet any solids).

For pull down, PBS and dexamethasone treated cytoplasmic and nuclear fractions were pre-cleared using 1 µg mouse IgG (Sigma) before incubation with 5 µg of either mouse IgG or mouse anti-GFP antibody (Roche) for an hour at 4°C. The samples were then incubated with protein G-sepharose beads (5x PBS

+ PI washed; GE) overnight. Next morning beads were washed 5x with PBS + PI before being mixed with an equal volume of 2x standard loading buffer (20% glycerol, 4% SDS, 0.004% bromophenol blue and 10% 2-mercaptoethanol) and denatured at 100°C for 5 min. Samples, in equal parts, were loaded on and separated on two different 8% SDS-PAGE gels at 120V with one electrophoresed for 90 minutes and the other for 15 minutes. A dual-colour protein ladder (7µl per lane; Bio-Rad) was used adjacent to sample lanes to determine molecular weight of bands. After electrophoresis, the gels were fixed in 7% glacial acetic acid in 40% (v/v) methanol solution of for an hour. Brilliant Blue G Colloidal (Sigma) was used as the protein staining suspension, into which the gel was placed for 1.5 hours. The gel was destained with 10% acetic acid in 25% (v/v) methanol for 60 seconds with shaking, rinsed with 25% methanol (which was discarded), then destained with 25% methanol overnight.

Gels electrophoresed for 90 minutes was used to visualize the purified proteins whereas the entire sample lanes were excised from the gel electrophoresed for 15 minutes and sent to Protein Nucleic Acid Chemistry Laboratory (University of Leicester) for peptide mass fingerprinting. Briefly, lanes were in-gel trypsin digested (Speicher, 2000) and proteolytic peptide fragments were analyzed by MALDI-ToF mass spectrometry using a Voyager DE-STR MALDI-ToF mass spectrometer (Applied Biosystems). The resulting MALDI-ToF spectrum peptide masses were searched against NCBI nr mus musculus protein database using MASCOT (Matrix Science). Mass spectrometry data for all samples were

loaded into the Scaffold (Proteome Software) for comparison and visualization. Proteins with two or more unique peptides of 95% significance were filtered and considered statistically significant identifications (**Appendix I**).

2.18 Lentiviral Fkbp5 gene silencing

Wild-type mice were intraperitoneally anaesthetized with ketamine/xylazine (100 and 10mg/kg, respectively), placed in stereotaxic apparatus and bilaterally injected with SMART vector 2.0 lentiviral shRNA technology (Dharmacon) to silence Fkbp5 gene in the amygdala. Three different targeting constructs equipped with human cytomegalovirus (hCMV) promoter and turboGFP reporter genes were tested. First, 0.3 μl of the lentivirus was injected at a point 1.7mm posterior to Bregma, 3.5mm lateral from the midline and 4.4mm ventral at 200 nl min^{-1} using the Nanofil syringe with a 33-gauge needle through an UMP-3.1 micropump (all from World Precision Instruments) mounted on Stoelting stereotaxic frame (**Figure 2.8**). After 5 min the needle was lowered to 5mm ventral and another 0.3 μl of the virus injected. The needle remained in place for another 5 min to prevent the backflow, slowly removed and the skin closed with Vetbond (3M). After two-week recovery, the region specificity of lentiviral injections was verified histologically by direct observation of the turbo GFP fluorescence on consecutive coronal sections spanning the amygdala using a Zeiss LSM5 Exciter confocal microscope (**Figure 2.9**). Amygdalae were dissected from stressed mice to determine *in vivo* knockdown efficiency of 3 different Fkbp5 targeting clones as compared to stress naïve non-targeting

control and uninjected mouse amygdalae by qRT-qPCR (**Figure 2.10A**; $F_{(3,12)} = 11.331$, $p < 0.001$; One-way ANOVA and **Figure 2.10B**; $F_{(2,9)} = 4.772$, $p < 0.05$; One-way ANOVA) and western blotting (**Figure 2.11**; $F_{(3,16)} = 32.349$, $p < 0.0001$; One-way ANOVA).

Table 2.2 List of Fkbp5 targeting SMART vector lentiviral shRNA constructs

Construct	Titer (TU/ml)	shRNA sequence
Non-targeting clone	2.66×10^8	TGGTTTACATGTTGTGTGA
Fkbp5 targeting clone 1	2.37×10^8	AAGGACATTTGATTGCCGA
Fkbp5 targeting clone 2	2.25×10^8	ATACTCAAACCCAAACGAA
Fkbp5 targeting clone 3	3.02×10^8	ATGCTGAGCTTATGTACGA

The most efficient Fkbp5 targeting clone 3 (~60% mRNA and protein knockdown efficiency) was used to silence Fkbp5 gene in all subsequent behavioural experiments. The restraint stress and behavioural experiments were performed two weeks after the intra-amygdala lentivirus injection as described below.

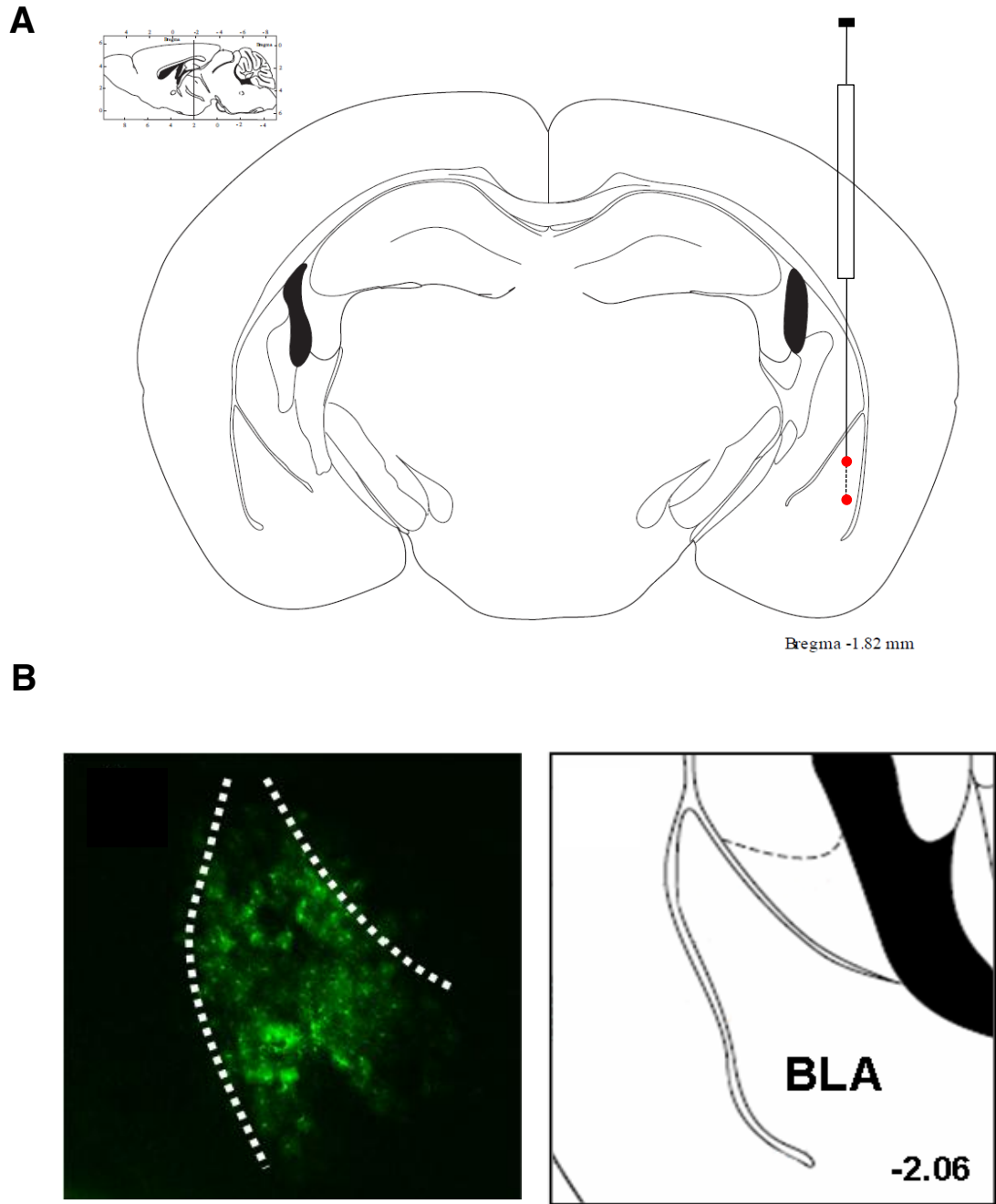


Figure 2.9 Verification of stereotaxic lentivirus injection into the basolateral complex of amygdala. (A) Coronal view of mouse brain at 1.8 mm posterior to Bregma (Adapted from Mouse Brain atlas by Paxinos & Franklin). Red dots indicate two injection sites: 4.4 mm and 5 mm ventral. (B) Brain sections were cut on vibrotome and turboGFP expression was visualized to verify viral transduction in the basolateral complex of amygdala. BLA, basolateral amygdala.

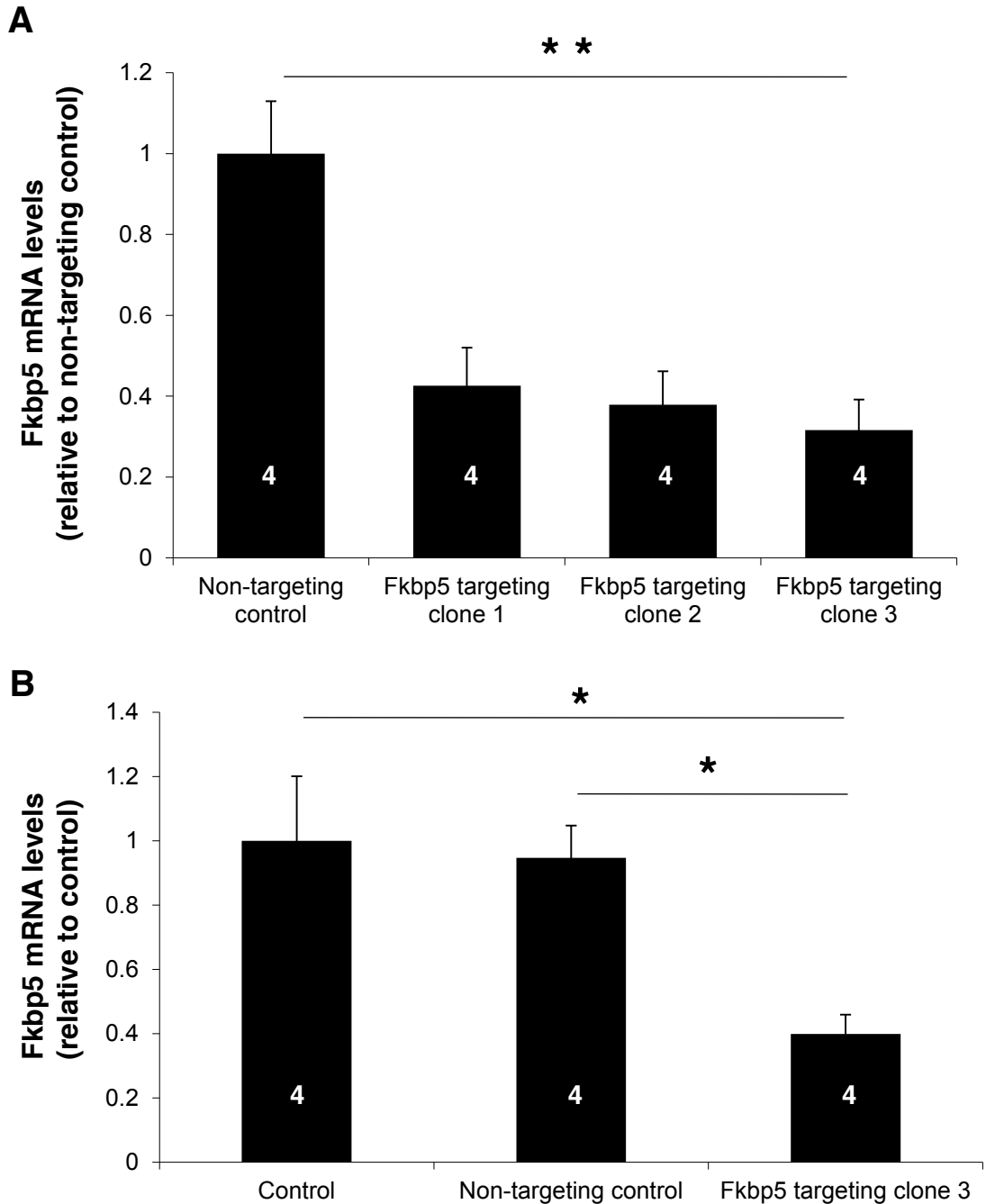


Figure 2.10 Lentivirus-mediated Fkbp5 gene silencing in amygdala. Wild type mice were stereotaxically injected with either non-targeting control or one of the Fkbp5 targeting clones. Post recovery period, Fkbp5 transcript levels in amygdala were measured using qRT-PCR. (A) Fkbp5 targeting clone 3 showed highest reduction in Fkbp5 levels compared to non-targeting control. (B) Compared to uninjected control, clone 3 injected mice had around 60% less Fkbp5 expression. Digits inside column indicate n. Data are shown as mean \pm s.e.m.

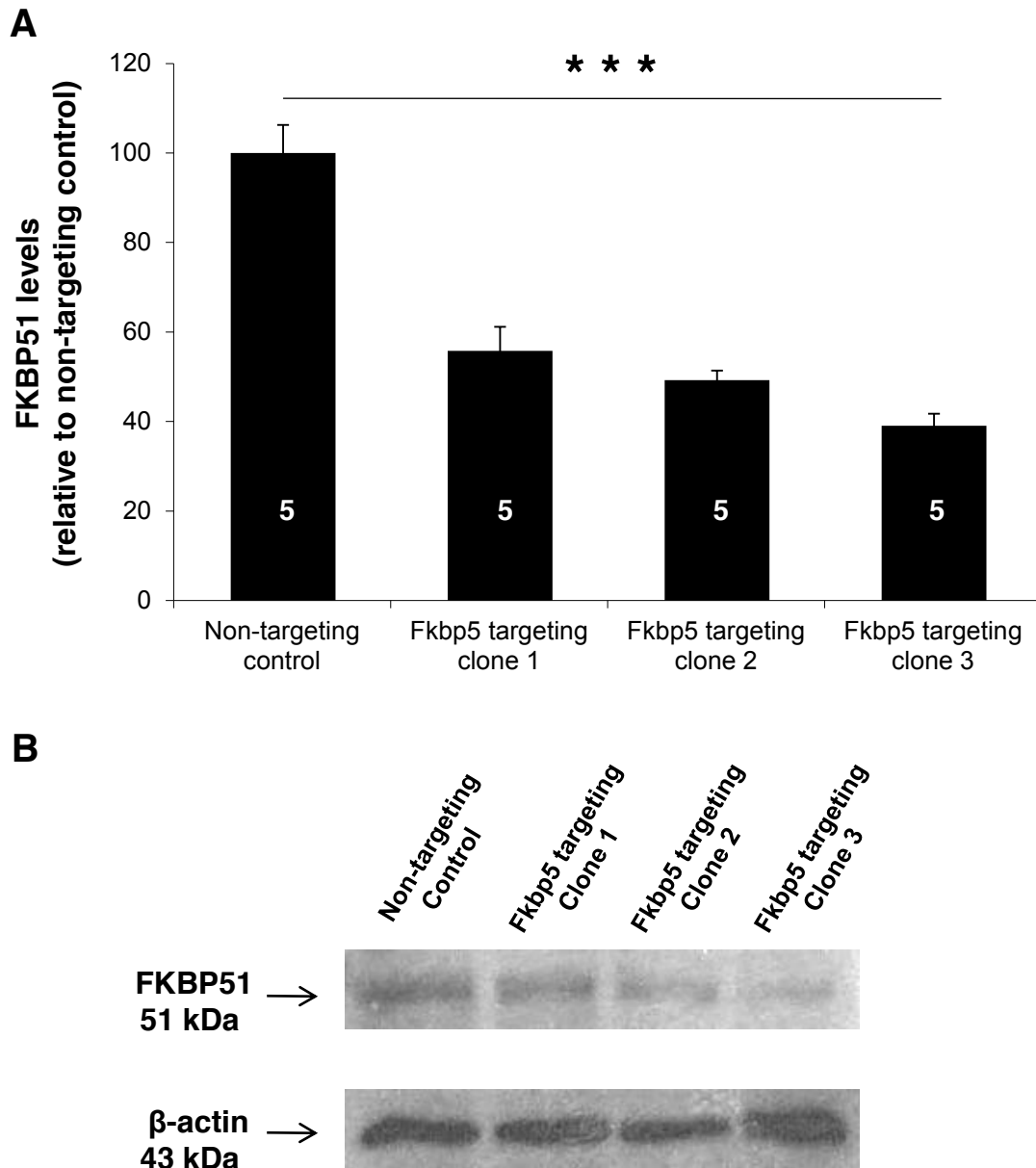


Figure 2.11 Stereotaxically injected lentivirus knockdowns FKBP51 in amygdala. FKBP51 levels in amygdala, dissected post-recovery from mice injected with non-targeting control and one of the Fkbp5 targeting clones, were measured using western blot method. (A) Amygdala homogenates in RIPA buffer were blotted for FKBP51 and normalized against actin. (B) Representative FKBP51 and actin western blots are shown for all the clones. Digits inside column indicate n. Data are shown as mean \pm s.e.m.

2.19 Elevated plus maze

The elevated-plus maze test was performed as previously described. The apparatus consisted of four non-transparent white Plexiglas arms: two enclosed arms (50 x 10 x 30 cm) that formed a cross shape with the two open arms (50 x 10 cm) opposite each other. The maze was 55 cm above the floor and dimly illuminated. Wild-type and *neuropsin*^{-/-} mice were tested 12 hours after the restraint stress. Mice were placed individually on the central platform facing an open arm, and allowed to explore the apparatus for 5 min. The maze was cleaned with 70% alcohol after each session to avoid any odorant cues. An overhead camera recorded the behaviour. The number of entries of the animal from the central platform to closed or open arms was counted.

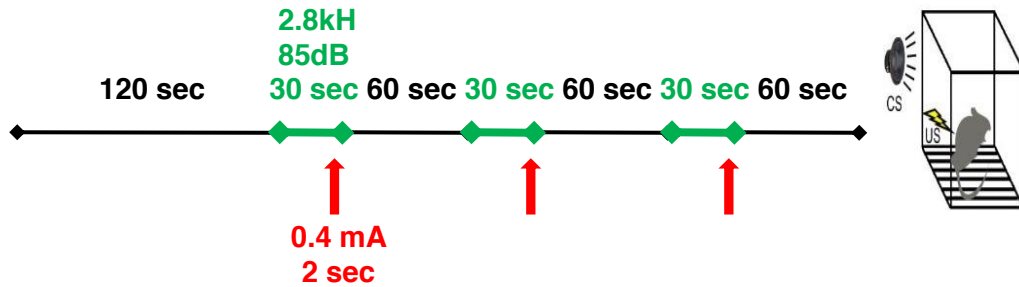
2.20 Open field

Mice were placed in a 50x50x50 cm plexiglas box and were left free to move during 10 min. The box was cleaned with 70% alcohol after each session to avoid any odorant cues. An overhead camera placed above the box recorded the session. Locomotor parameters were analysed with the ANY-MAZE software (Stoelting).

2.21 Fear conditioning

Mice were individually placed in the conditioning chamber (Coulbourn Instruments) for 2 minutes before they received three conditioned stimulus-unconditioned stimulus (CS-US) pairings (**Figure 2.12**). The last 2 seconds of the tone (CS, 30 sec, 2.8 kHz, 85dB) were paired with the footshock (US, 2 sec, 0.4mA) delivered through a grid floor. After training was completed mice remained in the conditioning chamber for one more minute and were then moved to their home cage. The next day the mice were placed back in the training chamber and freezing was monitored for 3 minutes to assess context-dependent learning. Cued-conditioning was evaluated 48h after training. The mouse was placed in a novel context (chamber with flat plexiglass floor and walls) for 2 minutes, after which the CS was delivered (2 minutes, 2.8 kHz, 85dB) and freezing was monitored. Data were analysed using FreezeView software (Coulbourn Instruments).

Day 1 Training



Day 2 Context testing



Day 3 Cued testing



Figure 2.12 Schematic diagram of the fear conditioning experimental protocol. On day 1, animals are trained to associate the tone (CS) with the electric foot shock (US). Animals are tested for contextual and cued memory on day 2 and 3 respectively. Green line indicates conditioned stimulus tone being played and red arrows indicate delivery of unconditioned stimulus foot shock. CS, Conditioned stimulus; US, Unconditioned stimulus.

2.22 miRNA microarray study

Wild-type control (n=12) and restrained stress mice (n=12) were anaesthetized intraperitoneally using sodium pentobarbital and transcardially perfused with ice-cold phosphate buffered saline (PBS). Amygdalae were isolated using a dissecting microscope in ice-cold ACSF (Glucose 25 mM, NaCl 115 mM, NaH₂PO₄ · H₂O 1.2 mM, KCl 3.3 mM, CaCl₂ 2 mM, MgSO₄ 1 mM, NaHCO₃ 25.5 mM, pH 7.4) and stored in RNAlater (Qiagen) at -20 °C until further processing. Total RNA enriched in small RNA was extracted using mirVANA kit (Applied Biosystems). RNA quantity and quality ($A_{260/280} > 1.80$) were measured using NanoDrop ND-1000 Spectrophotometer (Nanodrop Technologies). **RNA samples were sent to Febit Biomed gmbh (Germany) for miRNA expression profiling.** RNA samples were analyzed with the Geniom Realtime Analyzer (Febit Biomed gmbh) using the Geniom Biochip MPEA mus musculus (Febit Biomed gmbh) containing 7 replicates of reverse complement probes for all mature miRNAs and mature* sequences as annotated in the Sanger miRBase version 14.0 September 2009. RNA pulled from three mice was hybridized to one replicate giving a total n number of 4 samples per group. Briefly, samples were labeled with biotin using microfluidic-based enzymatic on-chip labeling of miRNAs (Vorwerk, 2008). Hybridization was performed automatically for 16 hours at 42 °C followed by automatic biochip washing and signal measurement. Signal enhancement process was combined with streptavidin-phycoerythrin detection of biotin to maximize signal sensitivity. Array images were analysed using the Geniom Wizard software (Febit Biomed gmbh). For each array, the

median signal intensity was extracted from the raw data file such that for each miRNA seven intensity values have been calculated corresponding to each replicate copy of miRNA-Base on the array. After background correction, median values were calculated from the seven replicate intensity values of each miRNA. The Febit Biomed gmbh provided a Bioinformatics report comprised of advanced microarray data analysis using R's LIMMA package including raw data, background corrected data and normalized data.

2.23 miRNA overexpression experiment

pEGP-miR vectors expressing stem loop precursor of stress-upregulated miRNAs (mmu-miR-483, mmu-miR-1192, mmu-miR-1224, mmu-miR-1892 & mmu-miR-1894-3p) and Null GFP control were purchased from Cell Biolabs as bacterial glycerol stocks. miRNA precursor cloned between BamHI and NheI sites (**Figure 2.13A**) is expressed in its native form preserving hairpin structure to ensure proper cleavage of miRNAs by endogenous processing machinery. Bacterial glycerol stock for all constructs were cultured on LB-agar plate supplemented with 100 µg/ml ampicillin, single colony picked grown in LB medium with 100 µg/ml ampicillin and plasmid DNA then extracted using Plasmid Mini Prep Columns (Qiagen). All the constructs were screened for the presence of the miRNA precursor (\approx 300bp) between BamHI and NheI sites. Following recommendation from NEB double digestion guide, plasmids were first digested with NheI (Reaction: 10 µl of plasmid; 3 µl of 10x NEBuffer II; 3 µl of 1 mg/mL BSA; 10 U of NheI enzyme and nuclease free water to yield a final

reaction volume of 30 μ l; an hour at 37°C) and subsequently with BamHI (Reaction: 30 μ l of NheI digested plasmid; final salt concentration adjusted to that of 1x NEBuffer III; 10 U of BamHI enzyme; an hour at 37°C). Non-digested, NheI digested and sequentially NheI & BamHI digested plasmids were analysed on a 1% agarose gel (**Figure 2.13B**). A band corresponding to precursor sequence was observed in sequentially digested mmu-miR-483 plasmid lanes at \approx 300bp but not in Null GFP control as expected. Similar to mmu-miR-483 plasmid, mmu-miR-1192, mmu-miR-1224, mmu-miR-1892 & mmu-miR-1894-3p plasmids also tested positive for the presence of miRNA precursor sequence (data not shown).

N2a cells cultured on polystyrene petri-dish (Nunclone, 56.7 cm²) in 10 ml medium were transiently transfected at 85-90% confluence with 16 μ g pEGP-miR constructs (Null GFP control, mmu-miR-483, mmu-miR-1192, mmu-miR-1224, mmu-miR-1892 & mmu-miR-1894-3p) and 40 μ l Lipofectamine as above. Cells were harvested 48 hours after transfection, RNA extracted using RNeasy micro kit (Qiagen), reverse transcribed and Fkbp5 mRNA levels quantified using qRT-PCR as mentioned in 2.5. Fkbp5 expression normalisation was carried out against two housekeeping genes: β -actin and glyceraldehydes-3-phosphate dehydrogenase (GAPDH), to rule out regulation of reference gene by stress-upregulated miRNAs leading to erroneous results.

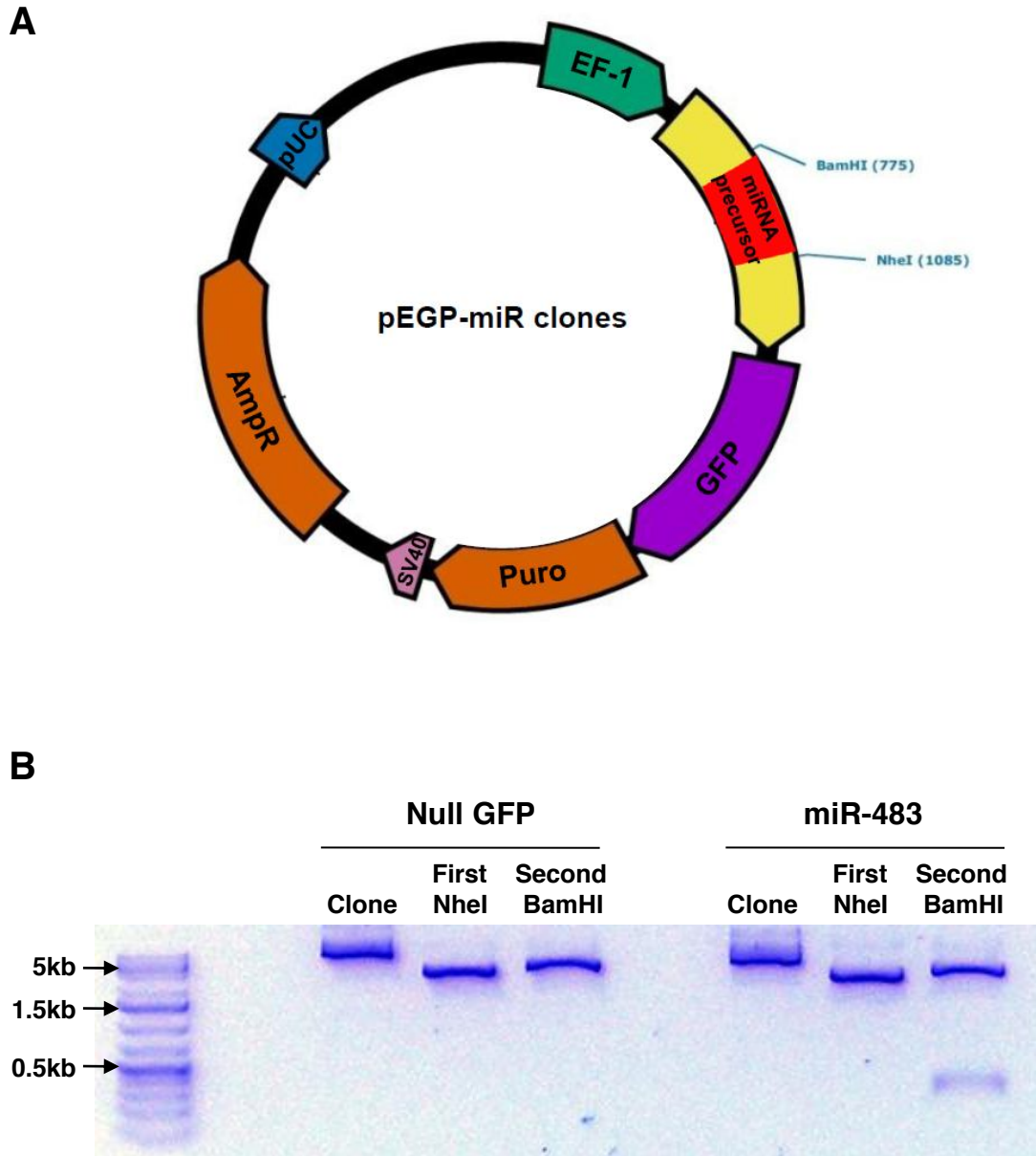


Figure 2.13 Validation of miRNA precursor expressing constructs. pEGP-miR constructs expressing stem-loop precursors of mouse miR-483, miR-1192, mir-1224, miR-1892, miR-1894-3p and null GFP were analysed for the precursor sequence cloned between NheI and BamHI sites. (A) Schematic map of miRNA precursor expressing pEGP-miR construct is shown. (B) Constructs were first digested with NheI and subsequently with BamHI and the digestion products were electrophoresed on 1% agarose gel.

2.24 Statistical Analysis

Analysis of variance (ANOVA) followed by a Tukey's post-hoc test was used for the entire study. SPSS (IBM) software was used for the statistical analysis of data. Results were considered statistically significant if the p-value was less than 0.05 ($p < 0.05$) and indicated by a star (*) on graphs. Where the p-value was less than 0.01 ($p < 0.01$) or 0.001 ($p < 0.001$) this is indicated by two (**) or three stars (***), respectively.

Chapter 3

Stress regulation of Fkbp5 in amygdala

3.1 Introduction

3.1.1 Neuropsin in synaptic plasticity

The neuropsin gene, encoding kallikrein-related endopeptidase KLK8, was first cloned from the hippocampus (Chen, 1995). Proneuropsin, the non-active precursor form of neuropsin, is constitutively present in synaptic vesicles. Various regulated and constitutive pathways trigger its extracellular release (Chen, 1995). Released proneuropsin matures to active neuropsin upon removal of the N-terminus activity masking peptide (Shimizu, 1998). Abundant expression of neuropsin in the hippocampus and amygdala neurons hinted towards its involvement in synaptic plasticity underlying learning and memory. In addition, the induction of the neuropsin gene by physiological stimuli such as long-term potentiation (LTP) and epileptogenic kindling further strengthened this hypothesis (Chen, 1995).

Indeed neuropsin, whose activation is NMDA receptor-dependent, cleaves the extracellular domain of L1-cell adhesion molecule (L1-CAM) to facilitate Schaffer-collateral LTP in the hippocampus. Blocking NMDA-dependent neuropsin activation inhibits the early phase of LTP without affecting basal synaptic transmission (Matsumoto-Miyai, 2003). In addition to the hippocampus, we have recently reported that the deletion of the neuropsin gene reduced the NMDA/AMPA current ratio in principal, basal amygdala neurons and impaired early LTP in the lateral-basal amygdala pathway

(Attwood, 2011). However, neuropsin involvement is not significant in the strong stimuli elicited late phase of LTP (Ishikawa, 2008). Synaptic tagging theory suggests that weakly stimulated synapse can capture newly synthesized proteins through synaptic tagging and convert into a persistent LTP synapse in absence of strong stimuli (Frey, 1997). This form of synaptic plasticity, crucial for non-stressful associative memory, is primarily believed to be neuropsin-dependent (Ishikawa, 2008 & 2011). Behavioural studies on neuropsin *-/-* mice complement the above electrophysiological findings. In line with neuropsin involvement in early LTP and late synaptic associativity, mice lacking neuropsin exhibit resistance to both acute and chronic stress-induced anxiety (Attwood, 2011). Hence, accumulating evidence indicate that neuropsin-mediated proteolysis facilitates neuronal plasticity at the neuron-extracellular matrix level.

3.1.2 EphB2 - NMDA clustering

Eph receptor family consists of 14 members, thus forming one of the largest groups of receptor tyrosine kinases. They interact with cell surface-bound ligands belonging to the ephrin family. Eph receptors are subdivided into two groups, EphA and EphB receptors, on the basis of extracellular domain homology and ligand preference (Arvanitis, 2008). Eph/ephrin signaling is bidirectional with both the receptors and the ligands transducing signaling events upon their interaction (Klein, 2009). Due to high expression of Eph

receptors in developing embryos their role was initially thought to be limited to neural developmental processes as an axon guidance molecule.

However during the past decade EphB2 receptor's direct interaction with NMDA channels has shifted the research focus onto their involvement in neuronal plasticity and synapse formation in the adult brain (Drescher, 2000). Extracellular domain of EphB2 interacts with NR1 subunit of the NMDA receptor after ephrinB1 treatment in neuronal cultures. EphrinB-mediated EphB2 stimulation significantly increased the density of NMDA receptor-positive synapses. The tyrosine kinase activity of EphB2, although not required for NR1 interaction, is crucial for synapse development (Dalva, 2000). EphrinB2 treatment induces EphB2 interaction with NMDA to potentiate NMDA-dependent Ca^{2+} influx, increases NR2B tyrosine phosphorylation and downstream gene expression in cortical neurons to facilitate neuronal plasticity (Takasu, 2002). EphB-NMDA clustering likely underlies the EphB/EphrinB signaling-induced, EphB kinase dependent dendritic spine formation (Penzes, 2003).

Consistent with previous findings, significantly smaller fraction of NR1 clustered with EphB receptors was found in EphB2^{-/-} mice, thus reducing synaptic NMDA currents and hippocampus LTP without affecting basal synaptic transmission and early LTP. Truncated EphB2 (devoid of the kinase activity) rescues impaired hippocampus-dependent learning of EphB2^{-/-} mice

(Henderson, 2001; Grunwald, 2001). Similarly, replenishing EphB2 in the dentate gyrus of human amyloid precursor protein transgenic mice reversed the impairment in NMDA-dependent synaptic strength and reversed the deficit in hippocampus-dependent spatial and non-spatial learning and memory assessed by Morris water maze and novel object recognition tests (Cisse, 2011). The phenotype of triple-knockout animals lacking EphB1, EphB2 and EphB3 suggested broader EphB receptors involvement in post-synaptic development. These mice displayed reduced AMPA receptor density in addition to lower NMDA clustering (Henkemeyer, 2003). Recently, a large multidomain protein Tiam1 has been shown to underlie EphB-NMDA clustering that facilitates proper synapse development. Tiam1 binds to EphB2-NMDA clusters through EphB2 (upon EphrinB stimulation) resulting in Rac-dependent actin remodeling crucial for dendritic spine formation (Tolias, 2005 & 2007).

An important aspect of EphB2 signaling is its modulation by extracellular proteases (Lin, 2008). Upon acute restraint stress neuropsin cleaves extracellular domain of EphB2 disrupting its interaction with NMDA receptors (Attwood, 2011). Higher membrane EphB2 protein levels in neuropsin^{-/-} mice together with a compensatory EphB2 gene upregulation in wild-type mice after stress are indicative of stress-induced EphB2 membrane trafficking. Consequently, stress increases the dynamics of EphB2-NR1 interaction resulting in enhanced NMDA receptor activity. Importantly, bilateral intra-amygdala injections of anti-EphB2 antibody into wild-type mice blocked the stress-triggered neuropsin

cleavage of EphB2 and recapitulated the stress-resistant phenotype observed in neuropsin^{-/-} mice (Attwood, 2011). Thus, extracellular neuropsin modulates EphB2-NMDA interaction to regulate synaptic plasticity and its behavioural consequences.

3.1.3 Stress molecule Fkbp5

Resistance of neuropsin^{-/-} mice to stress-induced anxiety, as measured in the elevated plus maze (Attwood, 2011), encouraged us to investigate the molecular mechanisms underlying their anxiolytic phenotype. Our microarray analysis approach identified Fkbp5 as amygdalar molecule showing differential upregulation in wild-type and neuropsin^{-/-} mice following stress. Therefore, I aimed to confirm our microarray findings using qRT-PCR in this chapter. Further, dissecting out the pathway underlying differential Fkbp5 regulation, we hypothesized that stress-triggered cleavage of EphB2 by neuropsin resulting in NMDA activation may drive Fkbp5 expression.

3.2 Results

Fkbp5 has been implicated in stress-related psychiatric disorders (Binder, 2009). Additionally, our microarray approach revealed differential Fkbp5 regulation in amygdala of neuropsin^{-/-} (NP^{-/-}) and wild-type (NP^{+/+}) mice (Attwood, 2011). We first aimed to confirm differential amygdalar Fkbp5 regulation in naïve and stressed wild-type and neuropsin^{-/-} mice. qRT-PCR confirmed genotype-dependent differences not only in basal but also in stress-induced regulation of the Fkbp5 gene in the amygdala (**Figure 3.1**; Two-way ANOVA; genotype effect $F_{(1,12)} = 10.281$, $p = 0.008$; stress effect $F_{(1,12)} = 181.249$, $p < 0.0001$; genotype \times stress interaction $F_{(1,12)} = 24.62$, $p < 0.0001$). Stress-induced Fkbp5 upregulation was attenuated in neuropsin^{-/-} mice (NP^{+/+} stress vs NP^{-/-} stress, $p < 0.001$) despite of their higher basal Fkbp5 levels (NP^{+/+} control vs NP^{-/-} control, $p < 0.05$). In contrast to 20-fold upregulation in wild type mice (NP^{+/+} control vs NP^{+/+} stress, $p < 0.001$), Fkbp5 was only 10-fold upregulated in neuropsin^{-/-} mice following 6 hours of restraint stress (NP^{-/-} control vs NP^{-/-} stress, $p < 0.001$).

Importantly, recombinant neuropsin injected into the basolateral complex of the amygdala rescued attenuated Fkbp5 upregulation in stressed neuropsin^{-/-} mice (**Figure 3.2**; Two-way ANOVA; genotype effect $F_{(1,14)} = 5.014$, $p = 0.042$; stress effect $F_{(1,14)} = 16.241$, $p = 0.001$; genotype \times stress interaction $F_{(1,14)} = 5.154$, $p = 0.04$).

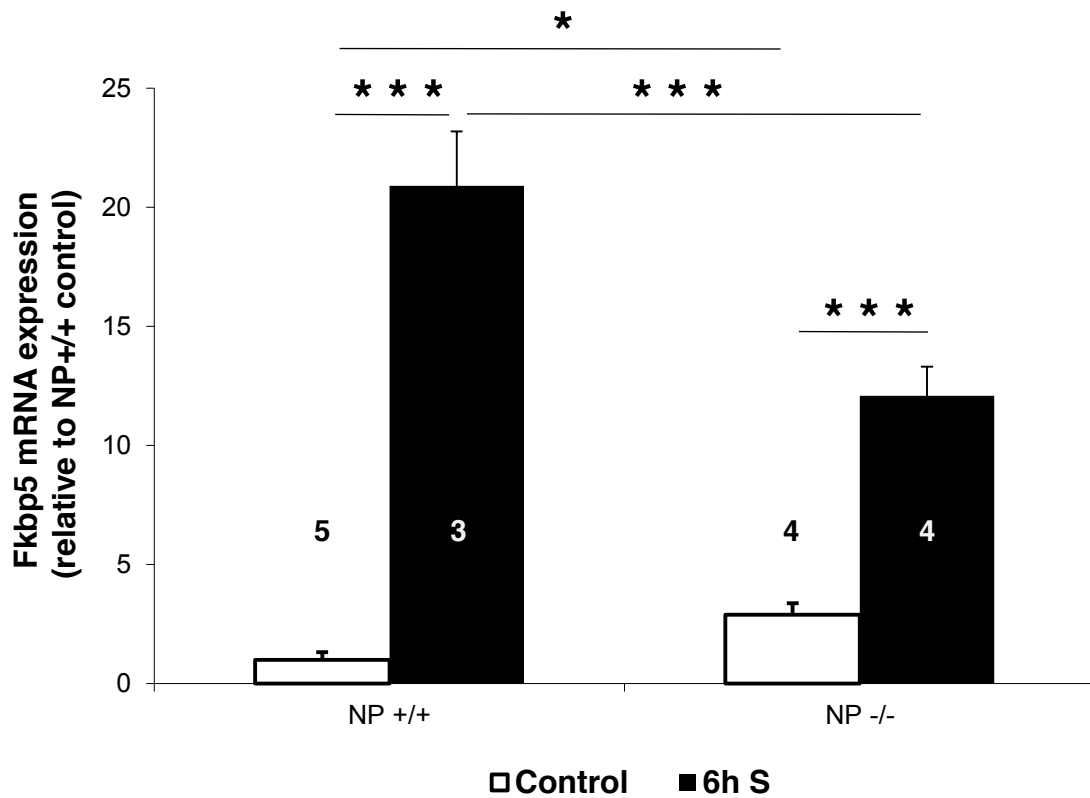


Figure 3.1 Stress-induced Fkbp5 upregulation is attenuated in neuropsin -/- mice. Fkbp5 transcript levels were measured in amygdala dissected from naïve and restraint stressed neuropsin+/+ and neuropsin -/- mice using qRT-PCR. Digits inside column indicate n. Data are shown as mean \pm s.e.m. NP, neuropsin; 6h S, 6 hours stress.

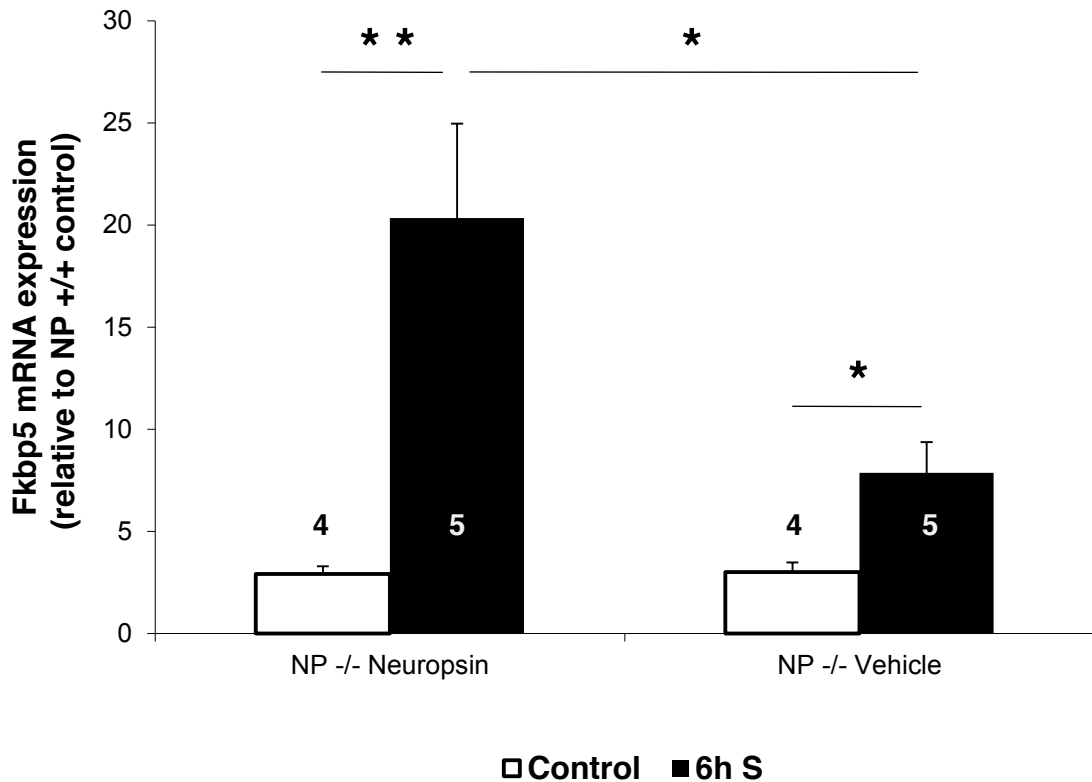


Figure 3.2 Intra-amygdala neuropeptide injection rescues attenuated Fkbp5 upregulation in neuropeptide-/- mice. Neuropeptide-/- mice were implanted with cannula aiming at basolateral complex of amygdala. Post recovery period, mice were injected with either vehicle or 50 nM recombinant neuropeptide in 1 μ l final volume followed by 6 hours of restraint stress in transparent plexiglass tubes. Amygdala was dissected from vehicle and neuropeptide injected naïve and stressed neuropeptide -/- mice and analysed for Fkbp5 mRNA levels using qRT-PCR. Digits inside column indicate n. Data are shown as mean \pm s.e.m. NP, neuropeptide; 6h S, 6 hours stress.

Neuropsin^{-/-} mice injected with exogenous neuropsin showed stress-induced Fkbp5 upregulation equivalent to that of wild-type mice (NP^{-/-} NP control vs NP^{-/-} NP stress, $p < 0.01$) whereas vehicle-injected stressed neuropsin^{-/-} mice still displayed the attenuation (NP^{-/-} vehicle control vs NP^{-/-} vehicle stress, $p < 0.05$; NP^{-/-} NP stress vs NP^{-/-} vehicle stress, $p < 0.05$). These findings confirmed the existence of neuropsin-dependent Fkbp5 regulatory pathways in the amygdala.

A large number of studies have identified Fkbp5 as a transcriptional target of GCs as discussed in chapter 1.5 (Jaaskelainen, 2011). Consistent with this we have found a well-conserved GRE located on the CpG island upstream of the transcription start site in the promoter region of Fkbp5 (Attwood, 2011). Thus, we wondered if corticosterone levels could underlie the differential Fkbp5 regulation in naïve and stressed wild type and neuropsin^{-/-} mice. Corticosterone enzyme-linked immunoassay confirmed dramatic elevations in plasma corticosterone levels of wild-type and neuropsin^{-/-} mice stressed for 30 minutes (**Figure 3.3; Table 3.1**; Two-way ANOVA; genotype effect $F_{(1,32)} = 2.743$, $p = 0.107$; stress effect $F_{(3,32)} = 358.48$, $p < 0.0001$; genotype \times stress interaction $F_{(3,32)} = 0.304$, $p = 0.822$). Corticosterone levels remained elevated in stressed mice after 90 minutes of recovery but had returned to baseline after 6 hours of recovery. However, neither basal nor stress-elevated corticosterone levels significantly differed between the genotypes indicating that the neuropsin-dependent component of Fkbp5 activation is independent of corticosterone levels.

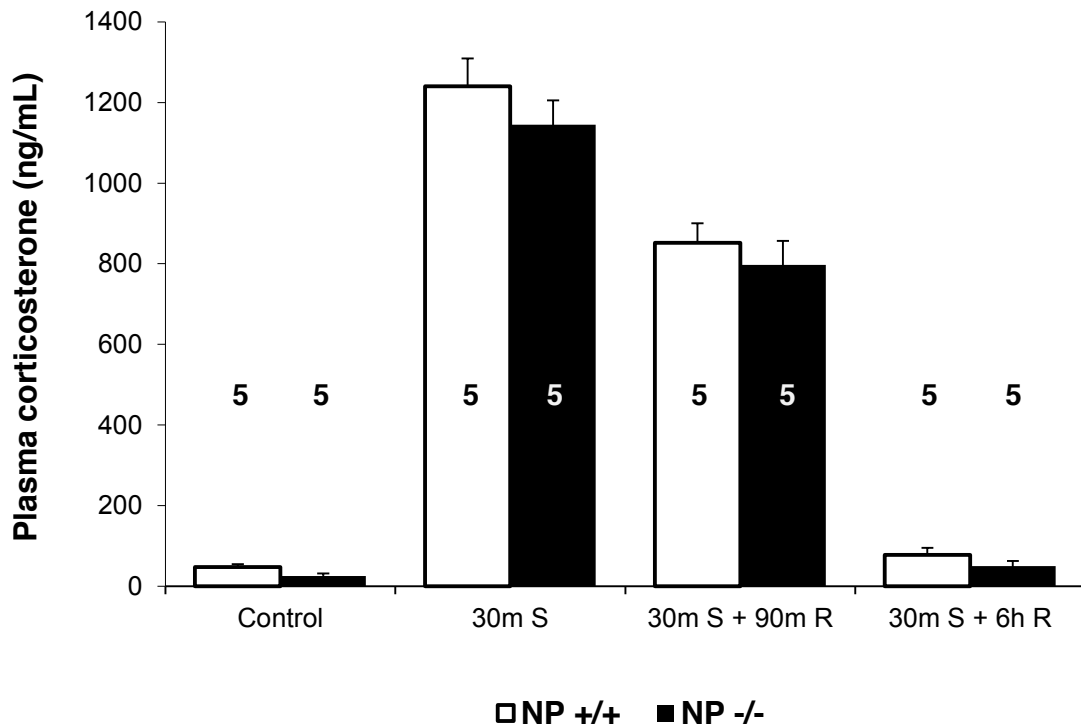


Figure 3.3 Differential Fkbp5 upregulation in neuropsin^{+/+} and neuropsin^{-/-} mice is independent of corticosterone. (A) Plasma corticosterone levels of neuropsin^{+/+} and neuropsin^{-/-} mice, subjected to no stress and 30 minutes of stress followed by various duration of recovery period, were measured using corticosterone enzyme immunoassay. Digits inside column indicate n. Data are shown as mean \pm s.e.m. NP, neuropsin; 30m S, 30 minutes stress; 90m R, 90 minutes recovery; 6h R, 6 hours recovery.

Table 3.1 Plasma corticosterone levels: Tukey's post-hoc results

Compared groups	p value
WT Control vs WT 30m S	p < 0.001
WT Control vs WT 30m S 90m R	p < 0.001
WT Control vs WT 30m S 6h R	p > 0.05
WT Control vs NP-/- control	p > 0.05
WT 30m S vs WT 30m S 90m R	p < 0.001
WT 30m S vs WT 30m S 6h R	p < 0.001
WT 30m S vs NP-/- 30m S	p > 0.05
WT 30m S 90m R vs WT 30m S 6h R	p < 0.001
WT 30m S 90m R vs NP-/- 30m S 90m R	p > 0.05
WT 30m S 6h R vs NP-/- 30m S 6h R	p > 0.05
NP-/- control vs NP-/- 30m S	p < 0.001
NP-/- control vs NP-/- 30m S 90m R	p < 0.001
NP-/- control vs NP-/- 30m S 6h R	p > 0.05
NP-/- 30m S vs NP-/- 30m S 90m R	p < 0.001
NP-/- 30m S vs NP-/- 30m S 6h R	p < 0.001
NP-/- 30m S 90m R vs NP-/- 30m S 6h R	p < 0.001

NP-/-, neuropsin-/-; 30m S, 30 mins stress; 90m R, 90 mins recovery; 6h R, 6 hours recovery

Extracellular serine protease neuropsin does not co-localise with the intracellular FKBP51 and therefore is unlikely to regulate the Fkbp5 gene expression directly. But stress-activated neuropsin cleaves the membrane bound tyrosine kinase EphB2 receptor in amygdala potentiating its interaction with the NMDA receptor (Attwood, 2011). EphB2 receptors modulate calcium influx through the NMDA channels to regulate gene expression; importantly interference with the EphB2 signaling has been previously linked to the regulation of Fkbp5 expression (Takasu, 2002; Genander, 2009). Therefore we hypothesized that neuropsin-mediated cleavage of EphB2 following stress promotes EphB2 interaction with NMDA receptor to regulate Fkbp5 expression. To study the effect of EphB2 cleavage by neuropsin on Fkbp5 expression we used an antibody raised against the extracellular portion of EphB2 to block the neuropsin cleavage of EphB2 in primary cultures of amygdala neurons. As shown in **Figure 3.4A** ($F_{(4,29)} = 19.04, p < 0.0001$; One-way ANOVA; **Table 3.2**), corticosterone and neuropsin had an additive effect inducing much higher upregulation in Fkbp5 compared to corticosterone alone. Anti-EphB2 antibody only blocked the neuropsin-dependent component of Fkbp5 upregulation. Anti-EphB2 antibody neither had any effect on its own nor affected the corticosterone-dependent Fkbp5 upregulation. Further, NMDA receptor stimulation mimicked the neuropsin-mediated upregulation in Fkbp5 expression (**Figure 3.4B**; One-way ANOVA; $p < 0.05$).

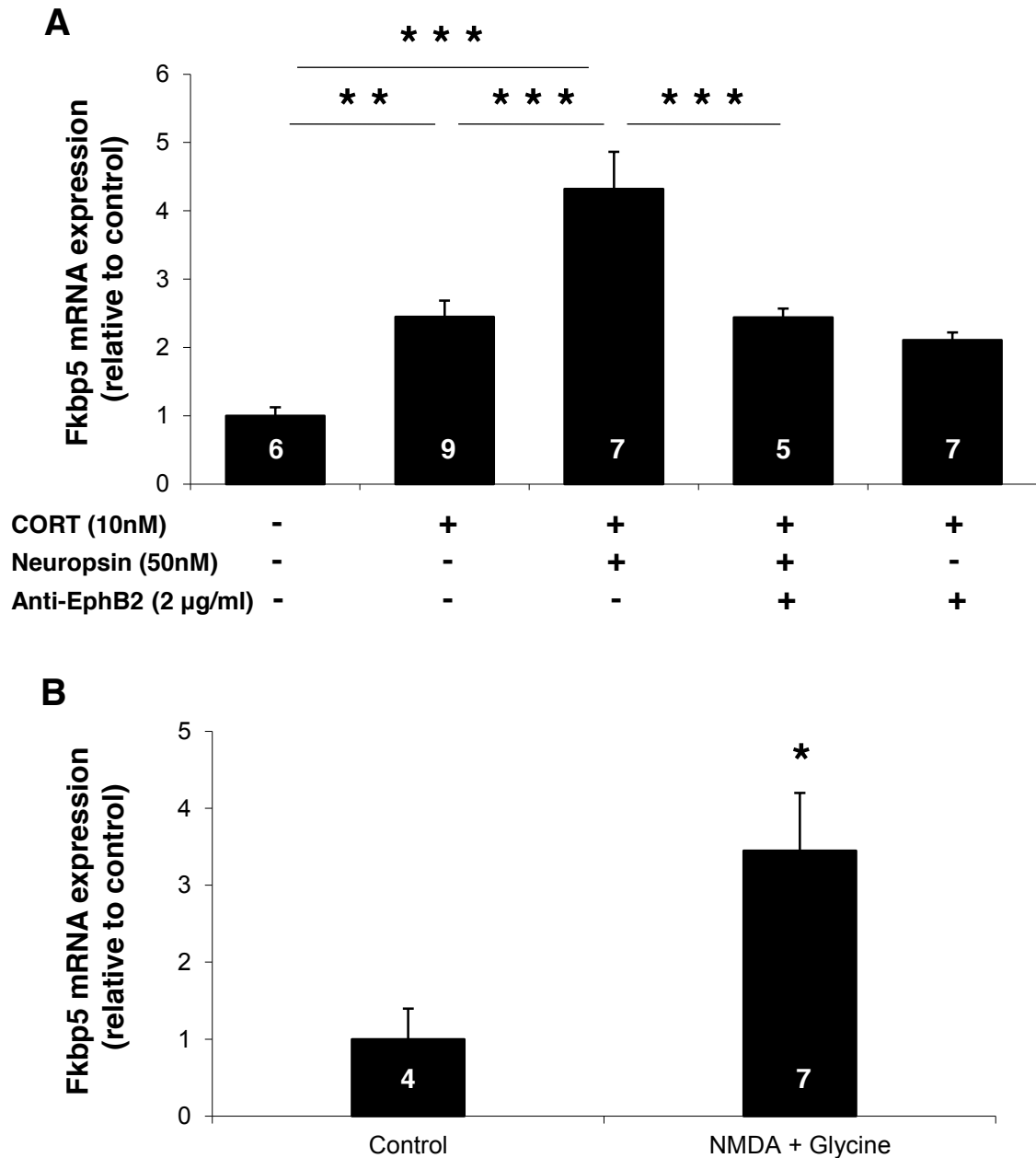


Figure 3.4 Anti-EphB2 antibody blocks and NMDA receptor agonist mimicks neuropsin-dependent Fkbp5 upregulation. Fkbp5 mRNA expression was measured using qRT-PCR in amygdala neurons treated for 6 hours with (A) vehicle, CORT + neuropsin, CORT + anti-EphB2 + neuropsin, CORT + anti-EphB2 and (B) 100 µM NMDA agonist + 10 µM glycine. EphB2 groups were treated with 2 µg/ml anti-EphB2 antibody 10 minutes before the experiment. Digits inside column indicate n. Data are shown as mean ± s.e.m. CORT, corticosterone; Anti-EphB2, Anti-EphB2 antibody; NMDA, NMDA receptor agonist.

Table 3.2 Fkbp5 expression in amygdala neurons: Tukey's post-hoc results

Compared groups	p value
control vs CORT	p < 0.01
control vs CORT + NP + EphB2	p < 0.01
control vs CORT + NP	p < 0.001
control vs CORT + EphB2	p < 0.05
CORT vs CORT + NP + EphB2	p > 0.05
CORT vs CORT + NP	p < 0.001
CORT vs CORT + EphB2	p > 0.05
CORT + NP vs CORT + NP + EphB2	p < 0.001
CORT + EphB2 vs CORT + NP + EphB2	p > 0.05
CORT + NP vs CORT + EphB2	p < 0.001

CORT, corticosterone; NP, neuropsin; EphB2, anti-EphB2 antibody

Thus, neuropsin cleaved EphB2 and stimulated NMDA to increase the Fkbp5 gene expression. Neuropsin-dependent mechanism acts in synergy with corticosterone-dependent mechanism to regulate Fkbp5 expression in the amygdala.

3.3 Discussion

High Fkbp5 levels have previously been associated with the propensity towards the development of stress-related psychiatric disorders (Binder, 2009). Intrigued by the stress-resistant phenotype of neuropsin-deficient mice, we conducted a microarray study that identified Fkbp5 as a molecule showing differential regulation in neuropsin^{-/-} mice. We confirmed these differences in basal and stress-induced expression of the Fkbp5 gene in the amygdala using qRT-PCR.

Restraint stress activates the HPA axis, elevating plasma corticosterone levels that accompany a robust, stress-induced Fkbp5 upregulation in wild-type mice amygdala. Complementary bioinformatics analysis of the Fkbp5 promoter region revealed the presence of a highly conserved glucocorticoid-binding site upstream of the transcription start site (Attwood, 2011). Steroid-occupied distal intronic GREs interact with the transcription machinery to induce Fkbp5 transcription via long-range activation (Makkonen, 2009; Paakinaho, 2010). Altered methylation pattern of CpGs in Fkbp5 promoter and intron 5 region by GCs have also been shown to increase Fkbp5 expression (Lee, 2010 & 2011). Hence our findings are consistent with Fkbp5 being a transcriptional target of GCs (Jaaskelainen, 2011).

Similar to neuropsin^{-/-} mice, mouse model of Rett syndrome lacking MeCP2 protein also exhibited higher basal Fkbp5 levels (Urduingio, 2008). Higher basal

Fkbp5 expression in *neuropsin*^{-/-} mice is not due to differences in resting plasma corticosterone levels (**Figure 3.3**). Surprisingly, despite equivalent elevations in corticosterone levels, *neuropsin*^{-/-} mice displayed attenuated Fkbp5 upregulation compared to stressed wild-type mice. Indicating *neuropsin*-dependent Fkbp5 upregulation following stress is independent of corticosterone. Similar glucocorticoid-independent Fkbp5 elevation has been described in MeCP2-deficient mice in which neither resting nor stress-elevated corticosterone levels differed from wild-type animals. MeCP2 binds to the methylated CpGs in the Fkbp5 genomic sequence and these CpGs are not demethylated by corticosterone treatment (Nuber, 2005). Thus, Fkbp5 shows epigenetic regulation independent of GCs that might potentially be modulated by *neuropsin*.

Extracellular serine protease *neuropsin* cleaves extracellular domain of tyrosine kinase EphB2 receptor following acute stress. Cleaved EphB2 dissociates from the NR1 subunit of the NMDA receptor and the phenomenon is accompanied by more frequent membrane insertions of new EphB2 receptors, thus increasing the dynamics of the EphB2-NR1 interaction (Attwood, 2011). Blocking EphB2 cleavage in the amygdala neurons with an anti-EphB2 antibody inhibits only *neuropsin*-dependent, but not the corticosterone-dependent, increase in Fkbp5 expression (**Figure 3.4A**). EphB2/NMDA association results in the increased transcription of plasticity-related genes (Takasu, 2002). Consistent with the above, NMDA receptor stimulation also mimicked the increase in Fkbp5

expression (**Figure 3.4B**). The differences in the regulation of Fkbp5 levels in response to stress between wild-type and neuropsin^{-/-} mice are consistent with the reduction of NMDA/AMPA current ratio in the pyramidal amygdala neurons in neuropsin^{-/-} mice (Attwood, 2011). Calcium influx through NMDA receptor leads to dissociation of MeCP2 from the BDNF gene promoter inducing its transcription (Chen, 2003; Martinowich, 2003). Therefore we speculate that neuropsin regulation of Fkbp5 might be epigenetic and involve NMDA-mediated separation of MeCP2 from the Fkbp5 genomic regions. This hypothesis is currently being tested experimentally.

Stress-induced Fkbp5 upregulation is attenuated in neuropsin^{-/-} mice amygdala compared to wild type mice (**Figure 3.1**). The magnitude of Fkbp5 upregulation in peripheral blood mononuclear cells at the time of trauma positively predicts development of PTSD in human subjects (Segman, 2005). Thus, attenuated Fkbp5 upregulation in neuropsin^{-/-} mice following stress could underlie their resistance to stress-mediated behavioural alterations. Importantly, recombinant neuropsin injected into the amygdala of neuropsin^{-/-} mice rescued the attenuation of stress-induced Fkbp5 upregulation and restored the anxiolytic behavioural phenotype of neuropsin^{-/-} mice towards normal (Attwood, 2011). Thus, our findings suggest the extent of Fkbp5 upregulation following stress may determine the behavioural manifestations of stress-mediated anxiety.

Chapter 4

Stress regulation of FKBP51 in amygdala

4.1 Introduction

Hsp90 co-chaperones FKBP51 and FKBP52 are dynamically active and show both cytoplasmic and nuclear localization in most cell lines. Quinta and colleagues observed that neuroblastoma N2a cell differentiation by FK506 involved FKBP52 replacement by FKBP51 in the transcriptionally active perinuclear domains and FKBP52 redistribution to the growth cones of growing neurites (Quinta, 2010). In GR signalling, cytoplasmic FKBP51 poorly interacts with dynein rendering the GR complex in cytoplasm (Tatro, 2009). Homologous FKBP52, unlike FKBP51, efficiently interacts with dynein/dynactin triggering nuclear translocation of the FKBP52 bound GR complex (Davies, 2002). Hence Hsp90 co-chaperones undergo function-specific dynamic subcellular rearrangements.

Stress-induced *Fkbp5* upregulation is attenuated in *neuropsin*^{-/-} mice amygdala compared to wild type mice (**Figure 3.1**). Therefore this chapter primarily aimed to study correlation between stress-induced *Fkbp5* gene and FKBP51 protein expression in the amygdala of wild type and *neuropsin*^{-/-} mice. Other aims included understanding previously unexplored aspects of amygdalar FKBP51 physiology in GR signaling. Hence, experiments intended to investigate the fate of FKBP51 replaced by FKBP52 upon steroid binding and interacting partners of nuclear FKBP51 to dissect its precise function in GR signaling.

4.2 Results

Following the *Fkbp5* studies, in order to characterize the differential biological response to stress more comprehensively amygdalar FKBP51 levels in control and stressed wild type and neuropsin^{-/-} mice were quantified using western blotting (**Figure 4.1**; Two-way ANOVA; genotype effect $F_{(1,14)} = 0.486$, $p = 0.497$; stress effect $F_{(1,14)} = 10.456$, $p = 0.006$; genotype \times stress interaction $F_{(1,14)} = 5.432$, $p = 0.035$). Stress upregulated FKBP51 levels in wild type mice by almost 2-fold (NP^{+/+} control vs NP^{+/+} stress, $p < 0.001$) whereas FKBP51 levels remained unchanged in neuropsin^{-/-} mice amygdala (NP^{-/-} control vs NP^{-/-} stress, $p > 0.05$). Two-way ANOVA showed significant effect of genotype \times stress interaction on FKBP51 expression despite no effect of genotype on its own. Hence, similar to *Fkbp5* gene, FKBP51 protein expression is also differentially regulated between both the genotypes after stress.

FKBP51, in its constitutive state, is bound to the GR-complex in the cytosol through Hsp90 (Sinars, 2003). To investigate FKBP51 regulation in the limbic system we first examined its expression in the amygdala neurons. Immunohistochemistry revealed that FKBP51 is abundantly expressed in the basolateral amygdala (**Figure 4.2**).

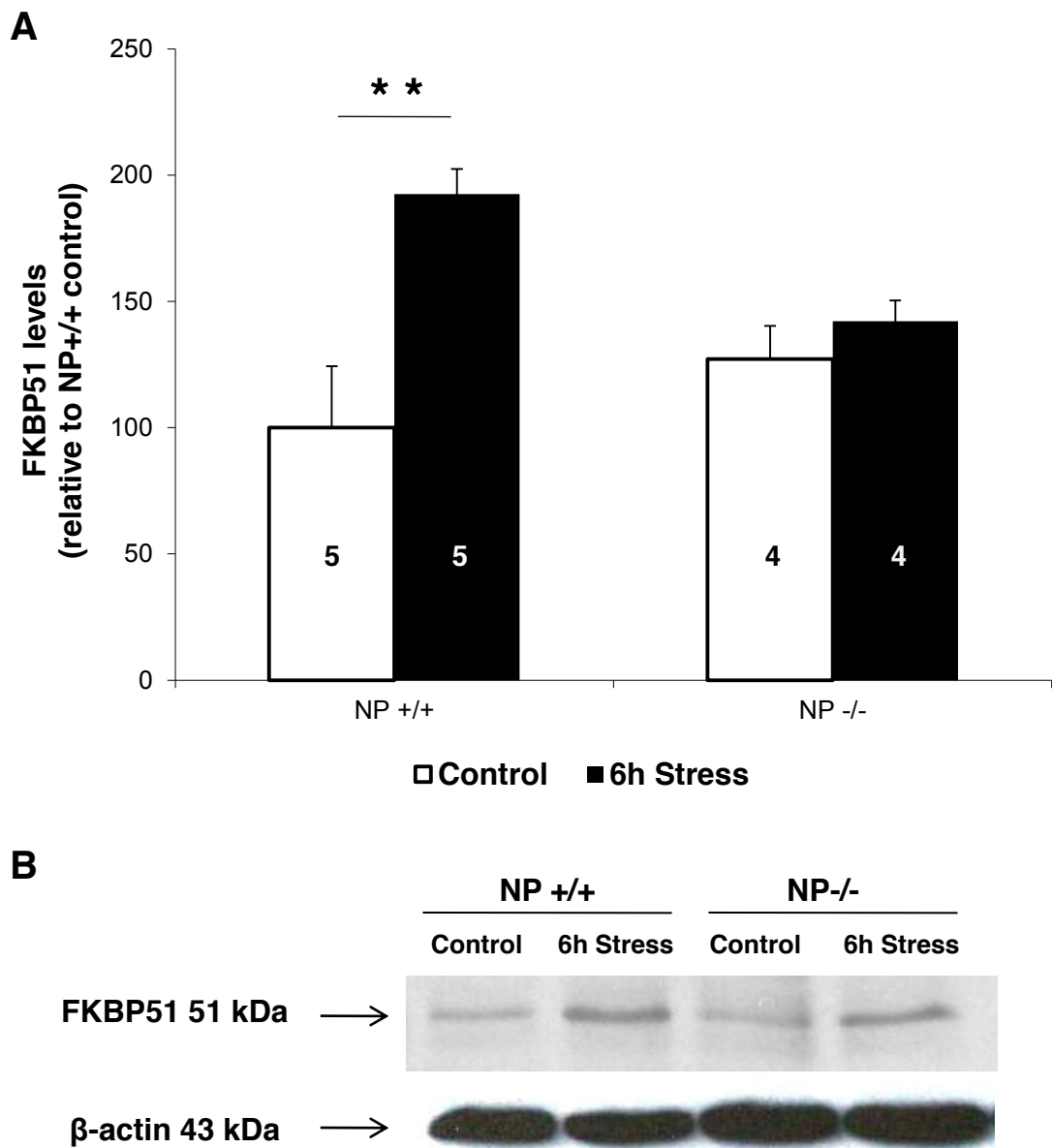


Figure 4.1 FKBP51 is stress-upregulated in neuropsin+/+ mice but not in neuropsin-/- mice. Amygdala was dissected from naïve and 6 hours stressed neuropsin+/+ and neuropsin-/- mice and homogenised in RIPA buffer. (A) Homogenates were blotted for FKBP51 and normalized against actin to measure stress-induced FKBP51 levels in both the genotypes. (B) Representative FKBP51 and actin western blots are shown for all the groups. Digits inside column indicate n. Data are shown as mean \pm s.e.m. NP, neuropsin; 6h Stress, 6 hours stress.

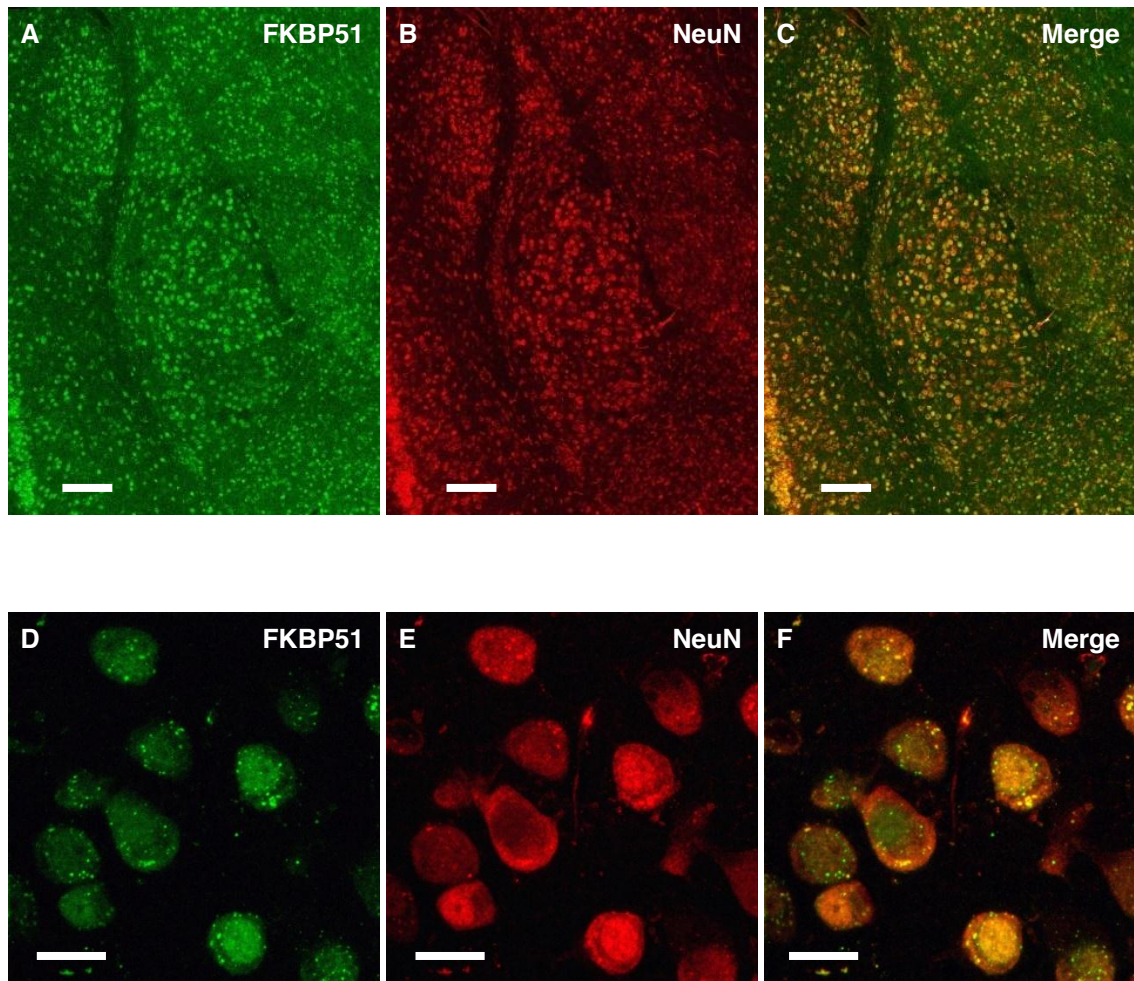


Figure 4.2 FKBP51 displays cytoplasmic and nuclear distribution in the amygdala neurons. Paraformaldehyde-fixed whole mice brains were cut to get free-floating 70 μm thick sections on vibratome. Sections were double stained for FKBP51 (A, D) and neuronal marker NeuN (B, E). Low (upper panel; scale bar, 200 μm) and high magnification (lower panel; scale bar, 20 μm) images were taken using a Zeiss confocal microscope. Merged images (C, F) revealed the majority of FKBP51 positive cells co-localised with NeuN in the amygdala.

Higher magnification (63x oil objective, lower panel) showed that FKBP51 immunoreactivity is present in the cytosol as well as the nucleus. In order to determine the FKBP51 expressing cell type, we performed double labelling for FKBP51 and neuronal nuclear marker NeuN. Merged images revealed a high degree of co-localization between NeuN and FKBP51 confirming neuronal phenotype of FKBP51 positive cells. Control sections labelled with only secondary antibodies failed to show any staining in the amygdala (data now shown).

Stimuli-dependent function specific transition between cellular compartments is a remarkable feature of Hsp90 immunophilins. For instance, upon treatment with immunosuppressive drug FK506, FKBP51 replaces FKBP52 in the perinuclear structures and suppresses neurite outgrowth in differentiating N2a cells (Quinta, 2010). To determine if FKBP51 undergoes subcellular rearrangement following stress, we determined the cytoplasmic and nuclear FKBP51 levels in wild type mice amygdala after 6 hours of stress with or without recovery using western blot. Amygdala tissue was fractionated to get four fractions rich in cytosol, membrane, nuclear and cytoskeletal proteins using a Subcellular Fractionation Kit (Perkin Elmer). Western blotting found markers calpain, EphA4, CREB and vimentin only in cytosol, membrane, nuclear and cytoskeletal protein rich fractions, respectively, confirming their purity (**Figure 4.3C**). Cytosol, membrane and cytoskeletal fractions in equal amounts constituted the cytoplasmic fraction.

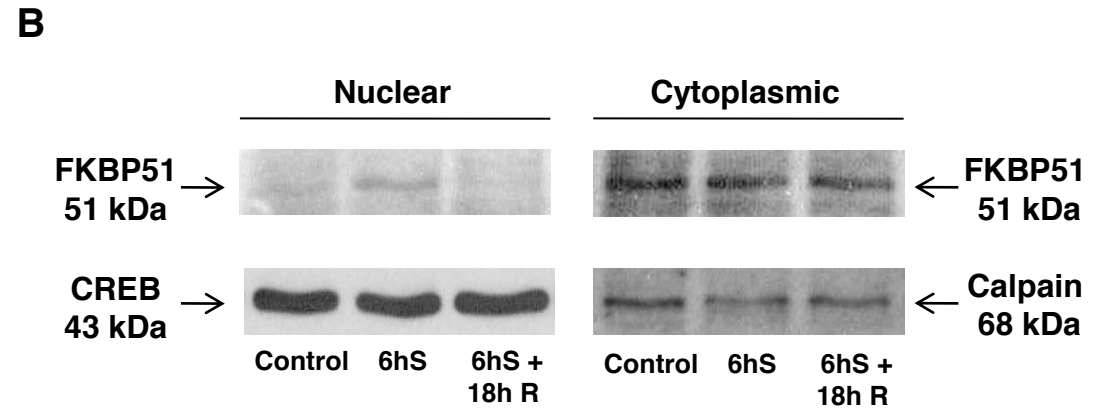
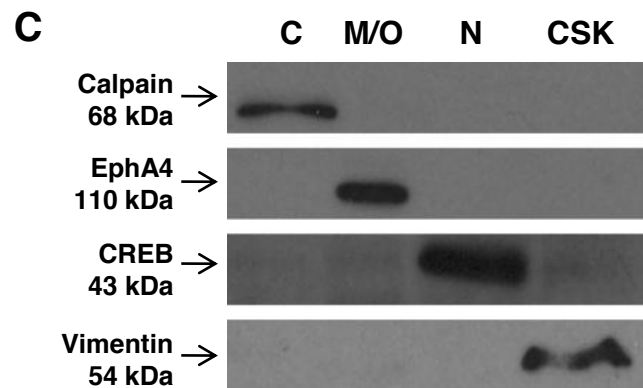
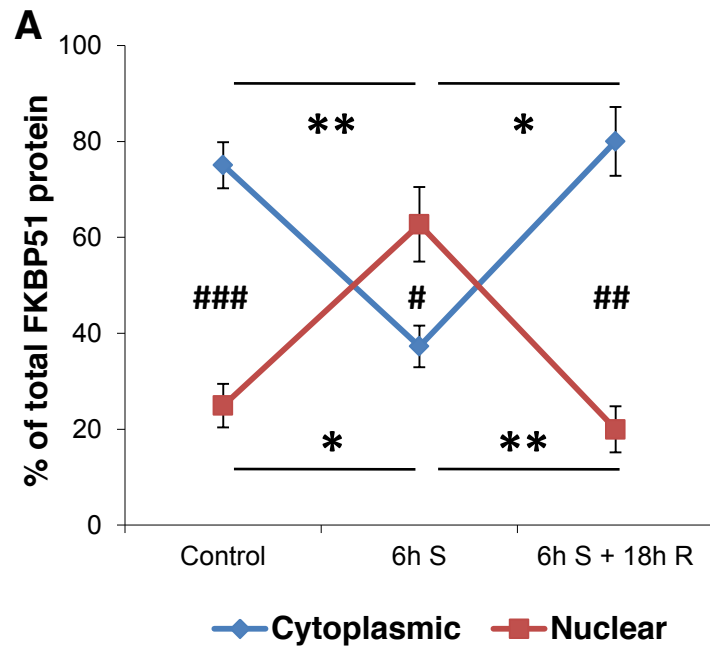


Figure 4.3 Stress triggers FKBP51 nuclear translocation in amygdala. Wild type mice underwent stress and stress followed by recovery period. Amygdalae were dissected and fractionated using subcellular fractionation kit. (C) Western blotting revealed presence of markers calpain, EphA4, CREB and vimentin only in cytosol, membrane, nuclear and cytoskeletal fractions, respectively, confirming purity of all fractions. (A) Total FKBP51 levels were measured by blotting cytoplasmic and nuclear fractions for FKBP51 and normalising to their respective markers calpain and CREB. FKBP51 levels in both fractions are shown as percentage of total FKBP51. (B) Representative cytoplasmic and nuclear fraction blots for FKBP51 and markers are shown. Data are shown as mean \pm s.e.m (n=6). *, intra-fraction significance; #, inter-fraction significance; 6h S, 6 hours stress; 6h S + 18h R, 6 hours stress followed by 18 hours recovery; C, cytosol; M/O, membrane/organelle; N, nuclear; CSK, cytoskeletal.

One-way ANOVA revealed a significant effect of stress on cytoplasmic and nuclear FKBP51 levels, depicted as percentage of the total FKBP51 (cytoplasmic + nuclear) detected (**Figure 4.3A & B; Table 4.1**; $F_{(5,30)} = 8.049$, $p < 0.0001$; One-way ANOVA). Under basal condition significantly large fraction of FKBP51 was present in the cytoplasm and a tiny amount in the nucleus as expected. But much to our surprise, FKBP51 undergoes cellular reshuffling after 6 hours of stress in the amygdala with simultaneous decline in cytoplasmic and elevation in nuclear FKBP51 levels. The basal FKBP51 localisation was restored after 18 hours of recovery. Hence, FKBP51 translocates to the nucleus following 6 hours of restraint stress in amygdala.

Table 4.1 FKBP51 nuclear translocation in amygdala: Tukey's post-hoc results

Compared groups	p value
Cyto Control vs Cyto 6h S	$p < 0.01$
Cyto Control vs Cyto 6h S 18h R	$p > 0.05$
Cyto Control vs Nucl control	$p < 0.001$
Cyto 6h S vs Cyto 6h S 18h R	$p < 0.05$
Cyto 6h S vs Nucl 6h S	$p < 0.05$
Cyto 6h S 18h R vs Nucl 6h S 18 R	$p < 0.01$
Nucl control vs Nucl 6h S	$p < 0.05$
Nucl control vs Nucl 6h S 18 R	$p > 0.05$
Nucl 6h S vs Nucl 6h S 18 h R	$p < 0.01$

Cyto, cytoplasm; Nucl, nuclear; 6h S, 6 hours stress; 6h S 18h R, 6 hours stress 18 hours recovery

To confirm stress-induced nuclear translocation of FKBP51 *in vitro*, Fkbp5 cDNA was cloned into mammalian pEGFP-N1 vector to express GFP-tagged FKBP51. N2a cells transiently transfected for 48 hours with Fkbp5-GFP construct were treated with dexamethasone for 6 hours followed by no recovery or 18 hours of recovery period. Cells were imaged at 63x magnification for GFP-tagged FKBP51 using confocal microscope to study the effect of dexamethasone treatment on FKBP51 cellular localisation. Untreated cells exhibited significantly more cytoplasmic GFP signal. In contrast, strong GFP signal was observed in the nucleus after 6 hours of dexamethasone treatment. The GFP signal was similar to untreated cells after 18 hours of wash following 6 hours of dexamethasone treatment (**Figure 4.4A**). Quantification of cytoplasmic and nuclear GFP signal intensity presented as percentage of total GFP intensity (cytoplasmic + nuclear) for each cell revealed that dexamethasone treatment induces nuclear concentration of FKBP51 and basal FKBP51 distribution is restored after 18 hours of recovery period (**Figure 4.4B; Table 4.2; $F_{(5,4428)} = 2161.4, p < 0.0001$; One-way ANOVA**). Hence, dexamethasone in N2a cells promotes FKBP51 cellular localisation pattern identical to the pattern that emerges in amygdala following 6 hours of restraint stress. Together, both experiments strengthen the finding that following dissociation from the GRC, FKBP51 translocates to the nucleus and returns to basal distribution post recovery period.

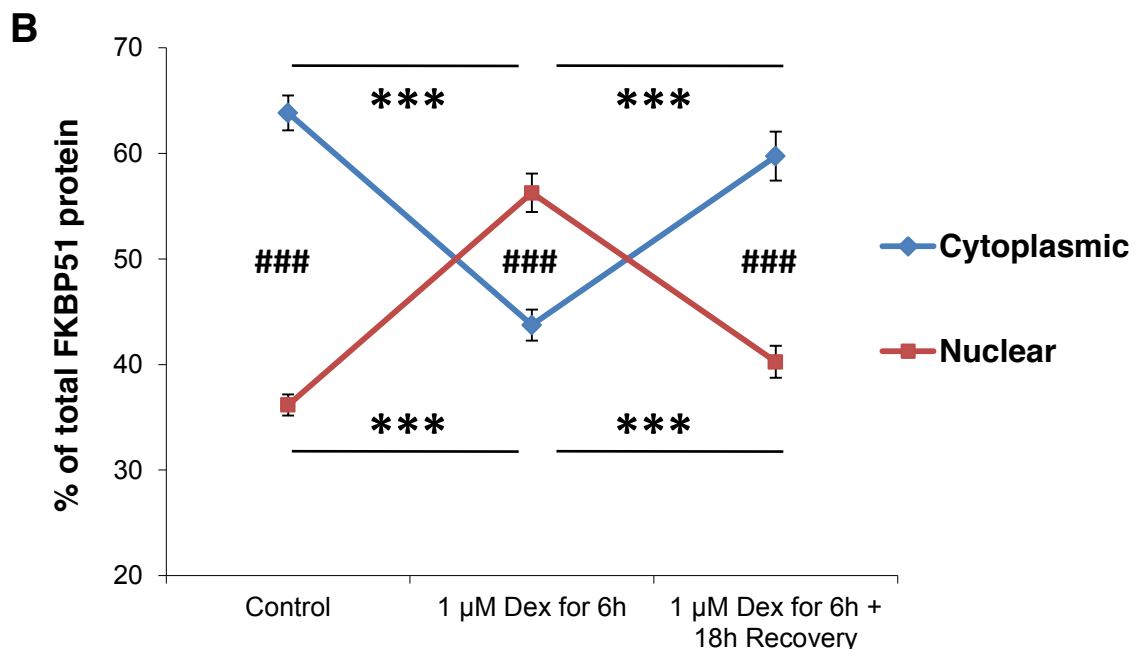
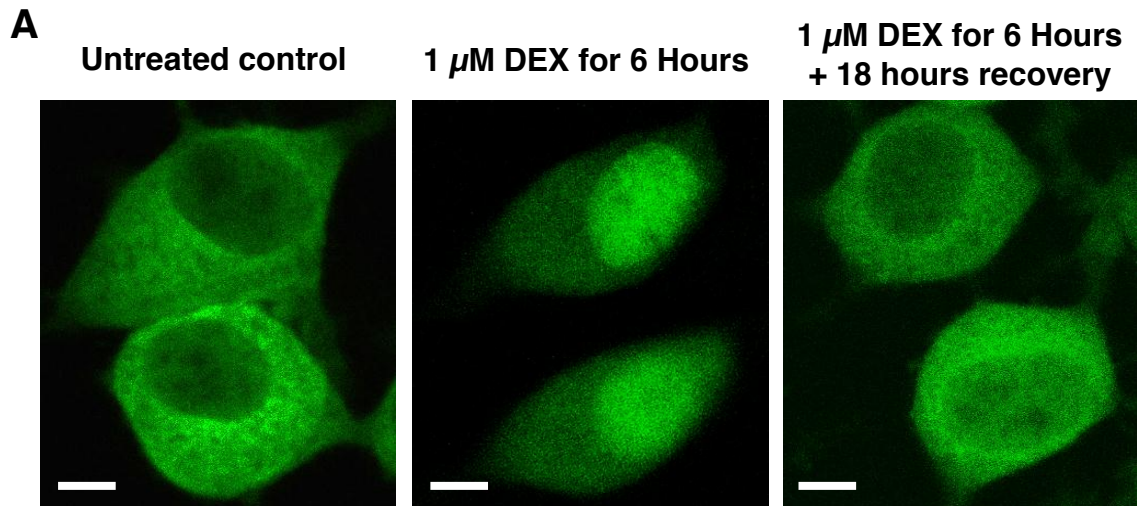


Figure 4.4 Dexamethasone promotes nuclear accumulation of FKBP51. Mouse neuroblastoma N2a cells were transfected with FKBP51-GFP construct for 48 hours and GFP-tag was imaged in live cells maintained at 37 °C and 5% CO₂ using confocal microscope to study FKBP51 localisation. (A) Representative confocal image of cells untreated, treated for 6 hours with dexamethasone and dexamethasone treatment followed by 18 hours of recovery. Scale bar, 5 μ m. (B) Green fluorescent intensity from cytoplasmic and nuclear region was measured using ImageJ software and combined to get total FKBP51 intensity for each cell. FKBP51 intensity in both fractions are shown as percentage of total FKBP51 intensity. Data for each group were collected from 4 different coverslips and around 150 cells from each coverslip. Data are shown as mean \pm s.e.m. *, intra-fraction significance; #, inter-fraction significance; 6h, 6 hours; 18h, 18 hours.

Table 4.2 FKBP51 nuclear translocation in N2a cells: Tukey's post-hoc results

Compared groups	p value
Cyto control vs Nucl control	p < 0.001
Cyto control vs Cyto Dex	p < 0.001
Cyto control vs Cyto Dex 18h R	p < 0.001
Nucl control vs Nucl Dex	p < 0.001
Nucl control vs Nucl Dex 18h R	p < 0.001
Cyto Dex vs Nucl Dex	p < 0.001
Cyto Dex vs Cyto Dex 18h R	p < 0.001
Nucl Dex vs Nucl Dex 18h R	p < 0.001
Cyto Dex 18h R vs Nucl Dex 18h R	p < 0.001

Cyto, cytoplasm; Nucl, nuclear; Dex 18h R, 6 hours dexamethasone treatment 18 hours recovery

We next set out to investigate the possible role of nuclear FKBP51 in GR signalling. BAG1, also known as RAP46, is another GR co-chaperone that binds to the GR-complex via Hsp70 and has been associated with the pathophysiology of stress-related disorders (Maeng, 2008). BAG1 translocates to the nucleus upon dexamethasone treatment and inhibits GR transcriptional activity by blocking the DNA binding site of GR (Schmidt, 2003). Therefore, we wondered if FKBP51 also bind to the DNA in the nucleus to inhibit the GR transcriptional activity. Modified chromatin immunoprecipitation was performed on amygdala from wild type control and stressed mice to find the answer. Sonicated chromatin (<500bp) was immunoprecipitated with an FKBP51 antibody.

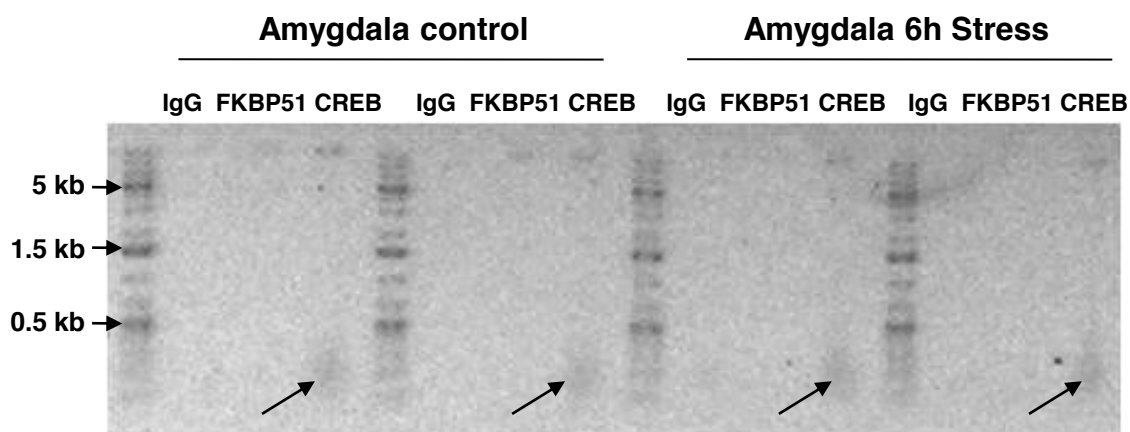


Figure 4.5 FKBP51 does not interact directly with DNA. Amygdalae from wild-type naïve and restrained stress mice were subjected to chromatin immunoprecipitation to study FKBP51 interaction with DNA. Paraformaldehyde cross-linked chromatin in amygdala homogenate was sonicated to get DNA fragments of average < 500bp. Sheared chromatin was immunoprecipitated with primary antibodies against rabbit IgG (negative control), FKBP51 (test) and CREB (positive control). Immunoprecipitated bead elute was reverse cross-linked and 1% agarose gel analysed. Arrows indicate immunoprecipitated chromatin smear in CREB samples. 6h Stress, 6 hours stress.

Since FKBP51 binding target genomic DNA sequence was not known, bead elutes were loaded onto 1% agarose gel to check the presence of any DNA fragment immunoprecipitated with anti-FKBP51 antibody (**Figure 4.5**). DNA fragments, absent in negative control rabbit IgG groups and present in positive control CREB groups, confirms the reliability of the experiment. Importantly no DNA fragments were observed in control and stressed amygdala samples immunoprecipitated with anti-FKBP51 antibody suggesting FKBP51 does not bind directly to the DNA. However, this does not rule out possibility of any indirect interaction between DNA and FKBP51.

Scaffolding protein FKBP51 promotes dephosphorylation of Akt at serine 473 by PHLPP phosphatases in cytoplasm and nucleus to determine chemosensitivity in cancer cells (Pei, 2009). Therefore we measured levels of Akt phosphorylated at serine 473 [pAkt(S473)] before and after stress in the amygdala, to determine involvement of FKBP51-facilitated Akt dephosphorylation in stress response. Quantification of western blots showed no significant changes in the pAkt(S473) levels after 5 minutes and 15 minutes of stress compared to control samples (**Figure 4.6**; $F_{(2,6)} = 0.9204$, $p = 0.4481$; One-way ANOVA). Thus, stress does not alter facilitation of Akt dephosphorylation by FKBP51.

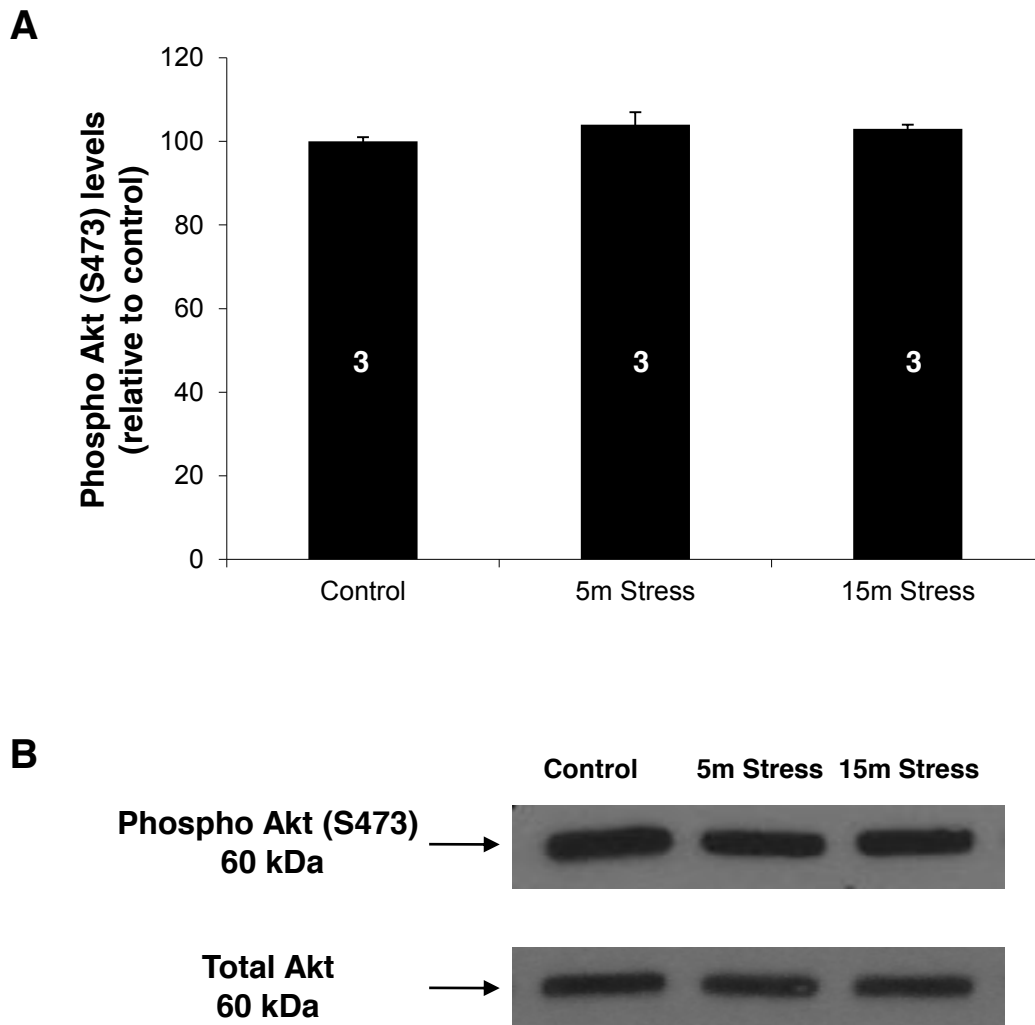


Figure 4.6 Stress does not affect Akt phosphorylation at serine 473 in amygdala. Amygdalae, dissected from naïve and stressed wild type mice, were homogenised in RIPA buffer. (A) Levels of Akt phosphorylated at serine 473 were measured and normalized to total Akt using western blot technique. (B) Representative western blots are depicted for Phospho Akt (S473) and total Akt. Digits inside column indicate n. Data are shown as mean \pm s.e.m. 5m, 5 minutes; 15m, 15 minutes.

Identification of interaction partners remains most popular approach to determine the function of a protein. Hence we performed pull down assay to find FKBP51 interacting cytoplasmic and nuclear proteins in vehicle and dexamethasone treated N2a cells transfected for 48 hours with Fkbp5-GFP construct. GFP-tagged FKBP51 complexes were immunoprecipitated using the antibody against the GFP tag due to high specificity of anti-GFP antibody whereas mouse IgG served as the control. Immunoprecipitated complexes were resolved on SDS-PAGE gel and stained with Brilliant Blue G-colloidal to visualise the proteins. Gel images for cytoplasmic and nuclear samples in **Figure 4.7** show strong bands at ≈ 79 kDa corresponding to GFP-tagged FKBP51 present only in anti-GFP antibody lanes. Peptide mass fingerprinting by MALDI-TOF mass spectrometry revealed a total of 31 proteins between IgG and GFP samples with at least two unique peptides of over 95% probability. With the applied filtering criteria (two unique peptides with over 95% probability) the predicted protein probability is $\approx 99\%$ (**Appendix I**). FKBP51 appeared at the top of the list (**Table 4.3**) only in GFP samples and not in the IgG samples assuring the reliability of the data. Apart from FKBP51, histone H1.4 was the only protein that immunoprecipitated with anti-GFP and not with IgG antibody and importantly in dexamethasone treated nuclear fraction. Thus, our results suggest that dexamethasone promotes FKBP51 interaction with histone H1.4 in the nucleus.

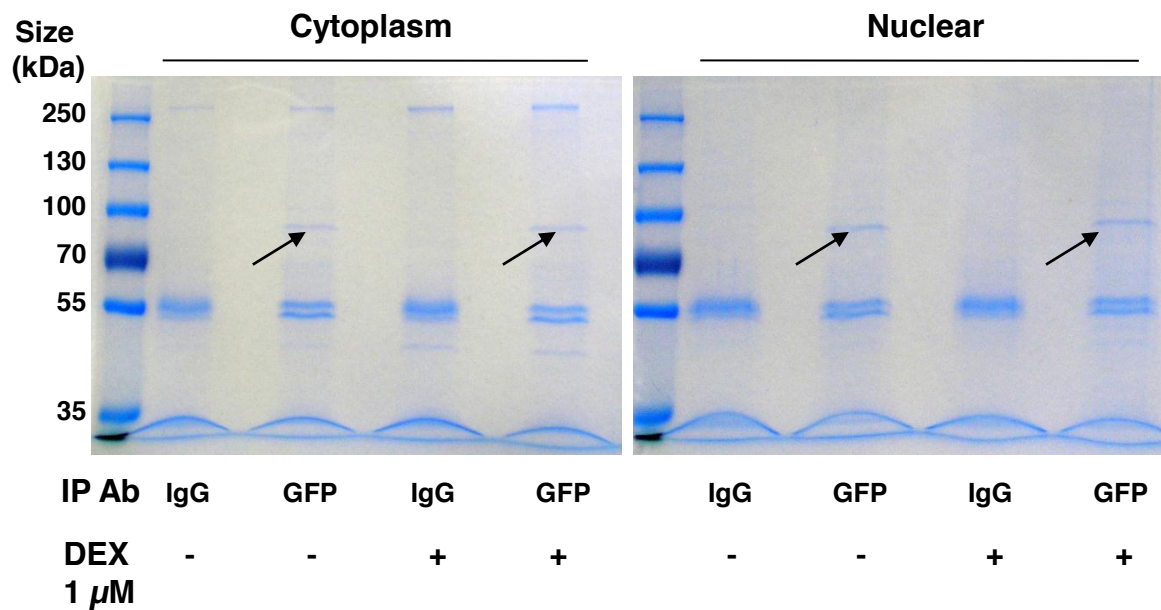


Figure 4.7 Proteomic analysis of cytoplasmic and nuclear FKBP51 interactome. N2a cells were transfected with FKBP51-GFP construct and treated for 6 hours with vehicle or dexamethasone 48 hours post-transfection. Harvested cells were fractionated to get cytoplasmic and nuclear proteins. FKBP51 complexes were immunoprecipitated from vehicle and dexamethasone treated cytoplasm and nuclear fractions with antibody against GFP-tag while IgG served as the negative control. Denatured elutes were electrophoresed on SDS-PAGE gels and Brilliant Blue G-Colloidal stained to visualize proteins. Representative images of Brilliant Blue G-Colloidal stained cytoplasmic and nuclear pull down gels are shown. Arrows point at GFP-tagged FKBP51 corresponding band (≈ 79 kDa), as expected. DEX, dexamethasone; IP ab, immunoprecipitating antibody; IgG, mouse IgG; GFP, anti-GFP antibody.

#	Visible?	Starred?	MS/MS View: Identified Proteins (31) Including 0 Decoys	Accession Number	Molecular Weight	Protein Grouping	Probability Legend:							
							1. Cyt PBS GFP UL01113-SP-01	2. Cyt DEX GFP UL01113-SP-02	3. Nucl PBS GFP UL01113-SP-03	4. Nucl DEX GFP UL01113-SP-04	5. Cyt PBS IgG UL01135-SP-01	6. Cyt DEX IgG UL01135-SP-02	7. Nucl PBS IgG UL01135-SP-03	8. Nucl DEX IgG UL01135-SP-04
1	<input checked="" type="checkbox"/>	<input type="checkbox"/>	Peptidyl-prolyl cis-trans isomerase FKBP5 OS=Mus mu...	51 kDa	15	15	19	19						
2	<input checked="" type="checkbox"/>	<input type="checkbox"/>	Tubulin beta-5 chain OS=Mus musculus GN=Tubb5 PE=...	50 kDa	8	6	10	11	18	14	20	18		
3	<input checked="" type="checkbox"/>	<input type="checkbox"/>	Actin, cytoplasmic 2 OS=Mus musculus GN=Actg1 PE=1.....	42 kDa	12	13	6	9	19	22	18	17		
4	<input checked="" type="checkbox"/>	<input type="checkbox"/>	Vimentin OS=Mus musculus GN=Vim PE=1 SV=3	54 kDa	2		3	8	12	10	19	21		
5	<input checked="" type="checkbox"/>	<input type="checkbox"/>	Elongation factor 1-alpha 1 OS=Mus musculus GN=Eef1.....	50 kDa	4	3	6	7	10	9	12	14		
6	<input checked="" type="checkbox"/>	<input type="checkbox"/>	Trypsin OS=Sus scrofa PE=1 SV=1	24 kDa	5	5	4	6	5	5	5	5		
7	<input checked="" type="checkbox"/>	<input type="checkbox"/>	Heat shock cognate 71 kDa protein OS=Mus musculus ...	71 kDa	5	2	8	6	21	19	24	25		
8	<input checked="" type="checkbox"/>	<input type="checkbox"/>	Heat shock protein HSP 90-beta OS=Mus musculus GN=...	83 kDa	4	2	9	5	25	14	26	29		
9	<input checked="" type="checkbox"/>	<input type="checkbox"/>	Alpha-enolase OS=Mus musculus GN=Eno1 PE=1 SV=3	47 kDa	2		2	5	14	11	15	20		
10	<input checked="" type="checkbox"/>	<input type="checkbox"/>	ATP synthase subunit alpha, mitochondrial OS=Mus mu.....	60 kDa	2		2	5	17	11	17	19		
11	<input checked="" type="checkbox"/>	<input type="checkbox"/>	Tubulin alpha-1A chain OS=Mus musculus GN=Tuba1a ...	50 kDa	6	5	4	4	18	16	18	17		
12	<input checked="" type="checkbox"/>	<input type="checkbox"/>	Asparagine synthetase [glutamine-hydrolyzing] OS=M.....	64 kDa				4	2		4	7		
13	<input checked="" type="checkbox"/>	<input type="checkbox"/>	Glyceraldehyde-3-phosphate dehydrogenase OS=Mus	36 kDa			3	3	10	7	10	10		
14	<input checked="" type="checkbox"/>	<input type="checkbox"/>	ATP synthase subunit beta, mitochondrial OS=Mus mu....	56 kDa	3		2	3	6	3	15	14		
15	<input checked="" type="checkbox"/>	<input type="checkbox"/>	Heterogeneous nuclear ribonucleoprotein D0 OS=Mus ...	38 kDa			2	2			4	3		
16	<input checked="" type="checkbox"/>	<input type="checkbox"/>	Delta-1-pyrroline-5-carboxylate synthase OS=Mus mu.....	87 kDa				2		2	3	2		
17	<input checked="" type="checkbox"/>	<input type="checkbox"/>	Endoplasmic reticulum chaperone protein OS=Mus mu.....	92 kDa			2	2	2		15	16		
18	<input checked="" type="checkbox"/>	<input type="checkbox"/>	Pyruvate kinase isozymes M1/M2 OS=Mus musculus G....	58 kDa				2	4	3	8	9		
19	<input checked="" type="checkbox"/>	<input type="checkbox"/>	40S ribosomal protein S3 OS=Mus musculus GN=Rps3 ...	27 kDa	2			2	4	6	8	6		
20	<input checked="" type="checkbox"/>	<input type="checkbox"/>	Tubulin alpha-1B chain OS=Mus musculus GN=Tuba1b ...	50 kDa		2		2	2	2	2	2		
21	<input checked="" type="checkbox"/>	<input type="checkbox"/>	Histone H1.4 OS=Mus musculus GN=Hist1h1e PE=1 SV=2....	22 kDa				2						
22	<input checked="" type="checkbox"/>	<input type="checkbox"/>	78 kDa glucose-regulated protein OS=Mus musculus G....	72 kDa			2		11	6	14	14		
23	<input checked="" type="checkbox"/>	<input type="checkbox"/>	T-complex protein 1 subunit zeta OS=Mus musculus GN.....	58 kDa			2		11	7	11	12		
24	<input checked="" type="checkbox"/>	<input type="checkbox"/>	T-complex protein 1 subunit alpha OS=Mus musculus G.....	60 kDa	2		3		10	7	11	10		
25	<input checked="" type="checkbox"/>	<input type="checkbox"/>	Heterogeneous nuclear ribonucleoprotein U OS=Mus m.....	88 kDa	3				5	4	11	12		
26	<input checked="" type="checkbox"/>	<input type="checkbox"/>	Heat shock protein HSP 90-alpha OS=Mus musculus GN.....	85 kDa			3		8		9	9		
27	<input checked="" type="checkbox"/>	<input type="checkbox"/>	T-complex protein 1 subunit epsilon OS=Mus musculus	60 kDa	2				6	3	8	7		
28	<input checked="" type="checkbox"/>	<input type="checkbox"/>	Guanine nucleotide-binding protein subunit beta-2-like.....	35 kDa	2				7	4	10	10		
29	<input checked="" type="checkbox"/>	<input type="checkbox"/>	Clathrin heavy chain 1 OS=Mus musculus GN=Cltc PE=1.....	192 kDa			2				12	9		
30	<input checked="" type="checkbox"/>	<input type="checkbox"/>	Ubiquitin OS=Mus musculus GN=Rps27a PE=1 SV=1	9 kDa	2				2		3	3		
31	<input checked="" type="checkbox"/>	<input type="checkbox"/>	T-complex protein 1 subunit eta OS=Mus musculus GN....	60 kDa			4				4	5		

Table 4.3 Mass spectrometric identification of proteins co-purified with cytosolic and nuclear FKBP51. Filtering criteria used were a minimum of 2 unique peptides with over 95% peptide probability. Proteins present in only either of the GFP and not in any IgG samples are highlighted in red boxes.

Together these results indicate that FKBP51 is differentially regulated in wild-type and *neuropsin*^{-/-} mice amygdala by stress reflecting the *Fkbp5* regulation. Scaffolding activity of FKBP51 indicated by pAkt(473) levels remains unaltered after stress. Importantly FKBP51 undergoes nuclear translocation in response to stress and dexamethasone where it interacts with linker histone H1.4 protein.

4.3 Discussion

Gene expression does not necessarily reflect active protein levels and therefore it is crucial to confirm that protein expression follows the gene expression accounting for the biological response. Stimulation of GR signalling with cortisol and dexamethasone for 6 hours results in simultaneous upregulation in *Fkbp5* gene and FKBP51 protein expression (Rees-Unwin, 2007; Billing, 2007). Consistent with this, increased *Fkbp5* expression is accompanied by elevation in FKBP51 protein levels in wild type mice amygdala (**Figure 4.1**). However FKBP51 levels remain unaltered in stressed *neuropsin*^{-/-} mice despite of attenuated upregulation in *Fkbp5* expression. Thus *neuropsin* genotype interaction with stress shows differential regulation of both *Fkbp5* gene and FKBP51 protein expression from the stressed wild type mice.

Our western blot and immunohistochemistry findings disagree with the view of Baughman and colleagues that murine FKBP51 is a T-cell specific immunophilin (Baughman, 1995). In contrast murine FKBP51 is considerably expressed in the amygdala, similar to the hippocampus (Touma, 2011). Double immunohistochemistry demonstrated that FKBP51 co-localises with amygdala neurons similar to primary human forebrain neurons (Tatro, 2009). Interestingly, the cellular localization of FKBP51 varies between different cell types (Staibano, 2011). Under basal condition, FKBP51 shows primarily nuclear staining in NTM-5 cells (Zhang, 2008). Amygdala neurons, on the other hand,

show diffused cytoplasmic and nuclear FKBP51 staining similar to mouse embryonic fibroblasts, rat intestinal epithelial and osteosarcoma cells (Llimited, 2008). Gallo and colleagues recently proposed FKBP51 as a primarily mitochondrial protein due to high levels of cytoplasmic FKBP51 co-localising with mitochondrial markers MitoTracker and proteins Cyt c, cyclooxygenase IV and Tom-20 in 3T3-L1 fibroblast cells. However, the authors argued that percentage of mitochondrial FKBP51 is variable and depends on factors such as cell type, passage number and growth conditions (Gallo, 2011). Cell-type dependent FKBP51 cellular localization pattern perhaps may determine its differential function.

FKBP immunophilins are not confined to any particular compartment in a static manner (Quinta, 2010). This notion is supported by our subcellular fractionation findings that restraint stress triggers nuclear translocation of FKBP51. In neuroblastoma N2a cells, GFP-tagged FKBP51 undergoes cytoplasmic-nuclear shuttling in response to dexamethasone treatment providing further *in vitro* evidence. Elevated FKBP51 concomitant with GR has been shown to translocate from cytoplasm to nucleus in rat thymus tissue after 15 minutes of restraint stress (Billing, 2008). FKBP51 also shows higher nuclear staining in 3T3-L1 fibroblasts upon steroid exposure compared to cells maintained in serum-free medium (Gallo, 2011). Our findings are consistent with the general consensus that FKBP51, unlike GR, do not completely abandon the cytoplasm/mitochondria and stress- and dexamethasone- triggered FKBP51

nuclear translocation represents concentration gradient shift rather than “all or none” phenomenon.

Despite the well-studied nuclear localization of FKBP51, how FKBP51 translocates to the nucleus still remains poorly understood. Interestingly our bioinformatics analysis of mouse FKBP51 amino acid sequence using web-based algorithms (TARGET 1.1, iPSORT, WoLFPSORT, ProteinProwler, pTARGET, CELLO, PA-SUB, SOSUISignal, PrediSi, SignalP, NucPred and LOCKey), although confirmed cytoplasmic and nuclear localization of FKBP51, did not predict any nuclear localization signal peptide. However, proteins not possessing their own nuclear localization signal peptide may interact with nuclear localization signal-containing cargo proteins to enter the nucleus (Nigg, 1997). For example following recruitment to the GRC, PPIase domain of homologous FKBP52 interacts with the intermediate chain of motor protein dynein to be actively transported to the nucleus (Galigniana, 2002). Evidences of FKBP51 PPIase domain interaction with dynein are divided since some suggests in favour of interaction although poor compared to FKBP52 (Zhang, 2008) whereas others argue no interaction at all (Wochnik, 2005). On the contrary the TPR domain has been observed to play an important role in determining cellular localization of FKBP51. Disrupting FKBP51 interaction with Hsp90, through treatment with Hsp90 competitive inhibitor radicicol and K352A-TPR domain mutation of FKBP51, promotes nuclear accumulation of FKBP51 (Gallo, 2011). Dissociation from the immunophilin-binding site on

Hsp90 dimer and in turn from the GRC confers a soluble state to unbound FKBP51. Likewise FKBP51 also attain soluble state following stress exposure or dexamethasone treatment since steroid binding to GR triggers dissociation of FKBP51 from the Hsp90-dimer and hence GRC (Davies, 2002). Therefore, FKBP51 similar to other soluble proteins of low molecular weight between 40-60 kDa can dynamically diffuse through the nuclear pore complex (Nigg, 1997). Hence neither the diffusion through the nuclear pore nor the interaction with transporter protein such as dynein can be ruled out.

Drawing comparisons between GR co-chaperones FKBP51 and BAG1 using modified chromatin immunoprecipitation revealed that following translocation to the nucleus, unlike BAG1, FKBP51 does not interact directly with DNA in a non-sequence specific manner to suppress GR-dependent transcription. However, FKBP51-mediated indirect regulation of GR transcriptional activity through an interacting protein partner still remains a possibility. Apart from psychiatric disorders, a crucial role of FKBP51 has also been demonstrated in cancer etiology and treatment (Wang, 2011). FKBP51 regulates phosphorylation of Akt to determine sensitivity to chemotherapeutic agents in cancer cells (Pei, 2009). FKBP51 levels inversely correlate with the Akt activity: higher FKBP51 results in reduced Akt activity leading to chemosensitivity. Although measuring pAkt(S473) levels after stress exposure suggests FKBP51 regulation of Akt is perhaps specific to cancer cells. Hence, FKBP51 may have different functions in different cell types.

Despite being a subject of debate, immunoprecipitation or pull-down followed by mass spectrometric identification of captured proteins is a widely used small-scale proteomic approach to identify novel interaction partners (Aebersold, 2003). Co-purification of non-specifically bound contaminants along with target protein is a major concern since routinely used sepharose beads can increasingly bind to more non-specific contaminants after longer incubation with HeLa cytoplasmic and nuclear fractions (Trinkle-Mulcahy, 2008). Counteractive measures such as stringent washing of immunoprecipitated complexes, although reduces the level of nonspecific binding, also poses a greater risk of removing bona fide protein partners interacting in sub-stoichiometric amounts or binding with lower affinity (Have, 2011). Therefore less stringent washing conditions were used to preserve all specific and less abundant interacting proteins. This strategy however resulted in higher background as shown in **Figure 4.7 & Table 4.3** and perhaps eclipsed known FKBP51 interacting proteins such as Hsp90. Protein of interest is often overexpressed with a fusion tag to overcome less abundant expression of native protein and lack of specific antibodies against the target protein (Have, 2011). Tagging FKBP51 with GFP did not interfere with dexamethasone triggered nuclear translocation of FKBP51 (**Figure 4.4**). Mass spectrometric identification of GFP tagged FKBP51 only in anti-GFP antibody immunoprecipitated cytoplasmic and nuclear fractions positively verified the experiment instigating more confidence. Nevertheless following the rule of thumb it is crucial to

validate any identified interaction using other technique, for example co-immunoprecipitation.

Between all GFP antibody immunoprecipitated groups, a total of 31 proteins were identified with \geq two unique peptides of over 95% probability. Comparison with the relevant mouse IgG controls discarded the non-specific contaminants and revealed FKBP51 interaction with nuclear protein histone H1.4 following dexamethasone treatment. Much higher sensitivity of mass spectrometry compared to Brilliant Blue G-colloidal staining accounts for identification of histone H1.4 as FKBP51 interacting protein despite of lack of clearly visible histone H1.4 corresponding band at \approx 22 kDa in the dexamethasone and anti-GFP antibody treated nuclear fraction lane (**Figure 4.7**).

Histone H1.4 (histone 1 isoform 4 or H1e) encoded by *Hist1h1e* gene belongs to the lysine-rich most divergent family of histone H1 also known as linker histone. Histone H1 family proteins, unlike other histones, do not form the nucleosome bead and instead binds to short stretches of DNA that link individual nucleosomes stabilising the chromatin fibre (Widom, 1998). Similar to core histones, linker H1 histones are also posttranslationally modified by phosphorylation, methylation, polyADP-ribosylation and acetylation to contribute to the regulation of gene expression (Jenuwein, 2001). Constitutive heterochromatin containing all four somatic H1 variants shows selective depletion of H1.4 from actively transcribed chromatin suggesting repressive

effects (Parseghian, 2000). Further histone H1.4 deficient mice exhibited strong attenuation of human β -globin transgene silencing (Alami, 2003). Therefore, co-immunoprecipitation confirmation of FKBP51 and histone H1.4 interaction would imply an unknown role of FKBP51 in gene expression regulation.

Chapter 5

Amygdalar Fkbp5 in stress-induced anxiety

5.1 Introduction

5.1.1 Measuring anxiety behaviour

Anxiety is an adaptive emotion characterized by psychological (e.g. worry, restlessness and fear) and physiological signs (e.g. sweating, increased heart rate and tremble). However, pathologically enhanced behavioural responsiveness to ambiguous threat due to hyperexcitability in the fear circuitry is expressed as clinical anxiety (Davis, 1998). Spielberger in 1966 conceptualized multifaceted anxiety defining individual's predisposition to respond as trait (innate) anxiety and anxiogenic stimulus- or experience-related anxiety as state anxiety (Endler, 2001). Importantly, behavioural tests described here measure situation-evoked (state) anxiety behaviour not the innate anxiety (Ohl, 2005). Anxiety-assessing behavioural methods can be divided into two categories: unconditioned or ethological tests (e.g. elevated plus-maze, open field) and conditioned tests (e.g. fear-potentiated startle) (Cryan, 2005). Given the highly debatable nature and complexities of behaviour paradigms only a brief literature review is provided of the tests employed in this study (Hogg, 1996).

Unconditioned tests are based on knowledge derived from studying animal's natural behaviour and involve assessing animal behaviour in presence of naturally fear inducing stimuli (Belzung, 2001). Rodents are naturally foraging species with innate exploratory behaviour to gain information about foraging

and any potential danger (Belzung, 1994). However, exposure to a novel unprotected area triggers exploratory as well as the fear drive leading to approach-avoidance conflict behaviour (Montgomery, 1955a). Unconditioned tests exploit these conflicting tendencies of animal to approach or avoid the unprotected spaces (Cryan, 2005). Aversive nature of the unprotected area is amplified in most tests by elevation and bright illumination of the area. The balance between desire to explore the unknown area and motivation to avoid danger determines animal's behaviour in these tests, indicative of generalized anxiety disorders and PTSD in humans (Ohl, 2005). Additionally due to ethical reasons, conditioned tests involving a significant pain element are less popular compared to ethological tests (Bourin, 2007).

Montgomery in 1955 reported rat's strong approach-avoidance conflict only in the open elevated alleyway and not in the closed alleyway of a Y-shaped apparatus (Montgomery, 1955b). Handley and colleagues in 1984 not just applied the elevated X maze to Montgomery's model but also successfully validated the method (Handley, 1984). Since then elevated plus-maze, first described in details by Pellow and colleagues in 1985, remain one of the most commonly used tool to screen anxiety modulating drugs and genetic & environmental factors (Pellow, 1985). Test is carried out in elevated, plus-shaped maze consisting of four arms: two opposing arms that form the unprotected aversive area and other two opposing closed arms protected by side walls. The animal is placed on the central platform interconnecting all four

arms and the behaviour is observed usually for 5-10 minutes. Elevated plus-maze apparatus combines three anxiogenic stimuli: height, open space and novelty. Spatiotemporal parameters such as number of entries and time spent in open arm, closed arm and centre are commonly measured (Walf, 2007). Ethological parameters such as number of head dips over the open & closed arms, stretch attend posture, rearing and sniffing could provide detail understanding of animal's behaviour on the maze (Walf, 2007). The rank-order of preference is closed > centre > open arm which is strengthened by anxiogenic and suppressed by anxiolytic stimuli. Open arm related parameters reflect the level of anxiety whereas total entries indicate animal's locomotor function (Lister, 1987). For example, anxiolytic drugs (diazepam and amylobarbitone) increased and putative anxiogenic agents (picrotoxin) decreased the number of entries by rats into the unprotected open arm (Handley, 1984). Elevated plus-maze is highly sensitive to environmental and procedural modifications (Carobrez, 2005). Various factors shown to affect animal's behaviour in the elevated plus maze include prior experience, illumination, width of the arm and social isolation among others (Bourin, 2007). Similar to other tests, elevated plus-maze apparatus, protocol and scoring method varies significantly from laboratory to laboratory (Hogg, 1996; Lewejohann, 2006).

Hall in 1936 measured rat's emotionality by means of defecation and ambulatory behaviour in a brightly illuminated round open field with surrounding walls. Emotional stimulation by predator encounter in rats

resulted in more defecation and marked reduction in ambulatory activity in the open field (Hall, 1936). Open field apparatus used varies from laboratory to laboratory in shape (round & square), size and intensity of illumination (dim to bright) (Ohl, 2005). Animals are placed in the same position and behaviour is usually monitored for 10 minutes. Mice display a strong tendency of staying close to the protected wall known as thigmotaxis and avoid entering the centre zone (Ohl, 2005). Parameters such as time spent, distance travelled and number of entries for centre and peripheral zone are calculated (Prut, 2003). Centre zone parameters indicate anxiety levels whereas total distance travelled is a measure of locomotion and exploratory behaviour (Bourin, 2007). Open field has significant predictive validity for both anxiolytic and anxiogenic drugs respectively increasing and decreasing the time spent by animals in the centre zone (Prut, 2003). Similar to elevated plus-maze, animal's behaviour in the open field test can also be influenced handling, procedural and environmental factors (Lewejohann, 2006).

5.1.2 Assessing learning and memory

Environmental factors influence behaviour by means of learning and memory mechanisms (Kandel, 1999). Definitions of learning and memory remain one of the most debated topics in the neuroscience fraternity (Sweatt, 2003). However, experimentally speaking, learning refers to acquisition of an altered behavioural response to a given stimulus resulting from an experience whereas memory represents the mechanisms of encoding, storing and retrieving the acquired

pattern of neuronal activation responsible for this altered behaviour after experience (Kandel, 1999; Sweatt, 2003). Memory is not a unitary phenomenon and multiple forms of memory vary in psychological characteristics, brain regions involved and neural mechanisms of encoding, storage, consolidation and retrieval. Given their diversity, not all forms of memory can be assessed by one particular test. Instead specific tests have been devised to study different aspects of learning and memory such as novel object recognition, Morris water maze, passive avoidance test, fear conditioning (FC), conditioned taste aversion, etc (Crawley, 1997).

Classical fear conditioning task is a form of associative learning that measures animal's ability to learn and remember association between environment and footshock (contextual), or between auditory tone and footshock (cued) (Maren, 2001). Animals are trained to associate neutral conditioned stimulus (CS), tone, with unconditioned stimulus (US), electric footshock, of aversive nature. CS presentation for 30 seconds end with a 2 seconds footshock and hence this procedure is also called delayed conditioning. FC to context is measured normally after 24 hours in the training chamber without tone and shock. Animals are placed 48 hours later in a chamber, different from the training, to assess cued FC in presence of tone. Animal's activity and freezing behaviour is recorded during all phases of the experiment. Increased freezing behaviour in the context of shock (contextual) and in response to conditioned tone (cued) indicates memory.

Regional lesion has been a common approach to identify neural circuitry involved in various forms of learning and memory (Eichenbaum, 2001). Classical view is that the hippocampus associates context with the footshock whereas association between tone and the footshock is amygdala-dependent (Maren, 2001). Importantly, where the associative role of the amygdala in FC is consensual, the contribution of the hippocampus to the contextual conditioning in mice is rather unclear. Electrolytic amygdala lesions impaired both context and cued conditioning whereas freezing solely to context was abolished in rats with damaged hippocampus (Phillips, 1992). Author proposed the amygdala as the brain region involved in formation of associative fear learning and memory. Hippocampus, in their view, served only as a sensory relay involved in association of context with the footshock. However, contradictory evidence also exists showing that hippocampal lesions have either no effect or only partial impairment on the context memory (Logue, 1997; Cho, 1999). Maren and colleagues observed that neurotoxic lesions of the dorsal hippocampus did not impair acquisition, but did disrupt the expression of the of contextual fear conditioning (Maren, 1997 & 1999). They postulated, two parallel, hippocampal and extrahippocampal, mechanisms compete with each other to support of contextual FC. Indeed some studies have reported that damaging perirhinal and postrhinal cortices, potential extrahippocampal candidates, pre-training or post-training remarkably impairs context-dependent FC (Buffalo, 1999; Bucci, 2000 & 2002; Lindquist, 2004). Importantly, basolateral amygdala serves as the locus of competition and hippocampus dominates the extrahippocampal

system in an intact system (Biedenkapp, 2009). Therefore, the amygdala is critical for acquisition and storage of cued memory whereas the hippocampus is a key region for context-dependent FC.

5.1.3 Fkbp5 in behaviour

GR transcriptional target Fkbp5 regulates GR sensitivity to determine one's stress coping behaviour and susceptibility to stress-related psychiatric disorders (Binder, 2009). Strong clinical evidence confirms positive correlation between "high induction" Fkbp5 genotypes (or single nucleotide polymorphisms) and development of depression and PTSD (Binder, 2009). Further, recently three studies have behaviourally phenotyped Fkbp5^{-/-} mice to better understand potential neurobehavioural effects of Fkbp5. Surprisingly Fkbp5 deletion affect neither the basal corticosterone levels nor the locomotion, stress-coping, anxiety-related, depression-like and exploratory behaviour in young mice (O'Leary III, 2011; Touma, 2011; Hartmann, 2011).

Stressed Fkbp5^{-/-} mice, on the other hand, spend significantly more time swimming and less time floating in forced swim test compared to stressed wild type mice in two independent studies (Touma, 2011; Hartmann, 2011). Complementing behaviour, psychological stress-induced elevations in corticosterone levels were attenuated in Fkbp5^{-/-} mice compared to their wild type littermates in different physiological paradigms and attenuation persisted even during recovery period (O'Leary III, 2011; Touma, 2011; Hartmann, 2011).

Hence, enhanced GR sensitivity of Fkbp5^{-/-} mice following stress could underlie their more active coping behaviour in forced swim test (Touma, 2011; Hartmann, 2011). Even though chronically stressed Fkbp5^{-/-} mice did not show any anxiety-related behaviour in the open field and the elevated plus-maze test, despite their significantly lower locomotor activity (Hartmann, 2011).

Depressive symptoms show positive correlation with increased FKBP51 levels in HIV patients carrying high induction associated TT allele of rs1360780 (Tatro, 2010). Further in vivo evidence comes from behavioural studies of aged Fkbp5^{-/-} mice (O'Leary III, 2011). Interestingly in both tail-suspension and forced swim tests 17-20 months old Fkbp5^{-/-} mice displayed significantly less immobility compared to same age wild type mice. Nevertheless activity, motor performance, motor coordination, motor learning, anxiety-related behaviour, hippocampus-dependent and amygdala-dependent emotional learning & memory did not differ between aged Fkbp5^{-/-} and wild type mice when subjected to a battery of behavioural tests (O'Leary III, 2011).

Our lab has previously shown that acute restraint stress (6 hours) induces anxiety-like behaviour in elevated plus-maze test without affecting locomotion (Pawlak, 2003; Attwood, 2011). Importantly, this correlates with the robust upregulation in amygdala Fkbp5 gene expression after 6 hours of restraint stress (Figure 3.1). Hence, following the crucial role of Fkbp5 in stress-related coping behaviour, outlined in the literature above, we hypothesized a role of

amygdalar Fkbp5 in anxiety-related behaviour induced by severe stressful experiences. Therefore the primary aim of this chapter was to investigate the behavioural alterations in wild-type mice lacking amygdala-specific Fkbp5.

5.2 Results

Intra-amygdala stereotaxic injection of Fkbp5-targeting lentiviral shRNA particles silenced $\approx 60\%$ of Fkbp5s expression in the wild-type mice amygdala (Figure 2.10). Wild-type mice lacking local Fkbp5 in the amygdala were assessed on the elevated plus-maze for anxiety-like behaviour induced by restraint stress. Stress, genotype and stress \times genotype interaction did not significantly affect the number of total entries (**Figure 5.1A**; Two-way ANOVA; genotype effect $F_{(1,25)} = 1.382$, $p = 0.251$; stress effect $F_{(1,25)} = 0.044$, $p = 0.835$; genotype \times stress interaction $F_{(1,25)} = 2.060$, $p = 0.164$) and closed arm entries (**Figure 5.1C**; Two-way ANOVA; genotype effect $F_{(1,25)} = 0.064$, $p = 0.803$; stress effect $F_{(1,25)} = 0.353$, $p = 0.558$; genotype \times stress interaction $F_{(1,25)} = 0.049$, $p = 0.826$). However with regard to dimly illuminated open arm entries (**Figure 5.1B**), two-way ANOVA revealed a significant effect of genotype ($F_{(1,25)} = 13.602$, $p = 0.001$) and stress \times genotype interaction ($F_{(1,25)} = 9.158$, $p = 0.006$) but not the stress ($F_{(1,25)} = 0.296$, $p = 0.591$).

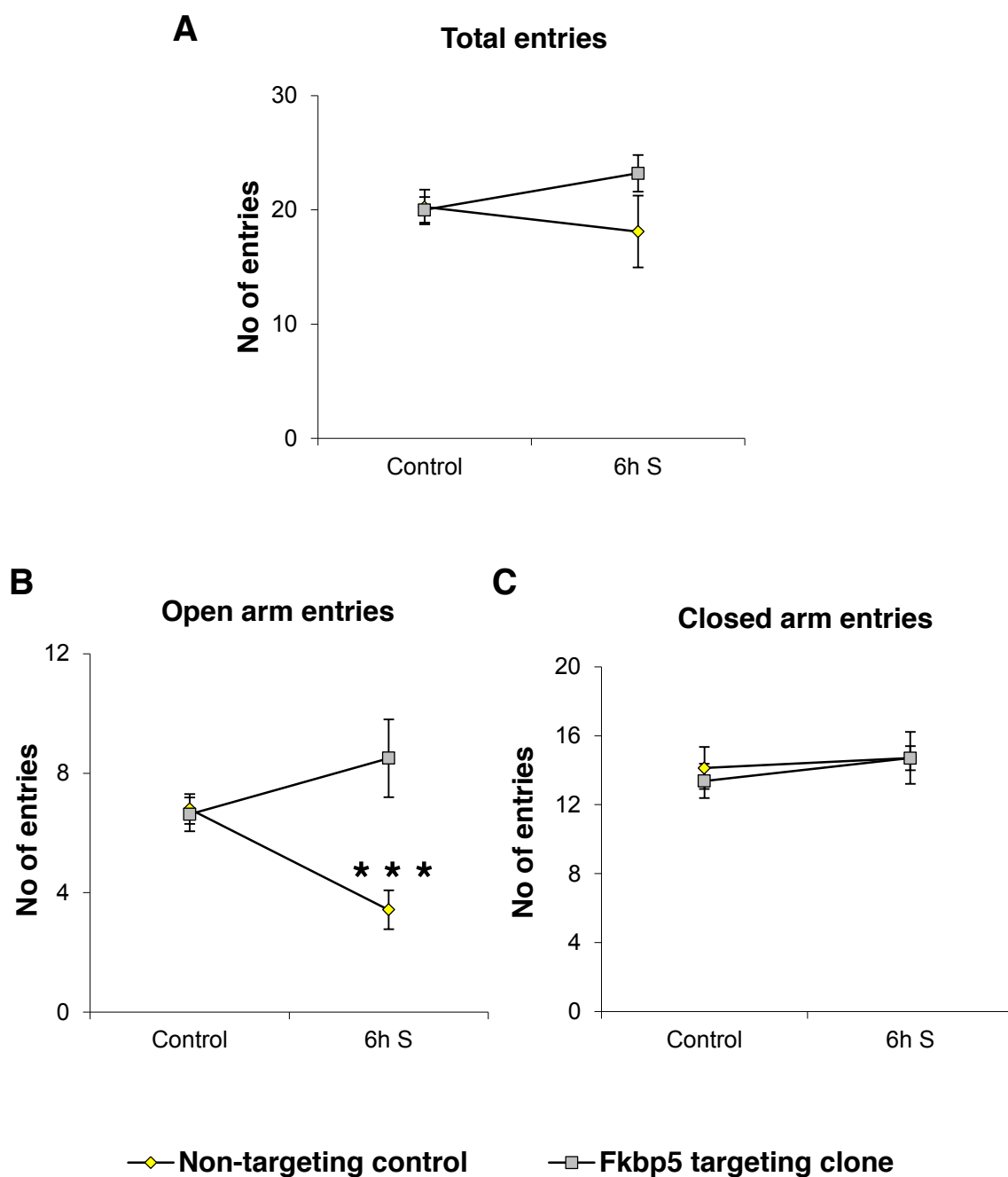


Figure 5.1 Amygdala-specific Fkbp5 silencing protects wild type mice from stress-induced anxiety in elevated plus maze. Wild-type mice, stereotaxically injected with either non-targeting control or Fkbp5 targeting clone, were subjected to restraint stress for 6 hours following recovery period. Next day animals were tested for stress-induced anxiety behaviour on the elevated plus maze. Animal's exploratory behaviour on the maze was recorded for 5 minutes and (A) total entries, (B) open arm entries and (C) closed arm entries were counted. Data are shown as mean \pm s.e.m. $n= 6-8$ per group. 6h S, 6 hours stress.

Non-targeting clone injected wild-type mice, following stress, entered the open arms significantly less compared to their non-stressed control littermates (Non-targeting control vs Non-targeting stress, $p < 0.05$), amygdalar Fkbp5-deficient non-stressed (Fkbp5 targeting control vs Non-targeting stress, $p < 0.05$) and stressed mice (Non-targeting stress vs Fkbp5 targeting stress, $p < 0.001$). Interestingly, elevated plus-maze open arm exploration of Fkbp5 targeting clone injected mice remains unaltered following stress (Fkbp5 targeting control vs Fkbp5 targeting stress, $p > 0.05$). Hence, silencing Fkbp5 in the amygdala confers anxiolytic phenotype to otherwise vulnerable wild-type mice.

Next the stress-induced alteration in exploratory behaviour of amygdala-specific Fkbp5 deficient mice was studied in the open field arena. The ANOVA failed to reveal significant effect of stress, genotype and stress \times genotype interaction on the total distance travelled (**Figure 5.2A**; Two-way ANOVA; genotype effect $F_{(1,24)} = 0.018$, $p = 0.895$; stress effect $F_{(1,24)} = 0.010$, $p = 0.921$; genotype \times stress interaction $F_{(1,24)} = 0.325$, $p = 0.574$), distance travelled in the perimeter (**Figure 5.2E**; Two-way ANOVA; genotype effect $F_{(1,24)} = 0.014$, $p = 0.907$; stress effect $F_{(1,24)} = 0.106$, $p = 0.748$; genotype \times stress interaction $F_{(1,24)} = 0.453$, $p = 0.507$) and time spent in the perimeter (**Figure 5.2F**; Two-way ANOVA; genotype effect $F_{(1,24)} = 1.595$, $p = 0.219$; stress effect $F_{(1,24)} = 1.826$, $p = 0.189$; genotype \times stress interaction $F_{(1,24)} = 3.451$, $p = 0.076$).

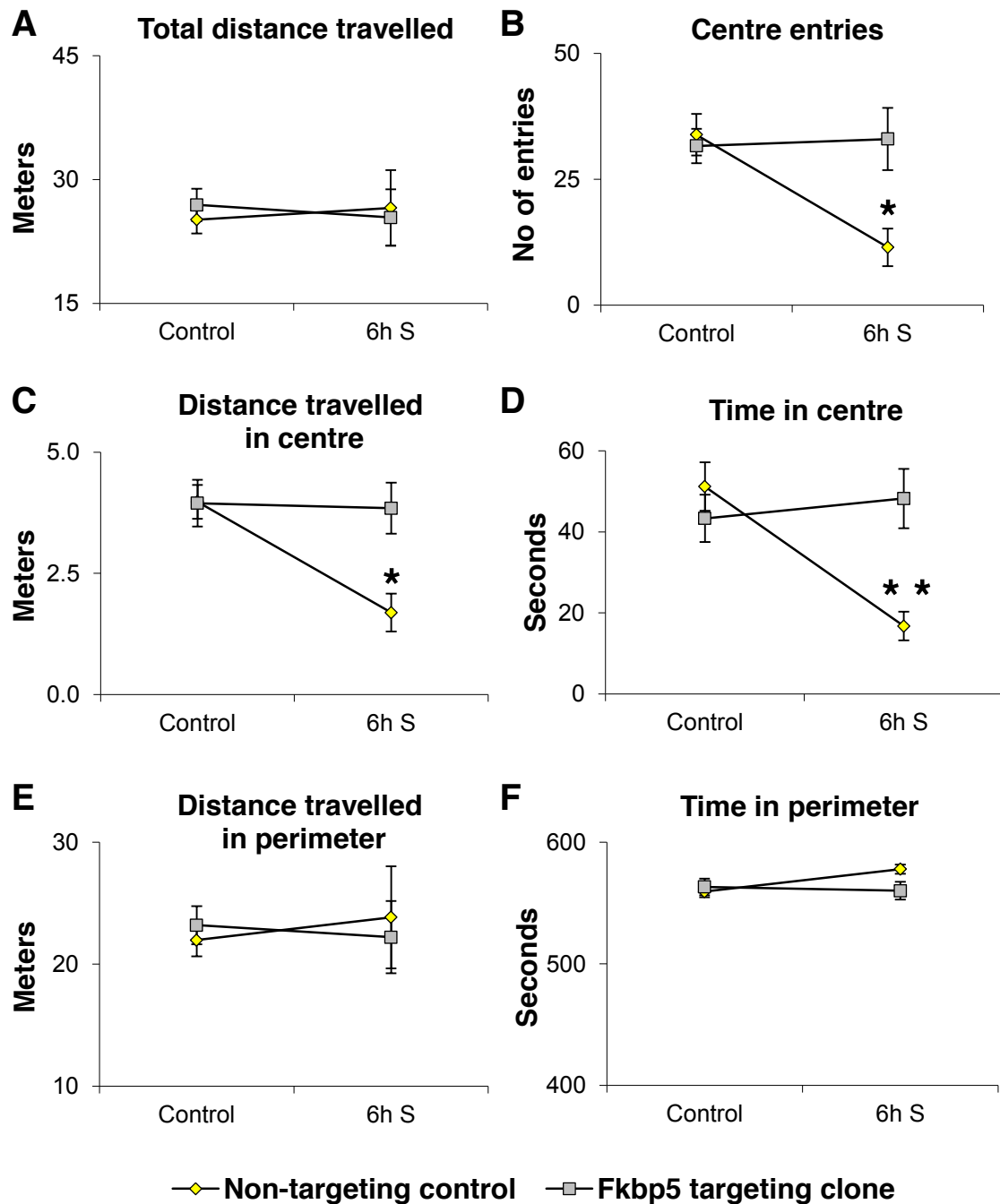


Figure 5.2 Silencing amygdalar Fkbp5 expression protects wild type mice from stress-induced suppression of exploratory behaviour in the open field. Wild type mice were injected with either non-targeting control or Fkbp5 targeting clone and restraint stressed for 6 hours post recovery period. Following day animal's exploratory behaviour in a novel open field environment was studied and recorded for 10 minutes using an overhead camera. ANY-MAZE software was used to calculate behavioural parameters: (A) total distance travelled, (B) centre entries, (C) distance travelled in centre, (D) time in centre, (E) distance travelled in perimeter and (F) time in perimeter. Data are shown as mean \pm s.e.m. n= 6-8 per group. 6h S, 6 hours stress.

Table 5.1 Number of centre zone entries: Tukey's post-hoc results

Compared groups	p value
NT NS vs NT 6h S	p < 0.05
Fkbp5 NS vs NT 6h S	p < 0.05
Fkbp5 NS vs Fkbp5 6h S	p > 0.05
NT 6h S vs Fkbp5 6h S	p < 0.05

NT, Non-targeting clone; Fkbp5, Fkbp5 targeting clone; NS, non stressed; 6h S, 6 hours stress

Table 5.2 Distance travelled in centre zone: Tukey's post-hoc results

Compared groups	p value
NT NS vs NT 6h S	p < 0.05
Fkbp5 NS vs NT 6h S	p < 0.01
Fkbp5 NS vs Fkbp5 6h S	p > 0.05
NT 6h S vs Fkbp5 6h S	p < 0.05

NT, Non-targeting clone; Fkbp5, Fkbp5 targeting clone; NS, non stressed; 6h S, 6 hours stress

Table 5.3 Time spent in centre zone: Tukey's post-hoc results

Compared groups	p value
NT NS vs NT 6h S	p < 0.01
Fkbp5 NS vs NT 6h S	p < 0.05
Fkbp5 NS vs Fkbp5 6h S	p > 0.05
NT 6h S vs Fkbp5 6h S	p < 0.01

NT, Non-targeting clone; Fkbp5, Fkbp5 targeting clone; NS, non stressed; 6h S, 6 hours stress

Conversely, significant genotype, stress and genotype \times stress interaction effects are revealed on centre zone parameters: number of entries (**Figure 5.2B; Table 5.1**; Two-way ANOVA; genotype effect $F_{(1,24)} = 4.552, p = 0.043$; stress effect $F_{(1,24)} = 5.398, p = 0.029$; genotype \times stress interaction $F_{(1,24)} = 6.905, p = 0.015$), distance travelled (**Figure 5.2C; Table 5.2**; Two-way ANOVA; genotype effect $F_{(1,24)} = 5.755, p = 0.025$; stress effect $F_{(1,24)} = 10.455, p = 0.004$; genotype \times stress interaction $F_{(1,24)} = 8.792, p = 0.007$) and time spent (**Figure 5.2D; Table 5.3**; Two-way ANOVA; genotype effect $F_{(1,24)} = 5.251, p = 0.031$; stress effect $F_{(1,24)} = 4.949, p = 0.036$; genotype \times stress interaction $F_{(1,24)} = 13.854, p = 0.001$).

Similar to the elevated plus maze, open field exploratory behaviour did not differ between stress-naïve non-targeting clone injected control and Fkbp5 targeting clone mice (**Figure 5.3**). However, non-targeting clone-injected mice displayed significant avoidance of unprotected center zone following stress despite unimpaired general locomotive activity. In contrast amygdala-specific Fkbp5-deficient stressed mice did not show any repulsive tendency towards the center zone since the number of entries, time spent and distance travelled did not differ between control and stressed mice implying a stress-resistant phenotype.

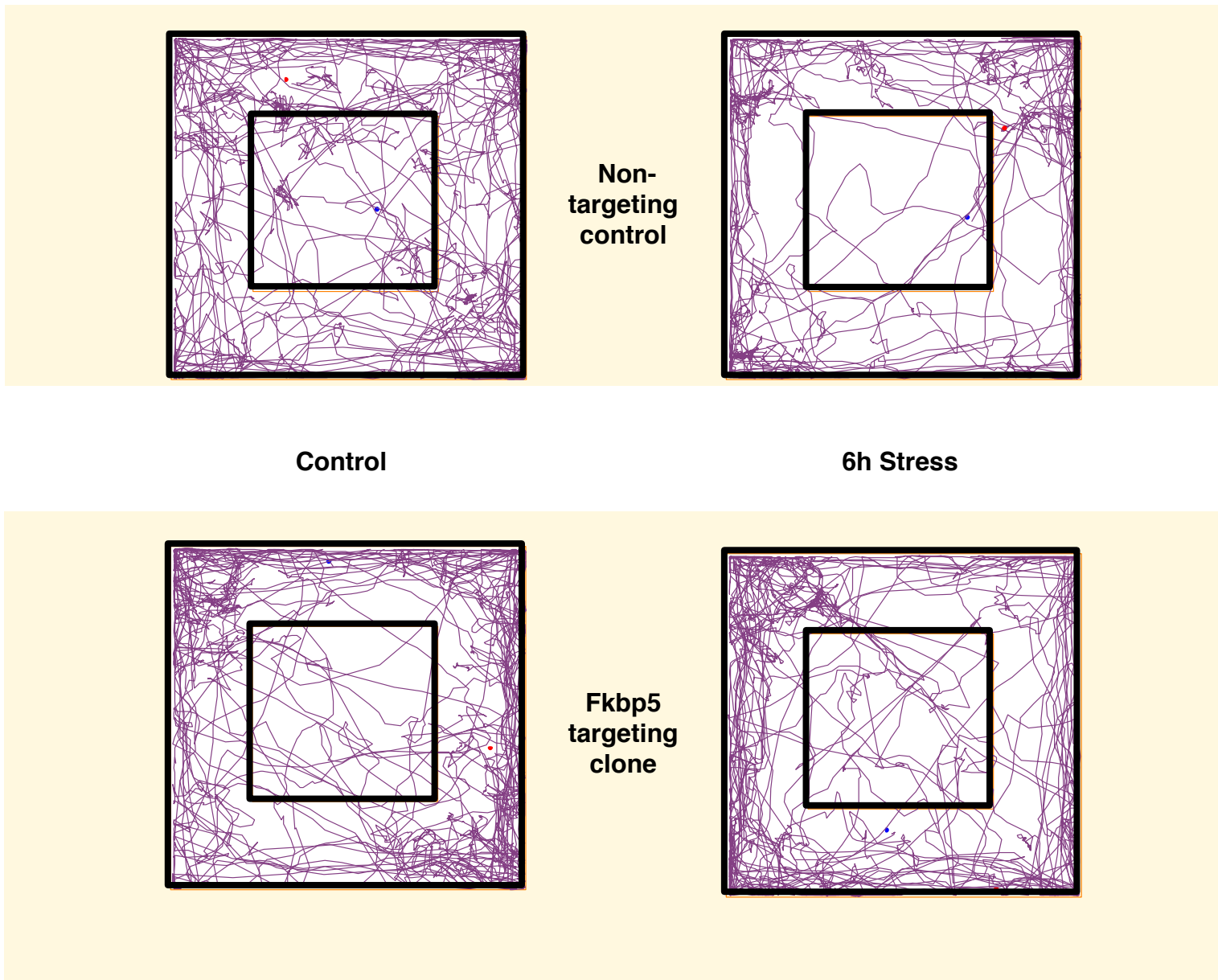


Figure 5.3 Representative track plots of animal's exploration pattern in the open field. Naïve and stressed wild type mice, injected with either non-targeting control or Fkbp5 targeting clone, were allowed to explore the open field for 10 minutes. Small square in the middle is defined as the centre zone and the outer square as the perimeter. The thin purple line indicates animal's movement in the open field recorded with an overhead camera. Plots were generated using ANY-MAZE software.

Pavlovian FC was performed on non-targeting and Fkbp5 targeting clone-injected mice to study the role of amygdalar Fkbp5 in fear learning and memory. After three trials, mice learned to associate the CS tone with the US electric footshock on training day. Retrieval of hippocampus-dependent contextual memory was evaluated 24 hours after training by re-exposing the mice to the training chamber and measuring the fear response indicated by immobility (**Figure 5.4; Table 5.4**). Two-way ANOVA showed a significant effect of only FC ($F_{(1,28)} = 60.452, p < 0.0001$) but not the genotype ($F_{(1,28)} = 1.160, p = 0.291$) and FC \times genotype interaction ($F_{(1,28)} = 0.635, p = 0.432$). Both genotypes showed around 20% more context retrieval freezing compared to baseline freezing (**Figure 5.4B & C**).

Table 5.4 Contextual memory: Tukey's post-hoc results

Compared groups	p value
NT baseline vs Fkbp5 baseline	$p > 0.05$
NT baseline vs NT retrieval	$p < 0.001$
NT baseline vs Fkbp5 retrieval	$p < 0.001$
Fkbp5 baseline vs NT retrieval	$p < 0.001$
Fkbp5 baseline vs Fkbp5 retrieval	$p < 0.001$
NT retrieval vs Fkbp5 retrieval	$p > 0.05$

NT, Non-targeting clone; Fkbp5, Fkbp5 targeting clone

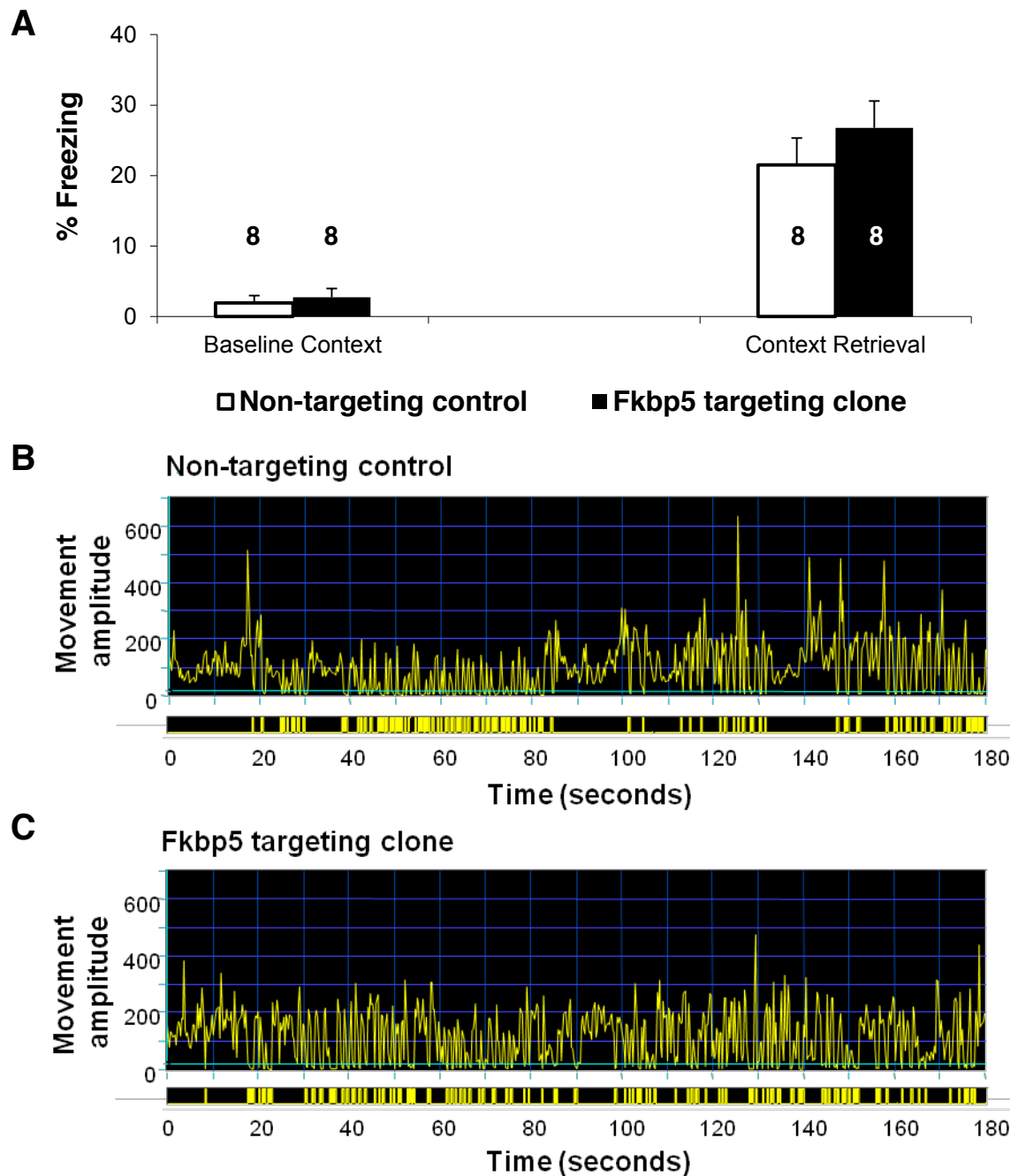


Figure 5.4 Deleting Fkbp5 gene in amygdala does not impair hippocampus-dependent memory in wild type mice. Non-targeting control or Fkbp5 targeting clone-injected mice were trained to associate the tone with the aversive foot shock. Next day mice were placed in the same chamber for 180 seconds and freezing was assessed to evaluate the hippocampus-dependent contextual memory. (A) FreezView software was used to quantify freezing. Representative traces of movement amplitude for (B) non-targeting control and (C) Fkbp5 targeting clone-injected mice during the context retrieval are depicted. Yellow bars in the panel below indicate lack of movement. Digits inside column indicate n. Data are shown as mean \pm s.e.m.

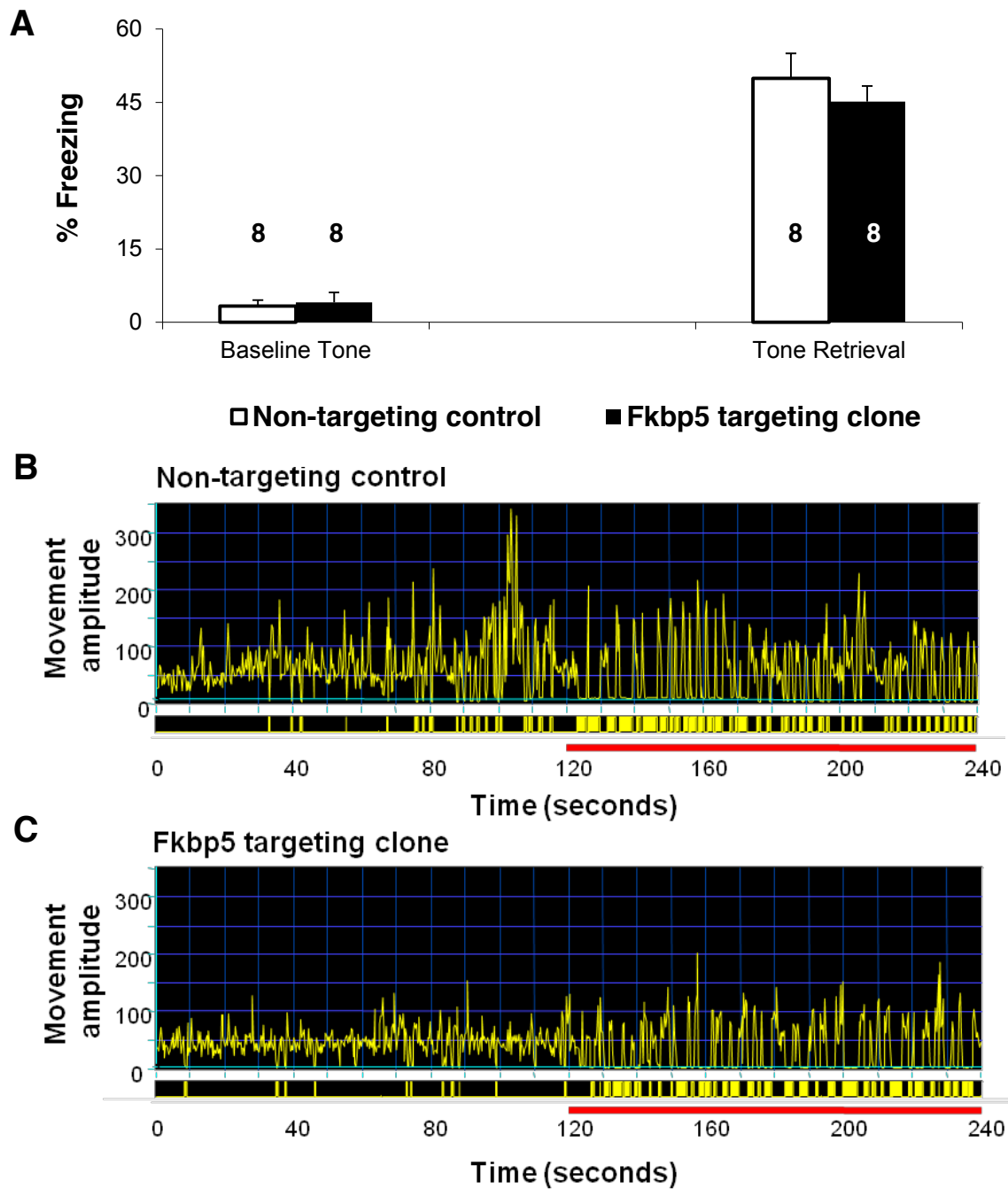


Figure 5.5 Amygdalar Fkbp5 is not involved in conditioned fear. Wild type mice, stereotaxically injected with either non-targeting control or Fkbp5 targeting clones, learned to pair conditioned tone with the electric foot shock on training day. Mice were placed in a different chamber from the training 48 hours later and the conditioned tone was played during the last 120 seconds. Animal's freezing behaviour in presence of tone was monitored to study amygdala-dependent cued memory and (A) quantified using FreezeView software. Representative traces of movement amplitude for (B) non-targeting control and (C) Fkbp5 targeting clone-injected mice during the tone retrieval are shown. Immobility is indicated by yellow bars in the below panel. Digits inside column indicate n. Data are shown as mean \pm s.e.m.

When tested for amygdala-dependent cued retrieval of fear 48 hours after training, both groups of animals significantly increased their immobility in response to the tone. However, the strength of the memory did not differ between both genotypes (**Figure 5.5; Table 5.5**; Two-way ANOVA; genotype effect $F_{(1,28)} = 0.392, p = 0.536$; FC effect $F_{(1,28)} = 184.176, p < 0.0001$; genotype \times FC interaction $F_{(1,24)} = 0.718, p = 0.404$). Non-targeting and Fkbp5 targeting clone injected mice showed robust freezing only during the tone presentation (**Figure 5.5B & C**).

Table 5.5 Cued memory: Tukey's post-hoc results

Compared groups	p value
NT baseline vs Fkbp5 baseline	$p > 0.05$
NT baseline vs NT retrieval	$p < 0.001$
NT baseline vs Fkbp5 retrieval	$p < 0.001$
Fkbp5 baseline vs NT retrieval	$p < 0.001$
Fkbp5 baseline vs Fkbp5 retrieval	$p < 0.001$
NT retrieval vs Fkbp5 retrieval	$p > 0.05$

NT, Non-targeting clone; Fkbp5, Fkbp5 targeting clone

5.3 Discussion

Silencing Fkbp5 in the amygdala did not impair the locomotor activity and anxiety-related behaviour in the stress naïve wild-type mice. None of the elevated plus-maze and open field test parameters measured differs significantly between non-stressed non-targeting control and Fkbp5 targeting clone injected wild-type mice. These results align with prior research investigating behavioural effects of global Fkbp5 deletion, which also demonstrated insignificant effect of Fkbp5 genotype on behavior under basal conditions (O'Leary III, 2011; Touma, 2011; Hartmann, 2011).

Restraint stress paradigm, involving neurogenic and psychogenic but no physical element, uses immobilization technique to trigger the stress response. Acutely stressed wild-type mice have previously been shown to exhibit significant anxiety-like behaviour in different anxiety measuring paradigms (Pawlak, 2003; Kumar, 2010; Attwood, 2011). The current study findings can confirm that exposure to acute immobilization restraint stress heightens anxiety behavior of non-targeting control injected wild-type mice without affecting the locomotion, as indicated by significantly decreased open arm entries in the elevated plus-maze and significantly increased avoidance of centre zone (number of entries, time spent and distance travelled) in the open field tests (**Figure 5.1 & 5.2 & 5.3**). Surprisingly though, amygdala-specific Fkbp5 deficient wild-type mice exposed to stress, in contrast, did not display

any fear of entering the open arm and exploring the centre of the open field arena in anxiety assessing behavioural tests (**Figure 5.1 & 5.2 & 5.3**). Therefore, neither the anxiety-related exploratory behavior nor the general locomotor activity was significantly altered by stress in wild-type mice lacking amygdalar Fkbp5.

Similar to amygdala-specific Fkbp5-deficient mice, conventional Fkbp5^{-/-} mice also exhibit more active stress-coping behaviour, although only in forced swim and not the elevated plus-maze and open field test, owing to their enhanced GR sensitivity, determined by significantly lower corticosterone elevation following stress compared to wild-type mice in two independent studies (Touma, 2011; Hartmann, 2011). Importantly, Hartmann and colleagues failed to reproduce previously shown higher anxiety-like behaviour in the elevated plus-maze and the open field of wild-type mice subjected to chronic social defeat stress (Schmidt, 2007, Hartmann, 2011). These inconsistent findings question the reliability and reproducibility of the chronic social defeat stress paradigm. Also conventional knockout mice, although popular, always raise concerns over unknown and adaptive compensatory mechanisms (Touma, 2011). Devoid of any such masking mechanisms, wild-type mice lacking amygdalar Fkbp5 reveal their stress-resistant phenotype.

Silencing amygdala-specific Fkbp5 does not impair freezing in contextual and cued fear conditioning compared to wild-type controls (**Figure 5.4 & 5.5**).

Likewise, spatial and emotional memory remains unaffected by global Fkbp5 deletion (O'Leary III, 2011). Taken together, our results suggest that while amygdalar Fkbp5 deletion protects wild-type mice, exposed to restraint stress, from experiencing heightened unconditioned fear in unconditioned anxiety tests, conditioned fear remains unaffected.

Amygdalar Fkbp5 may differentially be involved in distinct neural mechanisms underlying unconditioned and conditioned fear related to stress responses. Amygdala is undisputedly a key brain region in neural circuitry of fear (Rosen, 2004). Basolateral complex of the amygdala receives sensory information from the thalamus and the cortex. Davis has proposed delineating the neural pathways involved in conditioned and unconditioned fear depending on the downstream, central nucleus of the amygdala (CeA) or the bed nucleus of the stria terminalis (BNST), region receiving projections from the basolateral complex (Davis, 2006). Both CeM and BNST receive inputs from the basolateral complex of amygdala and subsequently project to the hypothalamic and brainstem structures that mediate behavioural, autonomic and electrophysiological responses of fear and anxiety (Walker, 2003). Importantly, infusion of AMPA receptor antagonist into the basolateral amygdala disrupted both the conditioned and unconditioned phenomena (Walker, 1997). NMDA lesions of CeA but not the BNST, blocks the conditioned fear to explicit cues in fear potentiated startle (Hitchcock, 1987; Hitchcock, 1991; Lee, 1997). CRH- and light-enhanced startle, reflecting unconditioned fear, is blocked by NMDA

lesions only in the BNST region but not the CeA (LeDoux, 1988; Walker, 1997). Basolateral amygdala projections to CeA mediate rapid, phasic responses whereas basolateral amygdala output to BNST produces slower, sustained responses to unconditional threat (Walker, 2003; Davis, 2006). Most importantly, chronic immobilization stress-mediated increase in dendritic arborisation of neurons in the BNST, but not in CeA, underlies the facilitation of anxiety-like behaviour (Vyas, 2003).

In summary, knocking down amygdalar Fkbp5 in wild-type mice, while does not impair basal behaviour, under stressful environment confers more active coping behaviour and protective phenotype. Importantly, amygdalar Fkbp5 is only involved in unconditional fear or anxiety and not in the conditioned fear. Hence, both clinical evidence and mice behavioural data suggest Fkbp5 genotype affects behaviour only in interaction with environment.

Chapter 6

Stress-regulated amygdala miRNAs

6.1 Introduction

6.1.1 miRNA physiology

Non-coding RNAs constitute an important group of molecules participating in diverse developmental and regulatory events (Hunsberger, 2009). miRNAs are ~21 nucleotides long strands of genetic material that regulate post-transcriptional expression of almost one third coding mRNAs (Kosik, 2006). Mature miRNA biogenesis (**Figure 6.1**) involves a series of enzymatic events beginning with RNA-polymerase II-mediated transcription of long transcripts known as pri-miRNA. RNase III enzyme Drosha then cleaves the pri-miRNA transcript to ~70 nucleotide-long hairpin RNA called pre-miRNA, followed by translocation of the precursor to cytoplasm by nuclear export factor exportin 5. Another RNase III enzyme Dicer cleaves the stem-loop structure into imperfect ~21 base pairs long double-stranded RNA duplex. After unwinding of the duplex, strand with the lower thermodynamic stability at 5' end, also referred to as guide strand, is recruited to miRNA-induced silencing complex (miRISC; **Figure 6.1**) whereas the other strand in most cases is degraded (Kosik, 2006).

Mature miRNAs associate with any member of the argonaute protein family to form the miRISC followed by the complex's binding to the target mRNA through base pairing between partially complement miRNA and 3' - untranslated region (3' UTR) of the transcript (Bushati, 2007).

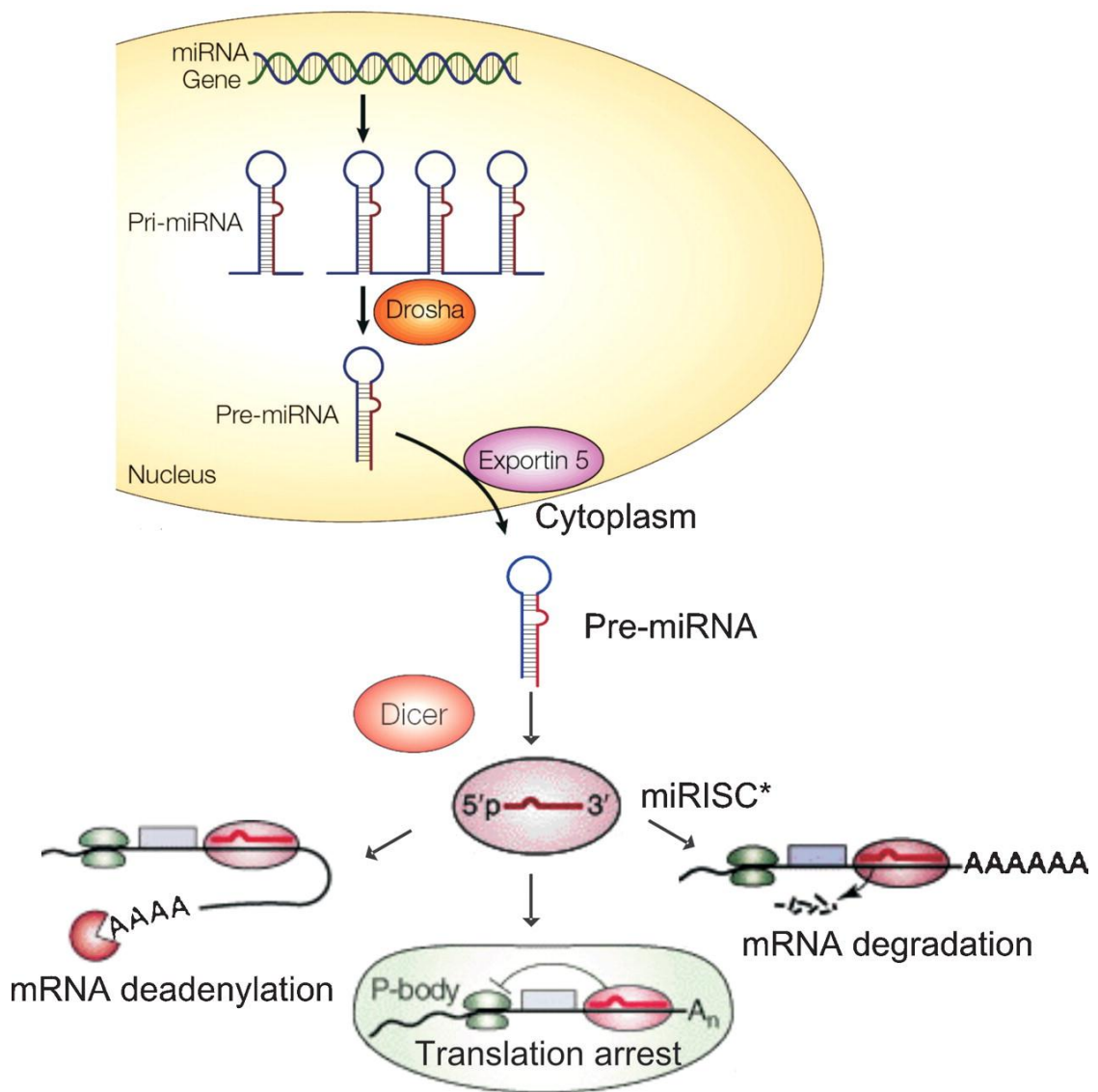


Figure 6.1 Schematic model of miRNA biogenesis and mechanism of action. Adapted from (Muhonen, 2009).

Classically miRNAs only negatively regulate mRNA translation into protein via mechanisms such as miRISC-triggered target transcript degradation through deadenylation and interference with target translation by inhibiting translation initiation, blocking translation elongation, promoting premature drop-off of the ribosome and degrading co-translational protein (Pillai, 2007; Cannell, 2008). Despite remarkable progress in our understanding of miRNA biology we struggle to understand the reason behind this diversity of mechanisms and precise molecular events that take place (Eulalio, 2008). Some argue that sequence and features of 3' UTR are important since 3' UTR region act as a docking site for complexes regulating mRNA stability and localization (Behm-Ansmant, 2006). In addition, miRISC-interacting proteins also have crucial roles in determining miRNA regulation (Buchan, 2007). Supporting evidence has surfaced showing that, contrary to the popular belief, an miRNA can both boost or block the translation of target mRNA depending on the miRISC interacting protein under different physiological conditions (Vasudevan, 2007 a&b). Nevertheless, a detailed understanding of miRNA mediated posttranscriptional regulation of mRNA is still in its infancy and more work is needed to understand their regulatory roles in critical physiological events.

6.1.2 miRNA, stress and synaptic plasticity

Regulatory role of miRNAs in the mature central nervous system is a rapidly growing field. Not because of abundant miRNA expression in the brain but mainly due to region specificity and enrichment of particular miRNAs

dominating the population of expressed miRNAs (Konecna, 2009). For example, brain specific miR-134, enriched in the synapto-dendritic compartment of mammalian hippocampal neurons, inhibits spine developmental protein Limk1 to regulate spine volume (Schratt, 2006). In addition, brain-derived neurotrophic factor (BDNF)-mediated synaptic activation releases the inhibitory effect of miR-134 on Limk1 translation (Schratt, 2006). Schratt and colleagues' pioneering work suggested that miRNAs regulating translation of dendrite-specific mRNAs might have a crucial role in stress-modulated structural form of synaptic plasticity in the basolateral amygdala and hence, associated behavioural imprints (Steward, 2001; Kelleher, 2004; Mitra, 2005). Indeed, in the frontal cortex region-specific transient alteration of miRNA levels have been observed in CD1 male mice stressed for 2 hours (Rinaldi, 2010). In addition, increased miR-18a expression resulting in reduced GR levels, in the paraventricular nucleus of the hypothalamus, determined impairment in HPA axis habituation and higher vulnerability of Fischer 344 rats to repeated restraint stress (Uchida, 2008). Moreover, acute immobilization stress-upregulated miR-134 and miR-183 in central nucleus of the rat amygdala both inhibits acetylcholinesterase transcript slicing factor, SC35, to regulate cholinergic neurotransmission in neuronal stress reaction (Meerson, 2010). Haramati and colleagues have recently reported that increased expression of stress-responding miR-34c in the central nucleus of the amygdala suppressed translation of corticotropin releasing factor receptor type 1 mRNA to protect C57BL/6J mice from stress-induced anxiety (Haramati, 2011). Hence in this

study, we aimed to examine amygdalar miRNA expression profile after 6 hours of restraint stress to explore the physiological role of miRNAs in the regulation of Fkbp5 during stress response, in the context of stress-related behaviour.

6.2 Results

miRNA expression profiling was carried out on mRNA extracted from amygdala tissues that were obtained from control and restraint stressed mice. During microarray procedures, measured intensity of the probes is affected by systemic spatial variability due to factors such as unequal distribution of RNA sample, non-specific binding of labelled sample to the array surface, processing effects such as deposits left after the wash stage, optical noise from the scanner and intensity-dependent dye effect (Burgueno, 2005). Spatial distribution plot determines the correlation between the intensity and location of the probes. In order to reduce the impact of spatial noise on estimation of gene expression, measured intensities were global background corrected by subtracting intensity of the blank probe containing only one single “T” nucleotide, spike-in labeling controls and hybridization controls. Spatial distribution image of raw data (**Figure 6.2A**) confirms a gradient effect of probe location on its intensity that is removed after global background correction (**Figure 6.2B**).

Normalisation aims to remove any obscuring systematic differences between samples that are not of biological origin (Pradervand, 2009). Mean-versus-standard deviation and box plots of raw data (**Figure 6.3A & C**) confirmed quadratic dependency of transcript variance on their mean. Variance stabilizing normalisation, described by Bolstad and colleagues, eliminates this dependency to make the variance independent of the mean and transforms intensity values to log-scale (Bolstad, 2003).

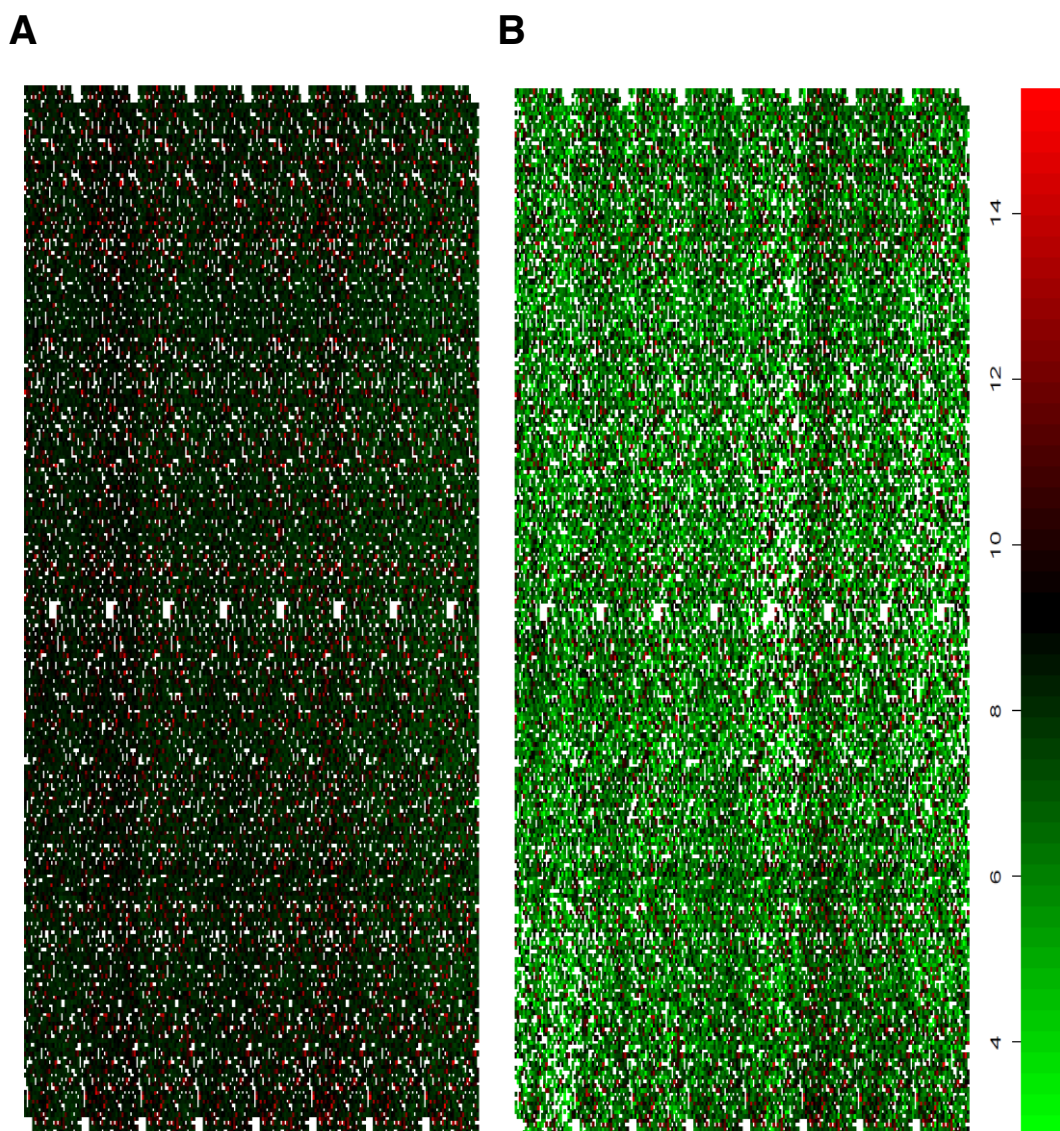


Figure 6.2 Spatial distribution of (A) raw and (B) local background corrected data. Red and green indicate up- and downregulation of the probe, respectively and the numeric scale bar denotes relative intensity values. Adapted from Febit's bioinformatics report.

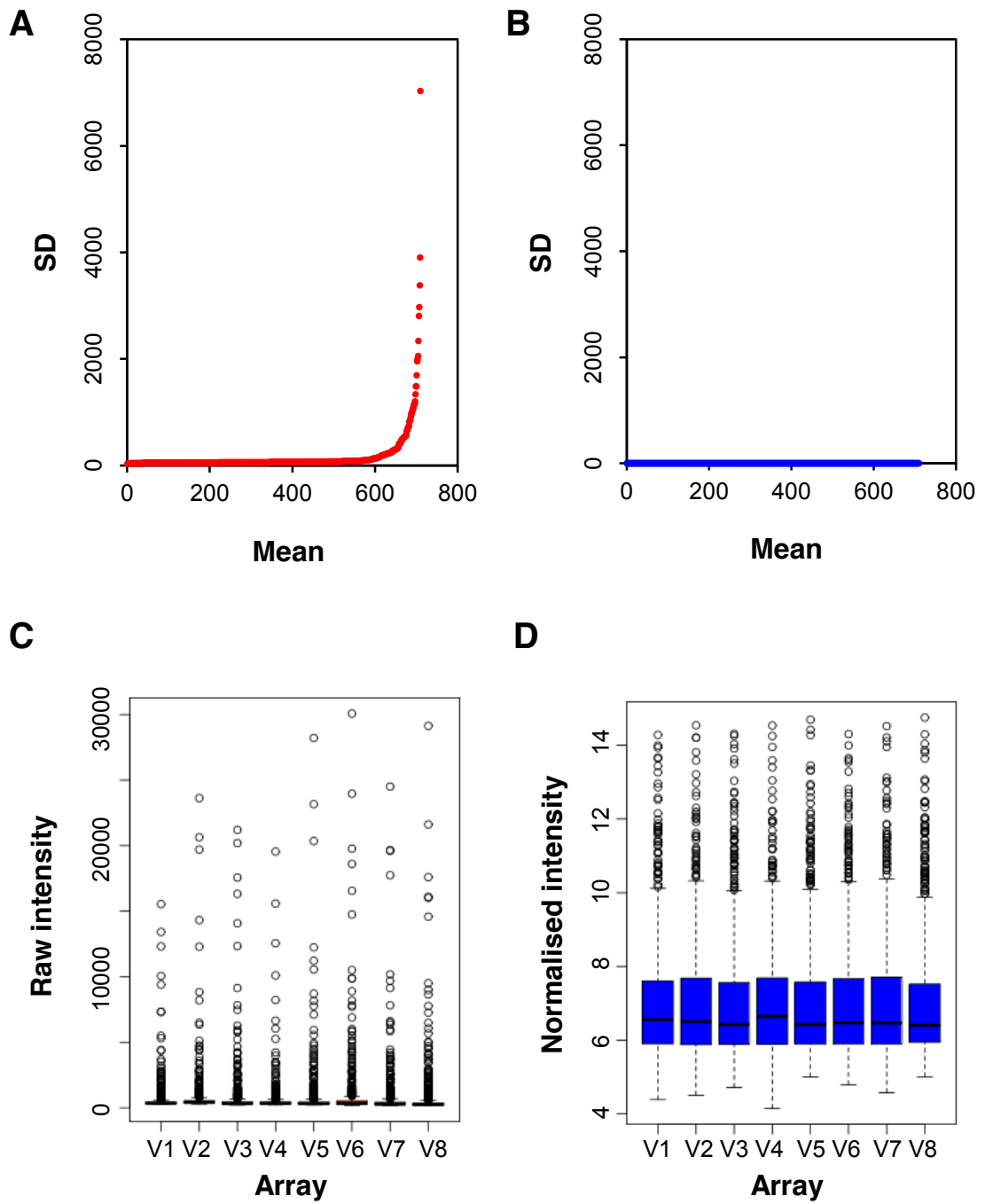


Figure 6.3 Variance stabilizing normalisation. Microarray raw data plotted on (A) mean versus standard deviation and (C) box plot revealed non-uniform distribution of raw data. Variance stabilizing normalised data plotted on (B) mean versus standard deviation and (D) box plot confirmed the positive influence of normalisation on data distribution.

Normalised data exhibited uniform distribution highlighting positive influence of normalisation in mean-versus-standard deviation and box plots (**Figure 6.3B & D**).

Correlation analysis represents Pearson correlation coefficients for inter and intra group samples calculated using probe intensity values (**Figure 6.4**). Biological replicates exhibited much higher correlation whereas control and stress, inter group, arrays comparison revealed lower correlation suggesting stress effect on intensity of probes. However the differences between inter and intra group correlation coefficient is rather smaller presumably because stress affects expression of only a fraction of miRNAs leaving majority of probes unchanged in biologically related samples.

Principal component analysis is a tool that compresses data dimensionality to identify the expression pattern by using covariance analysis between factors (Quackenbush, 2001). Screeplot indicates that first principal component carries the highest data variance and applying further principal components results in simultaneous reduction in degree of variances and data dimensionality (**Figure 6.5A**). Control and stressed samples display distinctive expression pattern from each other in three-dimension scatter plot of three principal components (**Figure 6.5B**).

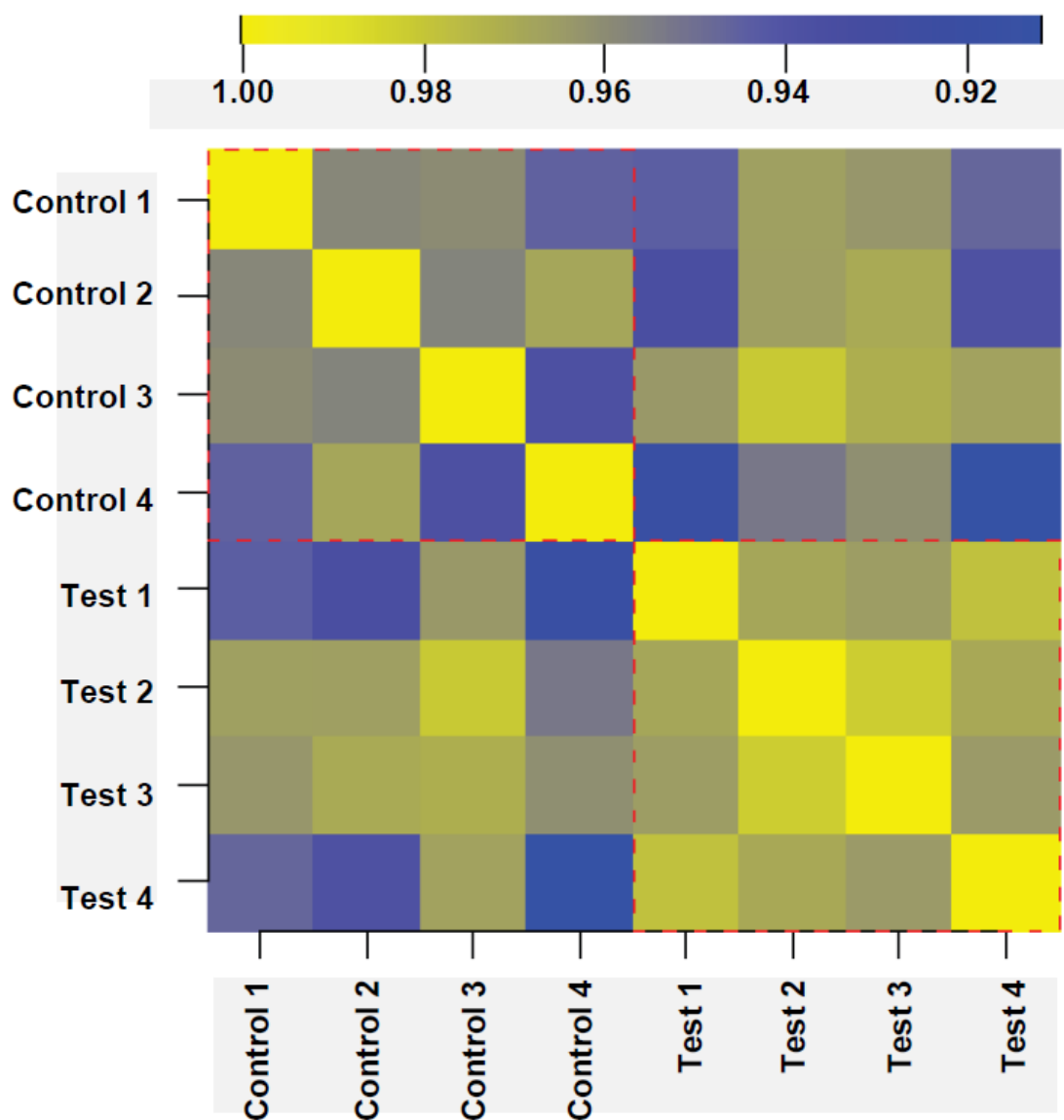


Figure 6.4 Correlation analysis. Correlation between replicates enclosed by red dashed boxes and samples between two groups are presented as a matrix. Blue and yellow indicate low and high correlation between the samples, respectively and the numeric scale bar denotes relative correlation coefficient value. Adapted from Febit's bioinformatics report.

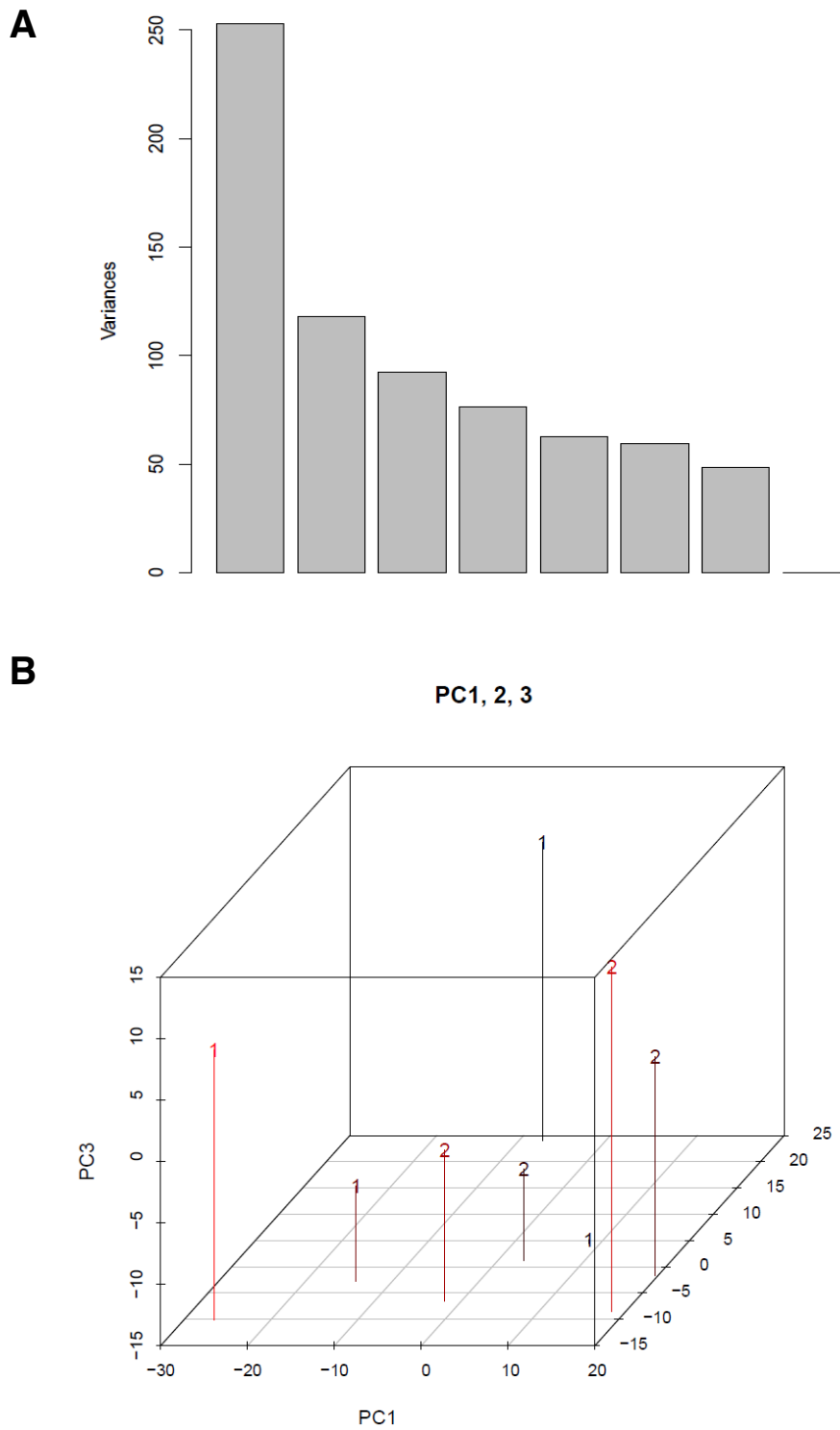


Figure 6.5 Principal component analysis. (A) Screenplot depicts eigenvalues for all the principal components. (B) Three dimension scatter plot of principal component analysis confirms control and test samples are clearly separate from each other. 1, control samples; 2, test/stress samples. Adapted from Febit's bioinformatics report.

Test versus control expression for all probes was compared to detect amygdala miRNAs differentially regulated by restraint stress. An R package, linear models for microarray data (LIMMA), was used to analyse t-Test and empirical Bayesian statistics p-value and p-value adjusted for multiple testing to control false discovery rate. **Table 6.1** represents the list of 20 top most deregulated miRNAs, of which 14 were up- and 6 were down-regulated after stress in the amygdala. However, for small sample size ($n \leq 6$) statistically stable and reliable empirical Bayesian adjusted p-value revealed only five significantly upregulated miRNAs showing more than threefold increase in expression. A volcano plot was generated to visualize the amygdala miRNAs most significantly (empirical Bayesian adjusted $p < 0.05$) and differentially expressed between control and stress samples (**Figure 6.6**).

Hierarchical clustering analysis identifies and pairwise aligns samples and individual probes on the basis of similarities in expression pattern measured using Euclidean distance (Eisen, 1998). Biological replicates clustered together as indicated by dendrogram for samples shown on top of the expression matrix (**Figure 6.7**). Importantly, clustering analysis of 29 highly variable miRNAs revealed one cluster consisted of three significantly stress upregulated amygdala miRNAs mmu-miR-1192, mmu-miR-1892 and mmu-miR-1894-3p (**Figure 6.7**). Therefore, expression of these three miRNAs is similarly regulated by stress in amygdala.

miRNA	Control median	Test median	Fold change	Log fold change	t-Test raw p-value	t-Test adjusted p-value	Empirical Bayesian raw p-value	Empirical Bayesian adjusted p-value
mmu-miR-483	7.752	9.336	4.877	1.585	0.073	0.572	0.000	0.001
mmu-miR-1224	6.051	7.503	4.273	1.452	0.060	0.572	0.000	0.031
mmu-miR-1892	7.086	8.237	3.160	1.151	0.081	0.572	0.000	0.031
mmu-miR-709	8.383	9.528	3.144	1.145	0.063	0.572	0.001	0.105
mmu-miR-1192	6.876	8.021	3.143	1.145	0.024	0.572	0.000	0.001
mmu-miR-1894-3p	7.219	8.356	3.119	1.137	0.063	0.572	0.000	0.006
mmu-miR-1897-5p	6.014	6.966	2.591	0.952	0.128	0.572	0.002	0.105
mmu-miR-1306	5.107	6.047	2.560	0.940	0.017	0.572	0.002	0.105
mmu-miR-376a	9.417	10.309	2.441	0.893	0.003	0.572	0.001	0.090
mmu-miR-150*	5.461	6.270	2.244	0.808	0.143	0.572	0.014	0.228
mmu-miR-1964	4.859	5.596	2.090	0.737	0.067	0.572	0.018	0.252
mmu-miR-669m	8.887	9.622	2.086	0.735	0.070	0.572	0.005	0.169
mmu-miR-32	7.082	6.328	0.470	-0.755	0.049	0.572	0.006	0.169
mmu-miR-703	7.695	6.887	0.446	-0.808	0.086	0.572	0.006	0.169
mmu-miR-470*	6.451	5.620	0.436	-0.831	0.013	0.572	0.001	0.098
mmu-let-7i*	7.798	6.929	0.419	-0.869	0.112	0.572	0.005	0.169
mmu-miR-711	7.641	6.762	0.415	-0.879	0.039	0.572	0.003	0.156
mmu-miR-666-3p	7.685	6.993	0.501	-0.691	0.207	0.572	0.053	0.327
mmu-miR-207	7.767	8.649	2.418	0.883	0.251	0.589	0.009	0.177
mmu-miR-34b-3p	6.598	7.521	2.515	0.922	0.601	0.818	0.049	0.327

Table 6.1 List of 20 amygdala miRNAs most deregulated by stress. miRNAs with empirical Bayesian adjusted $p < 0.05$ are highlighted in red. Modified from Febit's bioinformatics report.

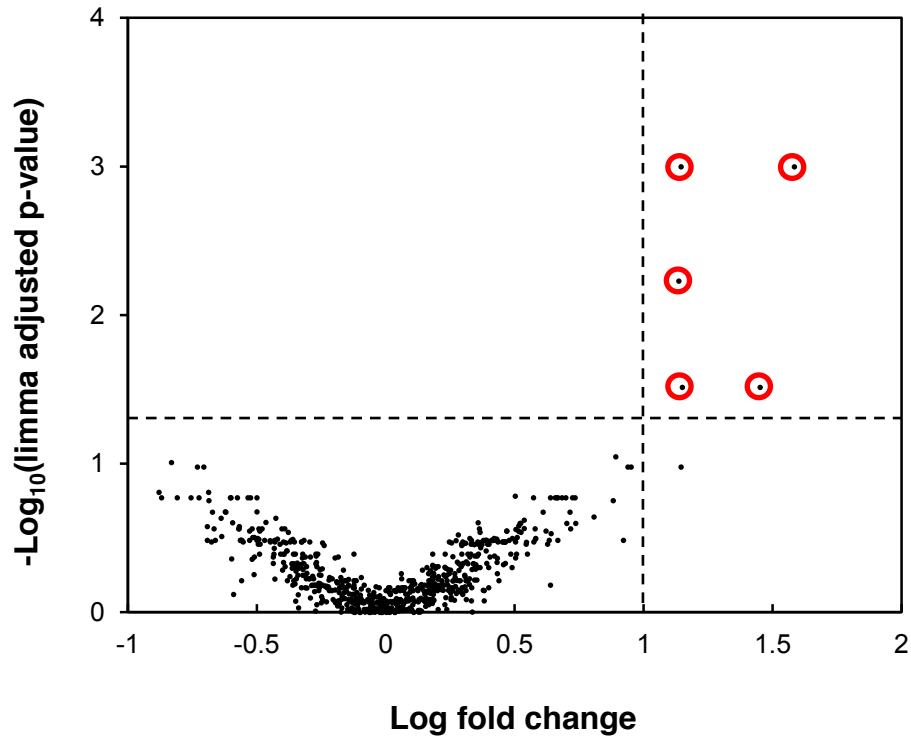


Figure 6.6 Volcano plot of test vs. control expression analysis. Data are plotted as logarithm of fold change for each miRNA probe on x-axis vs. $-\log_{10}(\text{limma adjusted p-value})$ on y-axis. Horizontal line represents the nominal significance level of 0.05. Vertical line represents the logarithmic fold change of 1 (≈ 2.72 fold change). Therefore, significantly stress-upregulated in red circles miRNAs are present in the top right quadrant.

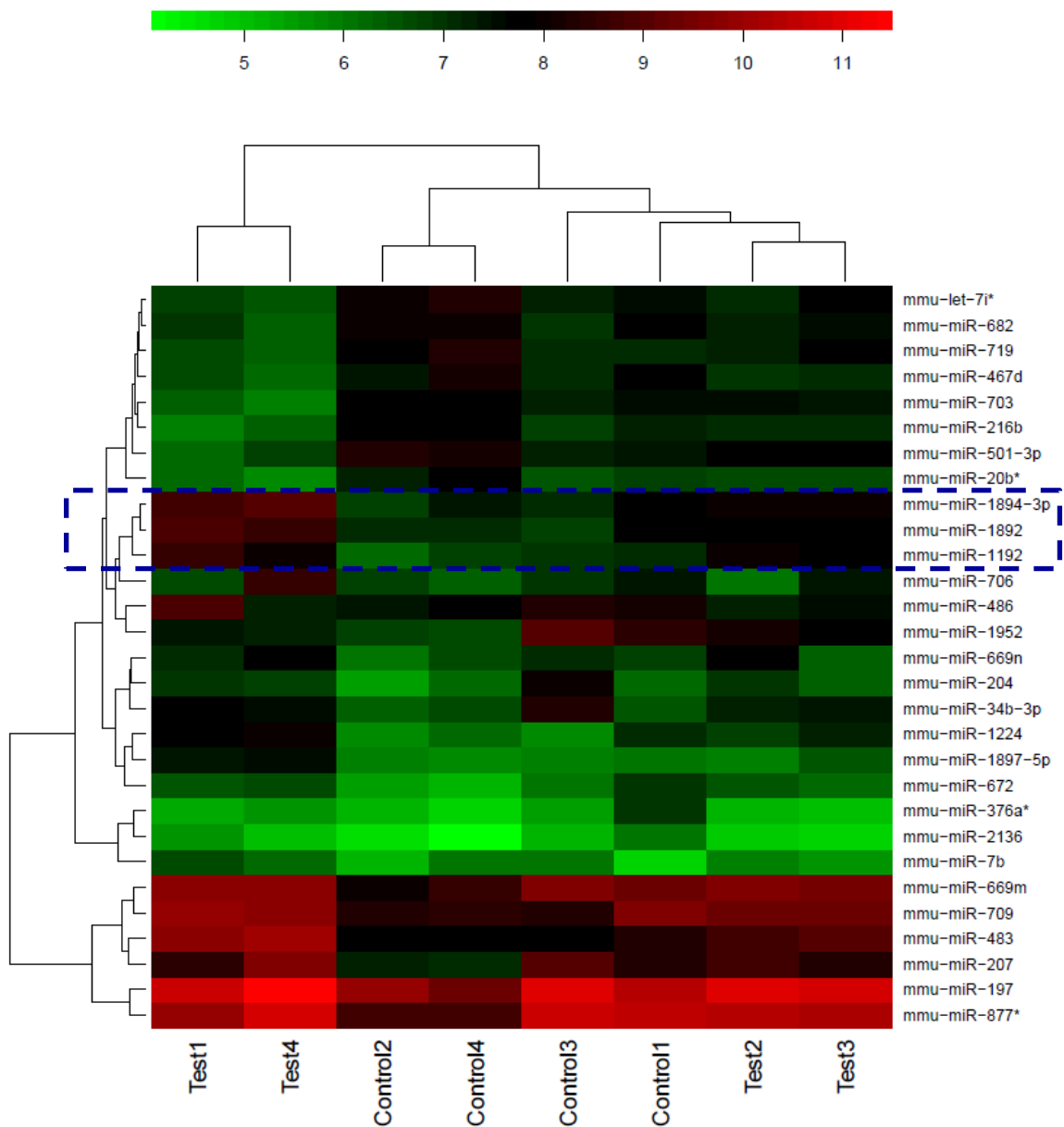


Figure 6.7 Heatmap of hierarchically clustered miRNA probes. Highest overall variability showing 29 miRNAs were clustered using Euclidean distance as a measure. Hierarchy dendrogram for probes are shown on the side and samples on top. Highlighted region outlines the cluster formed by stress-upregulated miRNAs. Red and green indicate up- and downregulation of the probe, respectively and the numeric scale bar denotes relative intensity values. Adapted from Febit's bioinformatics report.

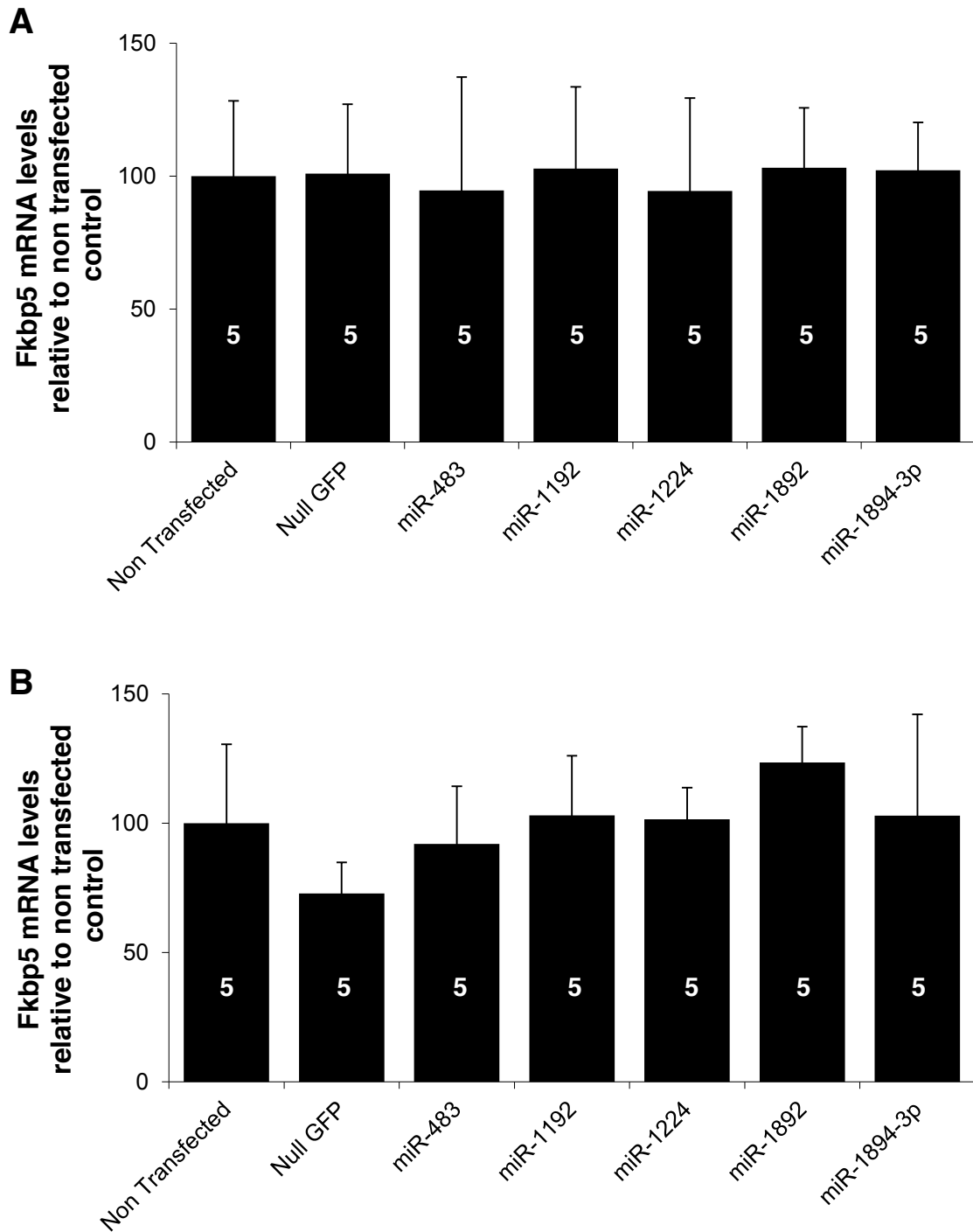


Figure 6.8 Overexpression of stress-upregulated miRNAs has no impact on Fkbp5 expression *in vitro*. Mouse neuroblastoma N2a cells were transfected with constructs overexpressing GFP, miR-483, miR-1192, miR-1224, miR-1892 and miR-1894-3p. RNA was extracted from cells 48 hours later and Fkbp5 transcript levels measured using qRT-PCR. Expression of Fkbp5 was normalized against two housekeeping genes: (A) β -actin and (B) GAPDH. Digits inside column indicate n. Data are shown as mean \pm s.e.m.

Next, we investigated the effect of overexpression of stress upregulated amygdala miRNAs on *Fkbp5* mRNA levels. Mouse neuroblastoma N2a cells were transfected for 48 hours with constructs overexpressing either null GFP or precursors of mmu-miR-483, mmu-miR-1192, mmu-miR-1224, mmu-miR-1892 and mmu-miR-1894-3p. Extracted RNA analysed using qRT-PCR results showed that overexpression of these miRNAs did not cause any significant changes in *Fkbp5* transcript levels when normalised against β -actin (**Figure 6.8A**; One-way ANOVA; $F_{(6,28)} = 0.020$, $p = 1.00$) or GAPDH (**Figure 6.8B**; One-way ANOVA; $F_{(6,28)} = 0.492$, $p = 0.809$).

6.3 Discussion

Microarray experiment is an invaluable tool to study genome-wide expression profiling (Quackenbush, 2001). Exploiting the negative regulation of target mRNA by miRNAs, a commonly used approach is to correlate global mRNA and miRNA expression profiling to identify physiologically important miRNAs and their negatively correlated mRNA targets (Ruike, 2008). With an aim of understanding miRNA regulation of stress upregulated *Fkbp5*, microarray platform was employed to determine amygdala miRNAs differentially regulated by stress.

Baffling more than surprising, microarrays revealed only five amygdala miRNAs that were significantly elevated following stress (**Table 6.1**). Perhaps, microarray data statistical analysis using advanced empirical Bayesian method to compensate for our small n number (n=4 per group) and draw statistically reliable conclusions may have masked some genuine miRNAs. Moreover, Haramati and colleagues recently reported that different microarray platforms, Agilent and Affymetrix, although found some common upregulated miRNAs, but to a larger extent revealed drastically different miRNA expression profile for the same stressed amygdala samples, questioning reliability of the microarray technology (Haramati, 2011). Nevertheless, comparison of miRNA expression profile in the amygdala after 30 minutes and 6 hours of restraint stress elucidated dramatic differences in specific temporal miRNA patterns

underlining their physiological functions in the stress response (Haramati, 2011).

Referring to the classical view - negative post-transcriptional regulation of target mRNA by miRNA - no significantly down-regulated miRNAs were identified to correlate with elevated Fkbp5 in amygdala under stressful conditions (**Table 6.1**). Complementing our speculation, miRNA target prediction algorithms (TargetScan, miRDB, miRanda, Diana-MicroT, microRNA.org, EIMMo3 database and MicroTar) did not predict Fkbp5 as a target molecule of any stress-elevated five miRNAs. Experimentally Fkbp5 expression remains unaltered by overexpression of mmu-miR-483, mmu-miR-1192, mmu-miR-1224, mmu-miR-1892 and mmu-miR-1894-3p (**Figure 6.8 A & B**), further suggesting against any direct miRNA regulation of Fkbp5. It also suggests that stress-upregulated five miRNAs did not block a suppressor of Fkbp5 to indirectly elevate Fkbp5 by reducing suppressive effect. However, studying miRNA effect only on target mRNA level (as opposed to protein level) might not be adequate to draw firm conclusions. miRNAs, unlike siRNAs, can post-transcriptionally regulate target mRNA not only by degradation but also by interference with translation. Therefore, target protein levels also need to be evaluated in future to precisely identify potential miRNA-mRNA interactions.

In summary, our preliminary microarray findings suggest lack of regulation of Fkbp5 in amygdala by stress-related miRNAs.

Chapter 7

Concluding remarks & Future avenues

Severe acute restraint stress episode leads to elevated anxiety-like behaviour in wild-type mice but not in neuropsin-deficient mice (Pawlak, 2003; Attwood, 2011). This body of work explored potential mechanisms of genotypical differences in the behavioural manifestations of stress-mediated anxiety. **Figure 7.1** illustrates proposed model whereby stress regulation of GR co-chaperone, Fkbp5, in the amygdala may contribute to the stress-induced anxiety-like behaviour.

In Chapter 3, we uncovered that attenuated stress-induced upregulation of GR co-chaperone, Fkbp5, in neuropsin^{-/-} mice amygdala underlie their protective phenotype (**Figure 3.1**). Bilateral intra-amygdala injection of recombinant neuropsin restored the concomitant attenuated Fkbp5 elevation (**Figure 3.2**) and anxiolytic behaviour in neuropsin^{-/-} mice (Attwood, 2011). Stress upregulation of Fkbp5 expression is mediated through two independent pathways: corticosterone-dependent and previously unknown, corticosterone-independent pathway. Corticosterone binds to the GREs on the Fkbp5 promoter (Makkonen, 2009; Paakinaho, 2010; Attwood, 2011) and decreases DNA methyltransferase 1 to demethylate CpGs in the promoter and intron 5 region (Lee 2010; Lee 2011; Yang, 2012). Corticosterone-independent pathway, absent in neuropsin^{-/-} mice, involves extracellular domain of EphB2 receptor cleaved by stress-activated extracellular serine protease, neuropsin, facilitating NMDA receptor activity (Attwood, 2011). Elevated Fkbp5 expression in MeCP2-deficient mice independent of their plasma corticosterone levels (Nuber, 2005) suggest towards epigenetic nature of neuropsin-mediated Fkbp5 upregulation.

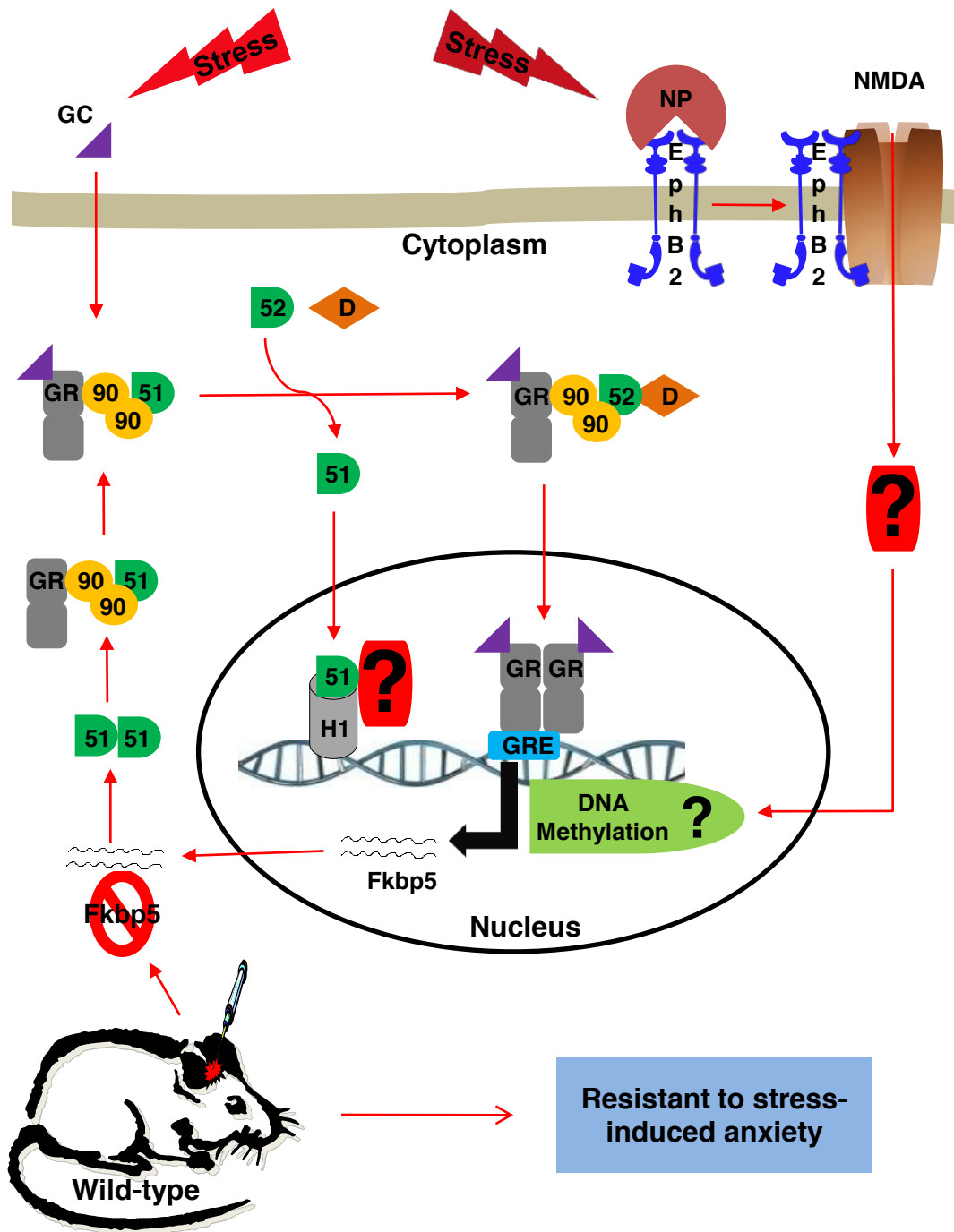


Figure 7.1 Stress regulation of amygdalar FKBP51. Two independent pathways mediate stress-induced FKBP5 expression upregulation in amygdala: corticosterone-dependent and neurotrophin-dependent. Mechanism downstream of neurotrophin pathway still remains unknown. FKBP51 translocates to nucleus following stress. Dexamethasone treatment promotes nuclear FKBP51 interaction with the linker histone H1. Amygdala (red dot)-specific Fkbp5 deletion protects vulnerable wild-type mice from stress-induced anxiety. GC, glucocorticoid; GR, glucocorticoid receptor; 51, FKBP51; 52, FKBP52; 90, Hsp90; D, dynein; GRE, glucocorticoid response element; NP, neurotrophin; NMDA, NMDA receptor; EphB2, EphB2 receptor; H1, histone 1.4.

Phosphorylation of transcription suppressor MeCP2 by calcium influx through NMDA receptor dissociates MeCP2 from the target gene inducing expression (Chen, 2003; Martinowich, 2003). As for epigenetic regulation of Fkbp5, quantitative chromatin immunoprecipitation could be employed to quantify MeCP2 binding to the Fkbp5 genomic sequence in control and stressed mice amygdala. Apart from stress paradigm, direct influence of NMDA receptor stimulation also needs to be studied on MeCP2 binding to the Fkbp5 genomic sequence to further strengthen the hypothesis.

Positive correlation between the extent of elevation in Fkbp5 at the time of trauma and development of PTSD has clinically been reported in human subjects (Segman, 2005). Moreover, Fkbp5 SNPs associated with higher Fkbp5 levels show significantly positive correlation with the development of stress-related psychiatric disorders (Binder, 2009). Clinically Fkbp5 has earned recognition as a genetic predictor of susceptibility to anxiety disorders in interaction with the stressful life events (Bevilacqua, 2012; van Zuiden, 2012). Complementing the clinical findings, significantly reduced elevation of corticosterone levels in stressed, genetic vulnerability factor, Fkbp5 deficient mice confers more active stress-related coping behaviour compared to stressed wild-type mice. Genetic deletion of Fkbp5 accounts for the enhanced GR sensitivity resulting in increased negative feedback of GR on HPA-axis, rapid termination of the stress response and hence, suppressed corticosterone levels (O'Leary III, 2011; Touma, 2011; Hartmann, 2011).

Chapter 5 findings revealed that silencing amygdala specific *Fkbp5* expression protects wild-type mice from severe acute stress-induced anxiogenic behaviour mediated through BNST. However, amygdalar *Fkbp5* deletion does not alter CeA-dependent freezing response to the conditioned fear. Speculatively, deletion of amygdala-specific *Fkbp5* leading to enhanced GR sensitivity, similar to that observed in *Fkbp5*^{-/-} mice, is rather an unlikely phenomenon. Supporting the notion, equivalent increase in plasma corticosterone levels of stressed wild-type and *neurospn*^{-/-} mice suggest that stress-resistant phenotype of *neurospn*^{-/-} mice is also independent of altered HPA-axis function (**Figure 3.3**). Additionally rescuing attenuated upregulation of amygdala specific *Fkbp5* by intra-amygdala *neurospn* injection alone restores the vulnerability to stress-induced anxiety in *neurospn*^{-/-} mice (**Figure 3.2**; Attwood, 2011). Therefore, our findings highlight previously unknown crucial amygdalar *Fkbp5* contribution to the stress-induced anxiety that is independent from *Fkbp5* regulation of GR sensitivity and HPA-axis function.

In addition to orchestrating the stress response, limbic brain structure, the amygdala, also acts as a relay station and storage site for traumatic emotional memories (LeDoux, 1994; Herman, 1997). Various psychological stress paradigms eliciting, either delayed or rapid, neuronal remodeling in the BLA exhibit concomitant heightened anxiety-like behaviour, and vice versa (Mitra, 2005). Acute restraint stress, paradigm employed in this study, induced

anxiogenic behaviour remains to be associated with plasticity changes in the BLA dendritic morphology using Golgi-staining technique.

Stress-regulation of amygdalar FKBP51, examined in chapter 4, confirmed the differential upregulation of FKBP51 between stressed wild-type (almost two-fold) and *neurospine*^{-/-} (unaltered) mice amygdala, reflecting the *Fkbp5* expression pattern (**Figure 4.1**). A remarkable aspect, however, is the stress-triggered dynamic nuclear translocation of predominantly cytoplasmic amygdalar FKBP51 in the wild-type mice (**Figure 4.3**). Proteomic analysis of nuclear FKBP51 interactome identified transcription regulator histone H1.4 as potential interaction partner portraying FKBP51 as modulator of histone H1.4-mediated gene expression (**Figure 4.7 & Table 4.3**).

Hence, we propose that, similar to GCs (Mitra, 2008), FKBP51-mediated modification of linker histone H1.4 transcription activity contributes to the stress-induced structural plasticity in the amygdala that underlies anxiety-like behaviour. Our hypothesis is further strengthened by a plethora of studies showing that posttranslational modification of histone proteins modulates transcription of genes required for long-lasting form of synaptic plasticity and memory (Borrelli, 2005; Barrett, 2008). For instance, stressful stimuli triggered activation of poly[ADP-ribose] polymerase 1 leads to polyADP-ribosylation modification of histone H1 required for long-term memory formation in the hippocampus (Virag, 2002; Cohen-Armon, 2004; Fontan-Lozano, 2010). Scaffolding protein FKBP51 has previously been shown to modulate

posttranslational phosphorylation of Akt in cancer cells (Pei, 2009). Although experimentally differential BLA neuronal remodeling in stressed wild-type and amygdala specific *Fkbp5* deficient mice needs to be investigated using Golgi staining. Speculatively, resilience of *neuropsin*^{-/-} mice to stress-induced anxiety is not due to impaired nuclear translocation of FKBP51 since stress-triggered nuclear translocation of FKBP51 in the amygdala is unlikely to be disrupted by *neuropsin*. Therefore, hypothetical involvement of FKBP51 in epigenetic mechanism of neuronal plasticity is although crucial, the magnitude of amygdalar FKBP51 elevation and its dynamic regulation in response to stress is undoubtedly indispensable for the stress-related behavioural manifestations.

To summarize, this study demonstrates that extent of stress-induced upregulation in amygdalar *Fkbp5* expression is directly proportional to the adverse anxiety-like behavioural effects of stress. Involvement of FKBP51 in stress response is not limited to its regulation of GR and the HPA-axis. Instead cytoplasmic amygdalar FKBP51 is transported across the nuclear membrane where it may modulate posttranslational modification of linker histone H1 contributing to the neuronal remodeling in amygdala. Most importantly, silencing *Fkbp5* expression in the amygdala protects wild-type mice from the stress-related anxiety behaviour. Therefore, pharmacological intervention of selective amygdalar *Fkbp5* in vulnerable individuals offers promising treatment regimen for stress-related anxiety disorders.

Appendix I

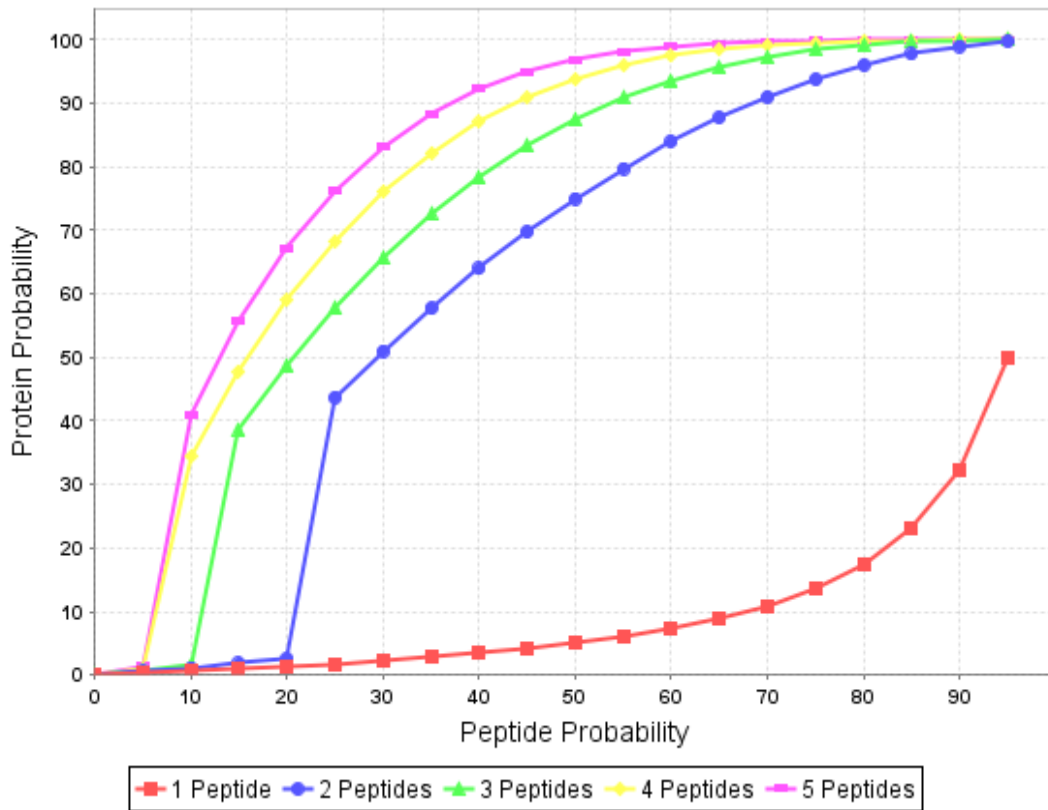


Figure I.1 Graphical presentation of relationship between protein and peptide probabilities. According to the plot, with 2 unique peptides of 95% probability predicted protein being correct are around 99%. Adopted from Scaffold user's manual.

Bibliography

- Aebersold R. A mass spectrometric journey into protein and proteome research. *J Am Soc Mass Spectrom* 14(7), 685-95, 2003.
- Aebersold R, Mann M. Mass spectrometry-based proteomics. *Nature* 422(6928), 198-207, 2003.
- Alami R, Fan Y, Pack S, Sonbuchner TM, Besse A, Lin Q, Greally JM, Skoultchi AI, Bouhassira EE. Mammalian linker-histone subtypes differentially affect gene expression in vivo. *Proc Natl Acad Sci U S A* 100(10), 5920-5, 2003.
- Appel K, Schwahn C, Mahler J, Schulz A, Spitzer C, Fenske K, Stender J, Barnow S, John U, Teumer A, Biffar R, Nauck M, Volzke H, Freyberger HJ, Grabe HJ. Moderation of adult depression by a polymorphism in the FKBP5 gene and childhood physical abuse in the general population. *Neuropsychopharmacology* 36(10), 1982-91, 2011.
- Arvanitis D, Davy A. Eph/ephrin signaling: networks. *Genes Dev* 22(4), 416-29, 2008.
- American Psychiatric Association. Diagnostic and statistical manual of mental disorders. Fourth edition, text revision. . In: Association AP, (Ed), Vol., Washington DC, 2000. .
- Attwood BK, Bourgoignon JM, Patel S, Mucha M, Schiavon E, Skrzypiec AE, Young KW, Shiosaka S, Korostynski M, Piechota M, Przewlocki R, Pawlak R. Neuropsin cleaves EphB2 in the amygdala to control anxiety. *Nature* 473(7347), 372-5, 2011.
- Banerjee A, Periyasamy S, Wolf IM, Hinds TD, Jr., Yong W, Shou W, Sanchez ER. Control of glucocorticoid and progesterone receptor subcellular localization by the ligand-binding domain is mediated by distinct interactions with tetratricopeptide repeat proteins. *Biochemistry* 47(39), 10471-80, 2008.
- Barent RL, Nair SC, Carr DC, Ruan Y, Rimerman RA, Fulton J, Zhang Y, Smith DF. Analysis of FKBP51/FKBP52 chimeras and mutants for Hsp90 binding and association with progesterone receptor complexes. *Mol Endocrinol* 12(3), 342-54, 1998.

- Barlow DH. Unraveling the mysteries of anxiety and its disorders from the perspective of emotion theory. *Am Psychol* 55(11), 1247-63, 2000.
- Barlow DH, Wincze J. DSM-IV and beyond: what is generalized anxiety disorder? *Acta Psychiatr Scand Suppl* 393, 23-9, 1998.
- Barrett RM, Wood MA. Beyond transcription factors: the role of chromatin modifying enzymes in regulating transcription required for memory. *Learn Mem* 15(7), 460-7, 2008.
- Baughman G, Harrigan MT, Campbell NF, Nurrish SJ, Bourgeois S. Genes newly identified as regulated by glucocorticoids in murine thymocytes. *Mol Endocrinol* 5(5), 637-44, 1991.
- Baughman G, Wiederrecht GJ, Campbell NF, Martin MM, Bourgeois S. FKBP51, a novel T-cell-specific immunophilin capable of calcineurin inhibition. *Mol Cell Biol* 15(8), 4395-402, 1995.
- Baughman G, Wiederrecht GJ, Chang F, Martin MM, Bourgeois S. Tissue distribution and abundance of human FKBP51, and FK506-binding protein that can mediate calcineurin inhibition. *Biochem Biophys Res Commun* 232(2), 437-43, 1997.
- Behm-Ansmant I, Rehwinkel J, Doerks T, Stark A, Bork P, Izaurralde E. mRNA degradation by miRNAs and GW182 requires both CCR4:NOT deadenylase and DCP1:DCP2 decapping complexes. *Genes Dev* 20(14), 1885-98, 2006.
- Belzung C, Griebel G. Measuring normal and pathological anxiety-like behaviour in mice: a review. *Behav Brain Res* 125(1-2), 141-9, 2001.
- Belzung C, Le Pape G. Comparison of different behavioral test situations used in psychopharmacology for measurement of anxiety. *Physiol Behav* 56(3), 623-8, 1994.
- Bevilacqua L, Carli V, Sarchiapone M, George DK, Goldman D, Roy A, Enoch MA. Interaction between FKBP5 and childhood trauma and risk of aggressive behavior. *Arch Gen Psychiatry* 69(1), 62-70, 2012.
- Biedenkapp JC, Rudy JW. Hippocampal and extrahippocampal systems compete for control of contextual fear: role of ventral subiculum and amygdala. *Learn Mem* 16(1), 38-45, 2009.
- Billing AM. Crosstalk between stress responses, mediators and the immune system: a proteomic approach. Department of Immunology, Doctoral thesis. University of Trier, Deutschland, 2008.

- Billing AM, Fack F, Renaut J, Olinger CM, Schote AB, Turner JD, Muller CP. Proteomic analysis of the cortisol-mediated stress response in THP-1 monocytes using DIGE technology. *J Mass Spectrom* 42(11), 1433-44, 2007.
- Binder EB. The role of FKBP5, a co-chaperone of the glucocorticoid receptor in the pathogenesis and therapy of affective and anxiety disorders. *Psychoneuroendocrinology* 34 Suppl 1, S186-95, 2009.
- Binder EB, Bradley RG, Liu W, Epstein MP, Deveau TC, Mercer KB, Tang Y, Gillespie CF, Heim CM, Nemeroff CB, Schwartz AC, Cubells JF, Ressler KJ. Association of FKBP5 polymorphisms and childhood abuse with risk of posttraumatic stress disorder symptoms in adults. *JAMA* 299(11), 1291-305, 2008.
- Binder EB, Salyakina D, Lichtner P, Wochnik GM, Ising M, Putz B, Papiol S, Seaman S, Lucae S, Kohli MA, Nickel T, Kunzel HE, Fuchs B, Majer M, Pfennig A, Kern N, Brunner J, Modell S, Baghai T, Deiml T, Zill P, Bondy B, Rupprecht R, Messer T, Kohnlein O, Dabitz H, Bruckl T, Muller N, Pfister H, Lieb R, Mueller JC, Lohmussaar E, Strom TM, Bettecken T, Meitinger T, Uhr M, Rein T, Holsboer F, Muller-Myhsok B. Polymorphisms in FKBP5 are associated with increased recurrence of depressive episodes and rapid response to antidepressant treatment. *Nat Genet* 36(12), 1319-25, 2004.
- Bolstad BM, Irizarry RA, Astrand M, Speed TP. A comparison of normalization methods for high density oligonucleotide array data based on variance and bias. *Bioinformatics* 19(2), 185-93, 2003.
- Bordi F, LeDoux JE. Response properties of single units in areas of rat auditory thalamus that project to the amygdala. II. Cells receiving convergent auditory and somatosensory inputs and cells antidromically activated by amygdala stimulation. *Exp Brain Res* 98(2), 275-86, 1994.
- Bordi F, LeDoux JE. Response properties of single units in areas of rat auditory thalamus that project to the amygdala. I. Acoustic discharge patterns and frequency receptive fields. *Exp Brain Res* 98(2), 261-74, 1994.
- Borrelli E, Nestler EJ, Allis CD, Sassone-Corsi P. Decoding the epigenetic language of neuronal plasticity. *Neuron* 60(6), 961-74, 2008.
- Bourin M, Petit-Demouliere B, Dhonnchadha BN, Hascoet M. Animal models of anxiety in mice. *Fundam Clin Pharmacol* 21(6), 567-74, 2007.
- Brent D, Melhem N, Ferrell R, Emslie G, Wagner KD, Ryan N, Vitiello B, Birmaher B, Mayes T, Zelazny J, Onorato M, Devlin B, Clarke G, DeBar L,

- Keller M. Association of FKBP5 polymorphisms with suicidal events in the Treatment of Resistant Depression in Adolescents (TORDIA) study. *Am J Psychiatry* 167(2), 190-7, 2010.
- Brent D, Melhem N, Turecki G. Pharmacogenomics of suicidal events. *Pharmacogenomics* 11(6), 793-807, 2010.
- Brown S, Schafer EA. An investigations into the functions of the occipital and temporal lobes of the monkey's brain. *Philosophical Transactions of the Royal Society London, Series B* B179, 303-27, 1888.
- Bucci DJ, Phillips RG, Burwell RD. Contributions of postrhinal and perirhinal cortex to contextual information processing. *Behav Neurosci* 114(5), 882-94, 2000.
- Bucci DJ, Saddoris MP, Burwell RD. Contextual fear discrimination is impaired by damage to the postrhinal or perirhinal cortex. *Behav Neurosci* 116(3), 479-88, 2002.
- Buchan JR, Parker R. Molecular biology. The two faces of miRNA. *Science* 318(5858), 1877-8, 2007.
- Buffalo EA, Ramus SJ, Clark RE, Teng E, Squire LR, Zola SM. Dissociation between the effects of damage to perirhinal cortex and area TE. *Learn Mem* 6(6), 572-99, 1999.
- Burguen J, Crossa J, Grimanelli D, Leblanc O, Autran D. Spatial Analysis of cDNA Microarray Experiments. *Crop Science* 45(2), 748-57, 2005.
- Bushati N, Cohen SM. microRNA functions. *Annu Rev Cell Dev Biol* 23, 175-205, 2007.
- Cannell IG, Kong YW, Bushell M. How do microRNAs regulate gene expression? *Biochem Soc Trans* 36(Pt 6), 1224-31, 2008.
- Carobrez AP, Bertoglio LJ. Ethological and temporal analyses of anxiety-like behavior: the elevated plus-maze model 20 years on. *Neurosci Biobehav Rev* 29(8), 1193-205, 2005.
- Chen WG, Chang Q, Lin Y, Meissner A, West AE, Griffith EC, Jaenisch R, Greenberg ME. Derepression of BDNF transcription involves calcium-dependent phosphorylation of MeCP2. *Science* 302(5646), 885-9, 2003.
- Chen ZL, Yoshida S, Kato K, Momota Y, Suzuki J, Tanaka T, Ito J, Nishino H, Aimoto S, Kiyama H, et al. Expression and activity-dependent changes of a

- novel limbic-serine protease gene in the hippocampus. *J Neurosci* 15(7 Pt 2), 5088-97, 1995.
- Cheung-Flynn J, Roberts PJ, Riggs DL, Smith DF. C-terminal sequences outside the tetratricopeptide repeat domain of FKBP51 and FKBP52 cause differential binding to Hsp90. *J Biol Chem* 278(19), 17388-94, 2003.
- Cho YH, Friedman E, Silva AJ. Ibotenate lesions of the hippocampus impair spatial learning but not contextual fear conditioning in mice. *Behav Brain Res* 98(1), 77-87, 1999.
- Cisse M, Halabisky B, Harris J, Devidze N, Dubal DB, Sun B, Orr A, Lotz G, Kim DH, Hamto P, Ho K, Yu GQ, Mucke L. Reversing EphB2 depletion rescues cognitive functions in Alzheimer model. *Nature* 469(7328), 47-52, 2011.
- Cohen-Armon M, Visochek L, Katzoff A, Levitan D, Susswein AJ, Klein R, Valbrun M, Schwartz JH. Long-term memory requires polyADP-ribosylation. *Science* 304(5678), 1820-2, 2004.
- Crawley JN, Paylor R. A proposed test battery and constellations of specific behavioral paradigms to investigate the behavioral phenotypes of transgenic and knockout mice. *Horm Behav* 31(3), 197-211, 1997.
- Cryan JF, Holmes A. The ascent of mouse: advances in modelling human depression and anxiety. *Nat Rev Drug Discov* 4(9), 775-90, 2005.
- Dalva MB, Takasu MA, Lin MZ, Shamah SM, Hu L, Gale NW, Greenberg ME. EphB receptors interact with NMDA receptors and regulate excitatory synapse formation. *Cell* 103(6), 945-56, 2000.
- Davies TH, Ning YM, Sanchez ER. A new first step in activation of steroid receptors: hormone-induced switching of FKBP51 and FKBP52 immunophilins. *J Biol Chem* 277(7), 4597-600, 2002.
- Davis M. Are different parts of the extended amygdala involved in fear versus anxiety? *Biol Psychiatry* 44(12), 1239-47, 1998.
- Davis M. Neural systems involved in fear and anxiety measured with fear-potentiated startle. *Am Psychol* 61(8), 741-56, 2006.
- Davis M, Shi C. The amygdala. *Curr Biol* 10(4), R131, 2000.
- de Kloet ER, Joels M, Holsboer F. Stress and the brain: from adaptation to disease. *Nat Rev Neurosci* 6(6), 463-75, 2005.

- Denny WB, Prapapanich V, Smith DF, Scammell JG. Structure-function analysis of squirrel monkey FK506-binding protein 51, a potent inhibitor of glucocorticoid receptor activity. *Endocrinology* 146(7), 3194-201, 2005.
- Denny WB, Valentine DL, Reynolds PD, Smith DF, Scammell JG. Squirrel monkey immunophilin FKBP51 is a potent inhibitor of glucocorticoid receptor binding. *Endocrinology* 141(11), 4107-13, 2000.
- Drescher U. Excitation at the synapse: Eph receptors team up with NMDA receptors. *Cell* 103(7), 1005-8, 2000.
- Drescher U. Eph receptor tyrosine kinases and their ligands in development. *Ernst Schering Res Found Workshop* (29), 151-64, 2000.
- Eichenbaum H. The hippocampus and declarative memory: cognitive mechanisms and neural codes. *Behav Brain Res* 127(1-2), 199-207, 2001.
- Eichenbaum H. The long and winding road to memory consolidation. *Nat Neurosci* 4(11), 1057-8, 2001.
- Eisen MB, Spellman PT, Brown PO, Botstein D. Cluster analysis and display of genome-wide expression patterns. *Proc Natl Acad Sci U S A* 95(25), 14863-8, 1998.
- Endler NS, Kocovski NL. State and trait anxiety revisited. *J Anxiety Disord* 15(3), 231-45, 2001.
- Eulalio A, Huntzinger E, Izaurralde E. Getting to the root of miRNA-mediated gene silencing. *Cell* 132(1), 9-14, 2008.
- Fontan-Lozano A, Suarez-Pereira I, Horrillo A, del-Pozo-Martin Y, Hmadcha A, Carrion AM. Histone H1 poly[ADP]-ribosylation regulates the chromatin alterations required for learning consolidation. *J Neurosci* 30(40), 13305-13, 2010.
- Frey U, Morris RG. Synaptic tagging and long-term potentiation. *Nature* 385(6616), 533-6, 1997.
- Galigniana MD, Harrell JM, Murphy PJ, Chinkers M, Radanyi C, Renoir JM, Zhang M, Pratt WB. Binding of hsp90-associated immunophilins to cytoplasmic dynein: direct binding and in vivo evidence that the peptidylprolyl isomerase domain is a dynein interaction domain. *Biochemistry* 41(46), 13602-10, 2002.

- Gallo LI, Lagadari M, Piwien-Pilipuk G, Galigniana MD. The 90-kDa heat-shock protein (Hsp90)-binding immunophilin FKBP51 is a mitochondrial protein that translocates to the nucleus to protect cells against oxidative stress. *J Biol Chem* 286(34), 30152-60, 2011.
- Genander M, Halford MM, Xu NJ, Eriksson M, Yu Z, Qiu Z, Martling A, Greicius G, Thakar S, Catchpole T, Chumley MJ, Zdunek S, Wang C, Holm T, Goff SP, Pettersson S, Pestell RG, Henkemeyer M, Frisen J. Dissociation of EphB2 signaling pathways mediating progenitor cell proliferation and tumor suppression. *Cell* 139(4), 679-92, 2009.
- Grad I, Picard D. The glucocorticoid responses are shaped by molecular chaperones. *Mol Cell Endocrinol* 275(1-2), 2-12, 2007.
- Gray TS, Bingaman EW. The amygdala: corticotropin-releasing factor, steroids, and stress. *Crit Rev Neurobiol* 10(2), 155-68, 1996.
- Greene LA, Rein G. Synthesis, storage and release of acetylcholine by a noradrenergic pheochromocytoma cell line. *Nature (London)* 268, 349-351, 1977.
- Grunwald IC, Korte M, Wolfer D, Wilkinson GA, Unsicker K, Lipp HP, Bonhoeffer T, Klein R. Kinase-independent requirement of EphB2 receptors in hippocampal synaptic plasticity. *Neuron* 32(6), 1027-40, 2001.
- Hall CS. Emotional behavior in the rat. III. The relationship between emotionality and ambulatory activity. *Journal of Comparative Psychology* 22(3), 345-52, 1936.
- Hammen C. Life events and depression: the plot thickens. *Am J Community Psychol* 20(2), 179-93, 1992.
- Hammen C, Davila J, Brown G, Ellicott A, Gitlin M. Psychiatric history and stress: predictors of severity of unipolar depression. *J Abnorm Psychol* 101(1), 45-52, 1992.
- Handley SL, Mithani S. Effects of alpha-adrenoceptor agonists and antagonists in a maze-exploration model of 'fear'-motivated behaviour. *Naunyn Schmiedebergs Arch Pharmacol* 327(1), 1-5, 1984.
- Haramati S, Navon I, Issler O, Ezra-Nevo G, Gil S, Zwang R, Hornstein E, Chen A. MicroRNA as repressors of stress-induced anxiety: the case of amygdalar miR-34. *J Neurosci* 31(40), 14191-203, 2011.

- Hartmann J, Wagner KV, Liebl C, Scharf SH, Wang XD, Wolf M, Hausch F, Rein T, Schmidt U, Touma C, Cheung-Flynn J, Cox MB, Smith DF, Holsboer F, Muller MB, Schmidt MV. The involvement of FK506-binding protein 51 (FKBP5) in the behavioral and neuroendocrine effects of chronic social defeat stress. *Neuropharmacology* 62(1), 332-9, 2012.
- Heim C, Newport DJ, Bonsall R, Miller AH, Nemeroff CB. Altered pituitary-adrenal axis responses to provocative challenge tests in adult survivors of childhood abuse. *Am J Psychiatry* 158(4), 575-81, 2001.
- Henderson JT, Georgiou J, Jia Z, Robertson J, Elowe S, Roder JC, Pawson T. The receptor tyrosine kinase EphB2 regulates NMDA-dependent synaptic function. *Neuron* 32(6), 1041-56, 2001.
- Henkemeyer M, Itkis OS, Ngo M, Hickmott PW, Ethell IM. Multiple EphB receptor tyrosine kinases shape dendritic spines in the hippocampus. *J Cell Biol* 163(6), 1313-26, 2003.
- Herman JP, Cullinan WE. Neurocircuitry of stress: central control of the hypothalamo-pituitary-adrenocortical axis. *Trends Neurosci* 20(2), 78-84, 1997.
- Herman JP, Figueiredo H, Mueller NK, Ulrich-Lai Y, Ostrander MM, Choi DC, Cullinan WE. Central mechanisms of stress integration: hierarchical circuitry controlling hypothalamo-pituitary-adrenocortical responsiveness. *Front Neuroendocrinol* 24(3), 151-80, 2003.
- Herman JP, Ostrander MM, Mueller NK, Figueiredo H. Limbic system mechanisms of stress regulation: hypothalamo-pituitary-adrenocortical axis. *Prog Neuropsychopharmacol Biol Psychiatry* 29(8), 1201-13, 2005.
- Hirata A, Yoshida S, Inoue N, Matsumoto-Miyai K, Ninomiya A, Taniguchi M, Matsuyama T, Kato K, Iizasa H, Kataoka Y, Yoshida N, Shiosaka S. Abnormalities of synapses and neurons in the hippocampus of neurotrophin-deficient mice. *Mol Cell Neurosci* 17(3), 600-10, 2001.
- Hitchcock J, Davis M. Lesions of the amygdala, but not of the cerebellum or red nucleus, block conditioned fear as measured with the potentiated startle paradigm. *Behav Neurosci* 100(1), 11-22, 1986.
- Hitchcock JM, Davis M. Fear-potentiated startle using an auditory conditioned stimulus: effect of lesions of the amygdala. *Physiol Behav* 39(3), 403-8, 1987.

- Hitchcock JM, Davis M. Efferent pathway of the amygdala involved in conditioned fear as measured with the fear-potentiated startle paradigm. *Behav Neurosci* 105(6), 826-42, 1991.
- Hogg S. A review of the validity and variability of the elevated plus-maze as an animal model of anxiety. *Pharmacol Biochem Behav* 54(1), 21-30, 1996.
- Horstmann S, Lucae S, Menke A, Hennings JM, Ising M, Roeske D, Muller-Myhsok B, Holsboer F, Binder EB. Polymorphisms in GRIK4, HTR2A, and FKBP5 show interactive effects in predicting remission to antidepressant treatment. *Neuropsychopharmacology* 35(3), 727-40, 2010.
- Hubler TR, Scammell JG. Intronic hormone response elements mediate regulation of FKBP5 by progestins and glucocorticoids. *Cell Stress Chaperones* 9(3), 243-52, 2004.
- Hunsberger JG, Austin DR, Chen G, Manji HK. MicroRNAs in mental health: from biological underpinnings to potential therapies. *Neuromolecular Med* 11(3), 173-82, 2009.
- Ishikawa Y, Horii Y, Tamura H, Shiosaka S. Neuropsin (KLK8)-dependent and -independent synaptic tagging in the Schaffer-collateral pathway of mouse hippocampus. *J Neurosci* 28(4), 843-9, 2008.
- Ishikawa Y, Tamura H, Shiosaka S. Diversity of neuropsin (KLK8)-dependent synaptic associativity in the hippocampal pyramidal neuron. *J Physiol* 589(Pt 14), 3559-73, 2011.
- Ising M, Depping AM, Siebertz A, Lucae S, Unschuld PG, Kloiber S, Horstmann S, Uhr M, Muller-Myhsok B, Holsboer F. Polymorphisms in the FKBP5 gene region modulate recovery from psychosocial stress in healthy controls. *Eur J Neurosci* 28(2), 389-98, 2008.
- Jaaskelainen T, Makkonen H, Palvimo JJ. Steroid up-regulation of FKBP51 and its role in hormone signaling. *Curr Opin Pharmacol* 11(4), 326-31, 2011.
- Jenuwein T. Re-SET-ting heterochromatin by histone methyltransferases. *Trends Cell Biol* 11(6), 266-73, 2001.
- Jenuwein T, Allis CD. Translating the histone code. *Science* 293(5532), 1074-80, 2001.
- Kandel ER, Pittenger C. The past, the future and the biology of memory storage. *Philos Trans R Soc Lond B Biol Sci* 354(1392), 2027-52, 1999.

- Kasckow JW, Regmi A, Gill PS, Parkes DG, Geraciotti TD. Regulation of corticotropin-releasing factor (CRF) messenger ribonucleic acid and CRF peptide in the amygdala: studies in primary amygdalar cultures. *Endocrinology* 138, 4774-4782, 1997.
- Kelleher RJ, 3rd, Govindarajan A, Tonegawa S. Translational regulatory mechanisms in persistent forms of synaptic plasticity. *Neuron* 44(1), 59-73, 2004.
- Kessler RC, Chiu WT, Demler O, Merikangas KR, Walters EE. Prevalence, severity, and comorbidity of 12-month DSM-IV disorders in the National Comorbidity Survey Replication. *Arch Gen Psychiatry* 62(6), 617-27, 2005.
- Kessler RC, Demler O, Frank RG, Olfson M, Pincus HA, Walters EE, Wang P, Wells KB, Zaslavsky AM. Prevalence and treatment of mental disorders, 1990 to 2003. *N Engl J Med* 352(24), 2515-23, 2005.
- Kirchheiner J, Lorch R, Lebedeva E, Seeringer A, Roots I, Sasse J, Brockmoller J. Genetic variants in FKBP5 affecting response to antidepressant drug treatment. *Pharmacogenomics* 9(7), 841-6, 2008.
- Klein DF. Prodromal symptoms in agoraphobia and panic disorder. *Am J Psychiatry* 146(6), 812-4, 1989.
- Klein DF, Klein HM. The utility of the panic disorder concept. *Eur Arch Psychiatry Neurol Sci* 238(5-6), 268-79, 1989.
- Klein R. Bidirectional modulation of synaptic functions by Eph/ephrin signaling. *Nat Neurosci* 12(1), 15-20, 2009.
- Kluver H, Busy PC. 'Psychic Blindness' and other symptoms following bilateral temporal lobectomy in rhesus monkeys. *American Journal of Physiology* 119, 352-3, 1937.
- Koenen KC, Saxe G, Purcell S, Smoller JW, Bartholomew D, Miller A, Hall E, Kaplow J, Bosquet M, Moulton S, Baldwin C. Polymorphisms in FKBP5 are associated with peritraumatic dissociation in medically injured children. *Mol Psychiatry* 10(12), 1058-9, 2005.
- Konecna A, Heraud JE, Schoderboeck L, Raposo AA, Kiebler MA. What are the roles of microRNAs at the mammalian synapse? *Neurosci Lett* 466(2), 63-8, 2009.

- Kosik KS. The neuronal microRNA system. *Nat Rev Neurosci* 7(12), 911-20, 2006.
- Kubista M, Andrade JM, Bengtsson M, Forootan A, Jonak J, Lind K, Sindelka R, Sjoback R, Sjogreen B, Strombom L, Stahlberg A, Zoric N. The real-time polymerase chain reaction. *Mol Aspects Med* 27(2-3), 95-125, 2006.
- Kumar A, Garg R, Prakash AK. Effect of St. John's Wort (*Hypericum perforatum*) treatment on restraint stress-induced behavioral and biochemical alteration in mice. *BMC Complementary and Alternative Medicine* 10(18), 1-6, 2010.
- Lamprecht R, LeDoux J. Structural plasticity and memory. *Nat Rev Neurosci* 5(1), 45-54, 2004.
- Lavebratt C, Aberg E, Sjöholm LK, Forsell Y. Variations in FKBP5 and BDNF genes are suggestively associated with depression in a Swedish population-based cohort. *J Affect Disord* 125(1-3), 249-55, 2010.
- LeDoux J. The amygdala. *Curr Biol* 17(20), R868-74, 2007.
- LeDoux JE. Emotion, memory and the brain. *Sci Am* 270(6), 50-7, 1994.
- LeDoux JE. Emotion circuits in the brain. *Annu Rev Neurosci* 23, 155-84, 2000.
- LeDoux JE, Iwata J, Cicchetti P, Reis DJ. Different projections of the central amygdaloid nucleus mediate autonomic and behavioral correlates of conditioned fear. *J Neurosci* 8(7), 2517-29, 1988.
- Lee RS, Tamashiro KL, Yang X, Purcell RH, Harvey A, Willour VL, Huo Y, Rongione M, Wand GS, Potash JB. Chronic corticosterone exposure increases expression and decreases deoxyribonucleic acid methylation of *Fkbp5* in mice. *Endocrinology* 151(9), 4332-43, 2010.
- Lee RS, Tamashiro KL, Yang X, Purcell RH, Huo Y, Rongione M, Potash JB, Wand GS. A measure of glucocorticoid load provided by DNA methylation of *Fkbp5* in mice. *Psychopharmacology (Berl)* 218(1), 303-12, 2011.
- Lee Y, Davis M. Role of the hippocampus, the bed nucleus of the stria terminalis, and the amygdala in the excitatory effect of corticotropin-releasing hormone on the acoustic startle reflex. *J Neurosci* 17(16), 6434-46, 1997.

- Lee Y, Davis M. Role of the septum in the excitatory effect of corticotropin-releasing hormone on the acoustic startle reflex. *J Neurosci* 17(16), 6424-33, 1997.
- Lee Y, Walker D, Davis M. Lack of a temporal gradient of retrograde amnesia following NMDA-induced lesions of the basolateral amygdala assessed with the fear-potentiated startle paradigm. *Behav Neurosci* 110(4), 836-9, 1996.
- Lekman M, Laje G, Charney D, Rush AJ, Wilson AF, Sorant AJ, Lipsky R, Wisniewski SR, Manji H, McMahon FJ, Paddock S. The FKBP5-gene in depression and treatment response--an association study in the Sequenced Treatment Alternatives to Relieve Depression (STAR*D) Cohort. *Biol Psychiatry* 63(12), 1103-10, 2008.
- Lewejohann L, Reinhard C, Schrewe A, Brandewiede J, Haemisch A, Gortz N, Schachner M, Sachser N. Environmental bias? Effects of housing conditions, laboratory environment and experimenter on behavioral tests. *Genes Brain Behav* 5(1), 64-72, 2006.
- Limited AS. Antibody Review to Mouse Anti FKBP51 ab46002. AbCam Incorporated, 2008.
- Lin KT, Sloniewski S, Ethell DW, Ethell IM. Ephrin-B2-induced cleavage of EphB2 receptor is mediated by matrix metalloproteinases to trigger cell repulsion. *J Biol Chem* 283(43), 28969-79, 2008.
- Lindquist DH, Jarrard LE, Brown TH. Perirhinal cortex supports delay fear conditioning to rat ultrasonic social signals. *J Neurosci* 24(14), 3610-7, 2004.
- Lister RG. The use of a plus-maze to measure anxiety in the mouse. *Psychopharmacology (Berl)* 92(2), 180-5, 1987.
- Logue SF, Paylor R, Wehner JM. Hippocampal lesions cause learning deficits in inbred mice in the Morris water maze and conditioned-fear task. *Behav Neurosci* 111(1), 104-13, 1997.
- Lopez JF, Akil H, Watson SJ. Neural circuits mediating stress. *Biol Psychiatry* 46(11), 1461-71, 1999.
- Luijk MP, Velders FP, Tharner A, van Ijzendoorn MH, Bakermans-Kranenburg MJ, Jaddoe VW, Hofman A, Verhulst FC, Tiemeier H. FKBP5 and resistant attachment predict cortisol reactivity in infants: gene-environment interaction. *Psychoneuroendocrinology* 35(10), 1454-61, 2010.

- Maeng S, Hunsberger JG, Pearson B, Yuan P, Wang Y, Wei Y, McCammon J, Schloesser RJ, Zhou R, Du J, Chen G, McEwen B, Reed JC, Manji HK. BAG1 plays a critical role in regulating recovery from both manic-like and depression-like behavioral impairments. *Proc Natl Acad Sci U S A* 105(25), 8766-71, 2008.
- Magee JA, Chang LW, Stormo GD, Milbrandt J. Direct, androgen receptor-mediated regulation of the FKBP5 gene via a distal enhancer element. *Endocrinology* 147(1), 590-8, 2006.
- Makkonen H, Kauhanen M, Paakinaho V, Jaaskelainen T, Palvimo JJ. Long-range activation of FKBP51 transcription by the androgen receptor via distal intronic enhancers. *Nucleic Acids Res* 37(12), 4135-48, 2009.
- Maren S. Neurotoxic or electrolytic lesions of the ventral subiculum produce deficits in the acquisition and expression of Pavlovian fear conditioning in rats. *Behav Neurosci* 113(2), 283-90, 1999.
- Maren S. Long-term potentiation in the amygdala: a mechanism for emotional learning and memory. *Trends Neurosci* 22(12), 561-7, 1999.
- Maren S. Neurobiology of Pavlovian fear conditioning. *Annu Rev Neurosci* 24, 897-931, 2001.
- Maren S, Aharonov G, Fanselow MS. Retrograde abolition of conditional fear after excitotoxic lesions in the basolateral amygdala of rats: absence of a temporal gradient. *Behav Neurosci* 110(4), 718-26, 1996.
- Maren S, Aharonov G, Fanselow MS. Neurotoxic lesions of the dorsal hippocampus and Pavlovian fear conditioning in rats. *Behav Brain Res* 88(2), 261-74, 1997.
- Maren S, Aharonov G, Stote DL, Fanselow MS. N-methyl-D-aspartate receptors in the basolateral amygdala are required for both acquisition and expression of conditional fear in rats. *Behav Neurosci* 110(6), 1365-74, 1996.
- Maren S, Quirk GJ. Neuronal signalling of fear memory. *Nat Rev Neurosci* 5(11), 844-52, 2004.
- Martinowich K, Hattori D, Wu H, Fouse S, He F, Hu Y, Fan G, Sun YE. DNA methylation-related chromatin remodeling in activity-dependent BDNF gene regulation. *Science* 302(5646), 890-3, 2003.

- Matsumoto-Miyai K, Ninomiya A, Yamasaki H, Tamura H, Nakamura Y, Shiosaka S. NMDA-dependent proteolysis of presynaptic adhesion molecule L1 in the hippocampus by neuropsin. *J Neurosci* 23(21), 7727-36, 2003.
- McEwen BS. The neurobiology of stress: from serendipity to clinical relevance. *Brain Res* 886(1-2), 172-89, 2000.
- McEwen BS. Protective and damaging effects of stress mediators: central role of the brain. *Prog Brain Res* 122, 25-34, 2000.
- McEwen BS. Allostasis and allostatic load: implications for neuropsychopharmacology. *Neuropsychopharmacology* 22(2), 108-24, 2000.
- McEwen BS. The neurobiology and neuroendocrinology of stress. Implications for post-traumatic stress disorder from a basic science perspective. *Psychiatr Clin North Am* 25(2), 469-94, ix, 2002.
- McEwen BS. Protection and damage from acute and chronic stress: allostasis and allostatic overload and relevance to the pathophysiology of psychiatric disorders. *Ann N Y Acad Sci* 1032, 1-7, 2004.
- Meerson A, Cacheaux L, Goosens KA, Sapolsky RM, Soreq H, Kaufer D. Changes in brain MicroRNAs contribute to cholinergic stress reactions. *J Mol Neurosci* 40(1-2), 47-55, 2010.
- Mehta D, Gonik M, Klengel T, Rex-Haffner M, Menke A, Rubel J, Mercer KB, Putz B, Bradley B, Holsboer F, Ressler KJ, Muller-Myhsok B, Binder EB. Using polymorphisms in FKBP5 to define biologically distinct subtypes of posttraumatic stress disorder: evidence from endocrine and gene expression studies. *Arch Gen Psychiatry* 68(9), 901-10, 2011.
- Mitra R, Jadhav S, McEwen BS, Vyas A, Chattarji S. Stress duration modulates the spatiotemporal patterns of spine formation in the basolateral amygdala. *Proc Natl Acad Sci U S A* 102(26), 9371-6, 2005.
- Mitra R, Sapolsky RM. Acute corticosterone treatment is sufficient to induce anxiety and amygdaloid dendritic hypertrophy. *Proc Natl Acad Sci U S A* 105(14), 5573-8, 2008.
- Miyata Y, Chambraud B, Radanyi C, Leclerc J, Lebeau MC, Renoir JM, Shirai R, Catelli MG, Yahara I, Baulieu EE. Phosphorylation of the immunosuppressant FK506-binding protein FKBP52 by casein kinase II: regulation of HSP90-binding activity of FKBP52. *Proc Natl Acad Sci U S A* 94(26), 14500-5, 1997.

- Montgomery KC. The relation between fear induced by novel stimulation and exploratory behavior. *J Comp Physiol Psychol* 48(4), 254-60, 1955.
- Montgomery KC, Monkman JA. The relation between fear and exploratory behavior. *J Comp Physiol Psychol* 48(2), 132-6, 1955.
- Montgomery KC, Segall M. Discrimination learning based upon the exploratory drive. *J Comp Physiol Psychol* 48(3), 225-8, 1955.
- Muhonen P, Holthofer H. Epigenetic and microRNA-mediated regulation in diabetes. *Nephrol Dial Transplant* 24(4), 1088-96, 2009.
- Nader K, Majidishad P, Amorapanth P, LeDoux JE. Damage to the lateral and central, but not other, amygdaloid nuclei prevents the acquisition of auditory fear conditioning. *Learn Mem* 8(3), 156-63, 2001.
- Nair SC, Rimerman RA, Toran EJ, Chen S, Prapapanich V, Butts RN, Smith DF. Molecular cloning of human FKBP51 and comparisons of immunophilin interactions with Hsp90 and progesterone receptor. *Mol Cell Biol* 17(2), 594-603, 1997.
- Nigg EA. Nucleocytoplasmic transport: signals, mechanisms and regulation. *Nature* 386(6627), 779-87, 1997.
- Nuber UA, Kriaucionis S, Roloff TC, Guy J, Selfridge J, Steinhoff C, Schulz R, Lipkowitz B, Ropers HH, Holmes MC, Bird A. Up-regulation of glucocorticoid-regulated genes in a mouse model of Rett syndrome. *Hum Mol Genet* 14(15), 2247-56, 2005.
- Ohl F. Animal models of anxiety. *Handb Exp Pharmacol* (169), 35-69, 2005.
- O'Leary JC, 3rd, Dharia S, Blair LJ, Brady S, Johnson AG, Peters M, Cheung-Flynn J, Cox MB, de Erausquin G, Weeber EJ, Jinwal UK, Dickey CA. A new anti-depressive strategy for the elderly: ablation of FKBP5/FKBP51. *PLoS One* 6(9), e24840, 2011.
- World Health Organization. The ICD-10 Classification of Mental and Behavioural Disorders: Clinical Descriptions and Diagnostic Guidelines. In: Organization. WH, (Ed), Vol., Geneva, 1992.
- Paakinaho V, Makkonen H, Jaaskelainen T, Palvimo JJ. Glucocorticoid receptor activates poised FKBP51 locus through long-distance interactions. *Mol Endocrinol* 24(3), 511-25, 2010.

- Papiol S, Arias B, Gasto C, Gutierrez B, Catalan R, Fananas L. Genetic variability at HPA axis in major depression and clinical response to antidepressant treatment. *J Affect Disord* 104(1-3), 83-90, 2007.
- Parseghian MH, Newcomb RL, Winokur ST, Hamkalo BA. The distribution of somatic H1 subtypes is non-random on active vs. inactive chromatin: distribution in human fetal fibroblasts. *Chromosome Res* 8(5), 405-24, 2000.
- Pawlak R, Magarinos AM, Melchor J, McEwen B, Strickland S. Tissue plasminogen activator in the amygdala is critical for stress-induced anxiety-like behavior. *Nat Neurosci* 6(2), 168-74, 2003.
- Pei H, Li L, Fridley BL, Jenkins GD, Kalari KR, Lingle W, Petersen G, Lou Z, Wang L. FKBP51 affects cancer cell response to chemotherapy by negatively regulating Akt. *Cancer Cell* 16(3), 259-66, 2009.
- Pellow S, Chopin P, File SE, Briley M. Validation of open:closed arm entries in an elevated plus-maze as a measure of anxiety in the rat. *J Neurosci Methods* 14(3), 149-67, 1985.
- Penzes P, Beaser A, Chernoff J, Schiller MR, Eipper BA, Mains RE, Huganir RL. Rapid induction of dendritic spine morphogenesis by trans-synaptic ephrinB-EphB receptor activation of the Rho-GEF kalirin. *Neuron* 37(2), 263-74, 2003.
- Perroud N. Suicidal ideation during antidepressant treatment: do genetic predictors exist? *CNS Drugs* 25(6), 459-71, 2011.
- Perroud N, Bondolfi G, Uher R, Gex-Fabry M, Aubry JM, Bertschy G, Malafosse A, Kosel M. Clinical and genetic correlates of suicidal ideation during antidepressant treatment in a depressed outpatient sample. *Pharmacogenomics* 12(3), 365-77, 2011.
- Phillips RG, LeDoux JE. Differential contribution of amygdala and hippocampus to cued and contextual fear conditioning. *Behav Neurosci* 106(2), 274-85, 1992.
- Pillai RS, Bhattacharyya SN, Filipowicz W. Repression of protein synthesis by miRNAs: how many mechanisms? *Trends Cell Biol* 17(3), 118-26, 2007.
- Pradervand S, Weber J, Thomas J, Bueno M, Wirapati P, Lefort K, Dotto GP, Harshman K. Impact of normalization on miRNA microarray expression profiling. *RNA* 15(3), 493-501, 2009.

- Pratt WB, Toft DO. Steroid receptor interactions with heat shock protein and immunophilin chaperones. *Endocr Rev* 18(3), 306-60, 1997.
- Prut L, Belzung C. The open field as a paradigm to measure the effects of drugs on anxiety-like behaviors: a review. *Eur J Pharmacol* 463(1-3), 3-33, 2003.
- Quackenbush J. Computational analysis of microarray data. *Nat Rev Genet* 2(6), 418-27, 2001.
- Quinta HR, Maschi D, Gomez-Sanchez C, Piwien-Pilipuk G, Galigniana MD. Subcellular rearrangement of hsp90-binding immunophilins accompanies neuronal differentiation and neurite outgrowth. *J Neurochem* 115(3), 716-34, 2010.
- Rees-Unwin KS, Craven RA, Davenport E, Hanrahan S, Totty NF, Dring AM, Banks RE, G JM, Davies FE. Proteomic evaluation of pathways associated with dexamethasone-mediated apoptosis and resistance in multiple myeloma. *Br J Haematol* 139(4), 559-67, 2007.
- Reynolds PD, Roveda KP, Tucker JA, Moore CM, Valentine DL, Scammell JG. Glucocorticoid-resistant B-lymphoblast cell line derived from the Bolivian squirrel monkey (*Saimiri boliviensis boliviensis*). *Lab Anim Sci* 48(4), 364-70, 1998.
- Reynolds PD, Ruan Y, Smith DF, Scammell JG. Glucocorticoid resistance in the squirrel monkey is associated with overexpression of the immunophilin FKBP51. *J Clin Endocrinol Metab* 84(2), 663-9, 1999.
- Riggs DL, Cox MB, Tardif HL, Hessling M, Buchner J, Smith DF. Noncatalytic role of the FKBP52 peptidyl-prolyl isomerase domain in the regulation of steroid hormone signaling. *Mol Cell Biol* 27(24), 8658-69, 2007.
- Riggs DL, Roberts PJ, Chirillo SC, Cheung-Flynn J, Prapapanich V, Ratajczak T, Gaber R, Picard D, Smith DF. The Hsp90-binding peptidylprolyl isomerase FKBP52 potentiates glucocorticoid signaling in vivo. *EMBO J* 22(5), 1158-67, 2003.
- Rinaldi A, Vincenti S, De Vito F, Bozzoni I, Oliverio A, Presutti C, Fragapane P, Mele A. Stress induces region specific alterations in microRNAs expression in mice. *Behav Brain Res* 208(1), 265-9, 2010.
- Roozendaal B, McEwen BS, Chattarji S. Stress, memory and the amygdala. *Nat Rev Neurosci* 10(6), 423-33, 2009.

- Rosen JB. The neurobiology of conditioned and unconditioned fear: a neurobehavioral system analysis of the amygdala. *Behav Cogn Neurosci Rev* 3(1), 23-41, 2004.
- Rosen JB, Schulkin J. From normal fear to pathological anxiety. *Psychol Rev* 105(2), 325-50, 1998.
- Roy A, Gorodetsky E, Yuan Q, Goldman D, Enoch MA. Interaction of FKBP5, a stress-related gene, with childhood trauma increases the risk for attempting suicide. *Neuropsychopharmacology* 35(8), 1674-83, 2010.
- Roy A, Hodgkinson CA, Deluca V, Goldman D, Enoch MA. Two HPA axis genes, CRHBP and FKBP5, interact with childhood trauma to increase the risk for suicidal behavior. *J Psychiatr Res* 46(1), 72-9, 2012.
- Ruike Y, Ichimura A, Tsuchiya S, Shimizu K, Kunimoto R, Okuno Y, Tsujimoto G. Global correlation analysis for micro-RNA and mRNA expression profiles in human cell lines. *J Hum Genet* 53(6), 515-23, 2008.
- Sandstrom NJ, Hart SR. Isolation stress during the third postnatal week alters radial arm maze performance and corticosterone levels in adulthood. *Behav Brain Res* 156(2), 289-96, 2005.
- Sapolsky RM. Stress and plasticity in the limbic system. *Neurochem Res* 28(11), 1735-42, 2003.
- Sarapas C, Cai G, Bierer LM, Golier JA, Galea S, Ising M, Rein T, Schmeidler J, Muller-Myhsok B, Uhr M, Holsboer F, Buxbaum JD, Yehuda R. Genetic markers for PTSD risk and resilience among survivors of the World Trade Center attacks. *Dis Markers* 30(2-3), 101-10, 2011.
- Sarginson JE, Lazzeroni LC, Ryan HS, Schatzberg AF, Murphy GM, Jr. FKBP5 polymorphisms and antidepressant response in geriatric depression. *Am J Med Genet B Neuropsychiatr Genet* 153B(2), 554-60, 2010.
- Scharf SH, Liebl C, Binder EB, Schmidt MV, Muller MB. Expression and regulation of the Fkbp5 gene in the adult mouse brain. *PLoS One* 6(2), e16883, 2011.
- Scheufler C, Brinker A, Bourenkov G, Pegoraro S, Moroder L, Bartunik H, Hartl FU, Moarefi I. Structure of TPR domain-peptide complexes: critical elements in the assembly of the Hsp70-Hsp90 multichaperone machine. *Cell* 101(2), 199-210, 2000.

- Schmidt MV, Sterlemann V, Ganea K, Liebl C, Alam S, Harbich D, Greetfeld M, Uhr M, Holsboer F, Muller MB. Persistent neuroendocrine and behavioral effects of a novel, etiologically relevant mouse paradigm for chronic social stress during adolescence. *Psychoneuroendocrinology* 32(5), 417-29, 2007.
- Schmidt U, Wochnik GM, Rosenhagen MC, Young JC, Hartl FU, Holsboer F, Rein T. Essential role of the unusual DNA-binding motif of BAG-1 for inhibition of the glucocorticoid receptor. *J Biol Chem* 278(7), 4926-31, 2003.
- Schratt GM, Tuebing F, Nigh EA, Kane CG, Sabatini ME, Kiebler M, Greenberg ME. A brain-specific microRNA regulates dendritic spine development. *Nature* 439(7074), 283-9, 2006.
- Segman RH, Shefi N, Goltser-Dubner T, Friedman N, Kaminski N, Shalev AY. Peripheral blood mononuclear cell gene expression profiles identify emergent post-traumatic stress disorder among trauma survivors. *Mol Psychiatry* 10(5), 500-13, 425, 2005.
- Selye H. Stress and disease. *Science* 122(3171), 625-31, 1955.
- Shemer J, Raizada MK, Masters BA, Ota A, LeRoith D. Insulin-like growth factor-I receptors in neuronal and glial cells. *J Biol Chem* 262, 7693-7699, 1987.
- Shimizu C, Yoshida S, Shibata M, Kato K, Momota Y, Matsumoto K, Shiosaka T, Midorikawa R, Kamachi T, Kawabe A, Shiosaka S. Characterization of recombinant and brain neuropsin, a plasticity-related serine protease. *J Biol Chem* 273(18), 11189-96, 1998.
- Shin LM, Liberzon I. The neurocircuitry of fear, stress, and anxiety disorders. *Neuropsychopharmacology* 35(1), 169-91, 2010.
- Shinozaki G, Jowsey S, Amer H, J MB, Colby C, Walker D, Black J, Rundell J, Stegall M, Mrazek DA. Relationship between FKBP5 polymorphisms and depression symptoms among kidney transplant recipients. *Depress Anxiety* 28(12), 1111-8, 2011.
- Sinars CR, Cheung-Flynn J, Rimerman RA, Scammell JG, Smith DF, Clardy J. Structure of the large FK506-binding protein FKBP51, an Hsp90-binding protein and a component of steroid receptor complexes. *Proc Natl Acad Sci U S A* 100(3), 868-73, 2003.
- Smith DF, Faber LE, Toft DO. Purification of unactivated progesterone receptor and identification of novel receptor-associated proteins. *J Biol Chem* 265(7), 3996-4003, 1990.

- Speicher KD, Kolbas O, Harper S, Speicher DW. Systematic analysis of peptide recoveries from in-gel digestions for protein identifications in proteome studies. *J Biomol Tech* 11(2), 74-86, 2000.
- Staibano S, Mascolo M, Ilardi G, Siano M, De Rosa G. Immunohistochemical analysis of FKBP51 in human cancers. *Curr Opin Pharmacol* 11(4), 338-47, 2011.
- Stechschulte LA, Sanchez ER. FKBP51- a selective modulator of glucocorticoid and androgen sensitivity. *Curr Opin Pharmacol* 11, 1-6, 2011.
- Steward O, Schuman EM. Protein synthesis at synaptic sites on dendrites. *Annu Rev Neurosci* 24, 299-325, 2001.
- Supriyanto I, Sasada T, Fukutake M, Asano M, Ueno Y, Nagasaki Y, Shirakawa O, Hishimoto A. Association of FKBP5 gene haplotypes with completed suicide in the Japanese population. *Prog Neuropsychopharmacol Biol Psychiatry* 35(1), 252-6, 2011.
- Swanson LW, Petrovich GD. What is the amygdala? *Trends Neurosci* 21(8), 323-31, 1998.
- Sweatt JD, Weeber EJ. Genetics of childhood disorders: LII. Learning and memory, part 5: human cognitive disorders and the ras/ERK/CREB pathway. *J Am Acad Child Adolesc Psychiatry* 42(7), 873-6, 2003.
- Takasu MA, Dalva MB, Zigmond RE, Greenberg ME. Modulation of NMDA receptor-dependent calcium influx and gene expression through EphB receptors. *Science* 295(5554), 491-5, 2002.
- Tatro ET, Everall IP, Kaul M, Achim CL. Modulation of glucocorticoid receptor nuclear translocation in neurons by immunophilins FKBP51 and FKBP52: implications for major depressive disorder. *Brain Res* 1286, 1-12, 2009.
- Tatro ET, Everall IP, Masliah E, Hult BJ, Lucero G, Chana G, Soontornniyomkij V, Achim CL. Differential expression of immunophilins FKBP51 and FKBP52 in the frontal cortex of HIV-infected patients with major depressive disorder. *J Neuroimmune Pharmacol* 4(2), 218-26, 2009.
- Tatro ET, Nguyen TB, Bousman CA, Masliah E, Grant I, Atkinson JH, Everall IP. Correlation of major depressive disorder symptoms with FKBP5 but not FKBP4 expression in human immunodeficiency virus-infected individuals. *J Neurovirol* 16(5), 399-404, 2010.

- Tatro ET, Scott ER, Nguyen TB, Salaria S, Banerjee S, Moore DJ, Masliah E, Achim CL, Everall IP. Evidence for Alteration of Gene Regulatory Networks through MicroRNAs of the HIV-infected brain: novel analysis of retrospective cases. *PLoS One* 5(4), e10337, 2010.
- ten Have S, Boulon S, Ahmad Y, Lamond AI. Mass spectrometry-based immuno-precipitation proteomics - the user's guide. *Proteomics* 11(6), 1153-9, 2011.
- Tolias KF, Bikoff JB, Burette A, Paradis S, Harrar D, Tavazoie S, Weinberg RJ, Greenberg ME. The Rac1-GEF Tiam1 couples the NMDA receptor to the activity-dependent development of dendritic arbors and spines. *Neuron* 45(4), 525-38, 2005.
- Tolias KF, Bikoff JB, Kane CG, Tolias CS, Hu L, Greenberg ME. The Rac1 guanine nucleotide exchange factor Tiam1 mediates EphB receptor-dependent dendritic spine development. *Proc Natl Acad Sci U S A* 104(17), 7265-70, 2007.
- Touma C, Gassen NC, Herrmann L, Cheung-Flynn J, Bull DR, Ionescu IA, Heinzmann JM, Knapman A, Siebertz A, Depping AM, Hartmann J, Hausch F, Schmidt MV, Holsboer F, Ising M, Cox MB, Schmidt U, Rein T. FK506 binding protein 5 shapes stress responsiveness: modulation of neuroendocrine reactivity and coping behavior. *Biol Psychiatry* 70(10), 928-36, 2011.
- Trinkle-Mulcahy L, Boulon S, Lam YW, Urcia R, Boisvert FM, Vandermoere F, Morrice NA, Swift S, Rothbauer U, Leonhardt H, Lamond A. Identifying specific protein interaction partners using quantitative mass spectrometry and bead proteomes. *J Cell Biol* 183(2), 223-39, 2008.
- Tsai SJ, Hong CJ, Chen TJ, Yu YW. Lack of supporting evidence for a genetic association of the FKBP5 polymorphism and response to antidepressant treatment. *Am J Med Genet B Neuropsychiatr Genet* 144B(8), 1097-8, 2007.
- U M, Shen L, Oshida T, Miyauchi J, Yamada M, Miyashita T. Identification of novel direct transcriptional targets of glucocorticoid receptor. *Leukemia* 18(11), 1850-6, 2004.
- Uchida S, Nishida A, Hara K, Kamemoto T, Suetsugi M, Fujimoto M, Watanuki T, Wakabayashi Y, Otsuki K, McEwen BS, Watanabe Y. Characterization of the vulnerability to repeated stress in Fischer 344 rats: possible involvement of microRNA-mediated down-regulation of the glucocorticoid receptor. *Eur J Neurosci* 27(9), 2250-61, 2008.

- Urduingio RG, Lopez-Serra L, Lopez-Nieva P, Alaminos M, Diaz-Uriarte R, Fernandez AF, Esteller M. Mecp2-null mice provide new neuronal targets for Rett syndrome. *PLoS One* 3(11), e3669, 2008.
- van Zuiden M, Geuze E, Willems HL, Vermetten E, Maas M, Amarouchi K, Kavelaars A, Heijnen CJ. Glucocorticoid receptor pathway components predict posttraumatic stress disorder symptom development: a prospective study. *Biol Psychiatry* 71(4), 309-16, 2012.
- Vasudevan S, Steitz JA. AU-rich-element-mediated upregulation of translation by FXR1 and Argonaute 2. *Cell* 128(6), 1105-18, 2007.
- Vasudevan S, Tong Y, Steitz JA. Switching from repression to activation: microRNAs can up-regulate translation. *Science* 318(5858), 1931-4, 2007.
- Velders FP, Kuningas M, Kumari M, Dekker MJ, Uitterlinden AG, Kirschbaum C, Hek K, Hofman A, Verhulst FC, Kivimaki M, Van Duijn CM, Walker BR, Tiemeier H. Genetics of cortisol secretion and depressive symptoms: a candidate gene and genome wide association approach. *Psychoneuroendocrinology* 36(7), 1053-61, 2011.
- Vermeer H, Hendriks-Stegeman BI, van der Burg B, van Buul-Offers SC, Jansen M. Glucocorticoid-induced increase in lymphocytic FKBP51 messenger ribonucleic acid expression: a potential marker for glucocorticoid sensitivity, potency, and bioavailability. *J Clin Endocrinol Metab* 88(1), 277-84, 2003.
- Virag L, Szabo C. The therapeutic potential of poly(ADP-ribose) polymerase inhibitors. *Pharmacol Rev* 54(3), 375-429, 2002.
- Vorwerk S, Ganter K, Cheng Y, Hoheisel J, Stahler PF, Beier M. Microfluidic-based enzymatic on-chip labeling of miRNAs. *N Biotechnol* 25(2-3), 142-9, 2008.
- Vyas A, Bernal S, Chattarji S. Effects of chronic stress on dendritic arborization in the central and extended amygdala. *Brain Res* 965(1-2), 290-4, 2003.
- Vyas A, Chattarji S. Modulation of different states of anxiety-like behavior by chronic stress. *Behav Neurosci* 118(6), 1450-4, 2004.
- Vyas A, Jadhav S, Chattarji S. Prolonged behavioral stress enhances synaptic connectivity in the basolateral amygdala. *Neuroscience* 143(2), 387-93, 2006.
- Vyas A, Mitra R, Shankaranarayana Rao BS, Chattarji S. Chronic stress induces contrasting patterns of dendritic remodeling in hippocampal and amygdaloid neurons. *J Neurosci* 22(15), 6810-8, 2002.

- Vyas A, Pillai AG, Chattarji S. Recovery after chronic stress fails to reverse amygdaloid neuronal hypertrophy and enhanced anxiety-like behavior. *Neuroscience* 128(4), 667-73, 2004.
- Walf AA, Frye CA. The use of the elevated plus maze as an assay of anxiety-related behavior in rodents. *Nat Protoc* 2(2), 322-8, 2007.
- Walker DL, Davis M. Anxiogenic effects of high illumination levels assessed with the acoustic startle response in rats. *Biol Psychiatry* 42(6), 461-71, 1997.
- Walker DL, Davis M. Double dissociation between the involvement of the bed nucleus of the stria terminalis and the central nucleus of the amygdala in startle increases produced by conditioned versus unconditioned fear. *J Neurosci* 17(23), 9375-83, 1997.
- Walker DL, Toufexis DJ, Davis M. Role of the bed nucleus of the stria terminalis versus the amygdala in fear, stress, and anxiety. *Eur J Pharmacol* 463(1-3), 199-216, 2003.
- Wan Y, Coxe KK, Thackray VG, Housley PR, Nordeen SK. Separable features of the ligand-binding domain determine the differential subcellular localization and ligand-binding specificity of glucocorticoid receptor and progesterone receptor. *Mol Endocrinol* 15(1), 17-31, 2001.
- Wang L. FKBP51 regulation of AKT/protein kinase B phosphorylation. *Curr Opin Pharmacol* 11(4), 360-4, 2011.
- Weinberg MS, Bhatt AP, Girotti M, Masini CV, Day HE, Campeau S, Spencer RL. Repeated ferret odor exposure induces different temporal patterns of same-stressor habituation and novel-stressor sensitization in both hypothalamic-pituitary-adrenal axis activity and forebrain c-fos expression in the rat. *Endocrinology* 150(2), 749-61, 2009.
- Weiskrantz L. Behavioral changes associated with ablation of the amygdaloid complex in monkeys. *J Comp Physiol Psychol* 49(4), 381-91, 1956.
- Westberry JM, Sadosky PW, Hubler TR, Gross KL, Scammell JG. Glucocorticoid resistance in squirrel monkeys results from a combination of a transcriptionally incompetent glucocorticoid receptor and overexpression of the glucocorticoid receptor co-chaperone FKBP51. *J Steroid Biochem Mol Biol* 100(1-3), 34-41, 2006.
- Widom J. Chromatin structure: linking structure to function with histone H1. *Curr Biol* 8(22), R788-91, 1998.

- Wiederrecht G, Hung S, Chan HK, Marcy A, Martin M, Calaycay J, Boulton D, Sigal N, Kincaid RL, Siekierka JJ. Characterization of high molecular weight FK-506 binding activities reveals a novel FK-506-binding protein as well as a protein complex. *J Biol Chem* 267(30), 21753-60, 1992.
- Willour VL, Chen H, Toolan J, Belmonte P, Cutler DJ, Goes FS, Zandi PP, Lee RS, MacKinnon DF, Mondimore FM, Schweizer B, DePaulo JR, Jr., Gershon ES, McMahon FJ, Potash JB. Family-based association of FKBP5 in bipolar disorder. *Mol Psychiatry* 14(3), 261-8, 2009.
- Wochnik GM, Ruegg J, Abel GA, Schmidt U, Holsboer F, Rein T. FK506-binding proteins 51 and 52 differentially regulate dynein interaction and nuclear translocation of the glucocorticoid receptor in mammalian cells. *J Biol Chem* 280(6), 4609-16, 2005.
- Woodruff PG, Boushey HA, Dolganov GM, Barker CS, Yang YH, Donnelly S, Ellwanger A, Sidhu SS, Dao-Pick TP, Pantoja C, Erle DJ, Yamamoto KR, Fahy JV. Genome-wide profiling identifies epithelial cell genes associated with asthma and with treatment response to corticosteroids. *Proc Natl Acad Sci U S A* 104(40), 15858-63, 2007.
- Xie P, Kranzler HR, Poling J, Stein MB, Anton RF, Farrer LA, Gelernter J. Interaction of FKBP5 with childhood adversity on risk for post-traumatic stress disorder. *Neuropsychopharmacology* 35(8), 1684-92, 2010.
- Yang X, Ewald ER, Huo Y, Tamashiro KL, Salvatori R, Sawa A, Wand GS, Lee RS. Glucocorticoid-induced loss of DNA methylation in non-neuronal cells and potential involvement of DNMT1 in epigenetic regulation of Fkbp5. *Biochem Biophys Res Commun*, 2012.
- Yehuda R. Post-traumatic stress disorder. *N Engl J Med* 346(2), 108-14, 2002.
- Yehuda R, Cai G, Golier JA, Sarapas C, Galea S, Ising M, Rein T, Schmeidler J, Muller-Myhsok B, Holsboer F, Buxbaum JD. Gene expression patterns associated with posttraumatic stress disorder following exposure to the World Trade Center attacks. *Biol Psychiatry* 66(7), 708-11, 2009.
- Yehuda R, Giller EL, Southwick SM, Lowy MT, Mason JW. Hypothalamic-pituitary-adrenal dysfunction in posttraumatic stress disorder. *Biol Psychiatry* 30(10), 1031-48, 1991.
- Yehuda R, Golier JA, Yang RK, Tischler L. Enhanced sensitivity to glucocorticoids in peripheral mononuclear leukocytes in posttraumatic stress disorder. *Biol Psychiatry* 55(11), 1110-6, 2004.

- Zhang X, Clark AF, Yorio T. FK506-binding protein 51 regulates nuclear transport of the glucocorticoid receptor beta and glucocorticoid responsiveness. *Invest Ophthalmol Vis Sci* 49(3), 1037-47, 2008.
- Zobel A, Schuhmacher A, Jessen F, Hofels S, von Widdern O, Metten M, Pfeiffer U, Hanses C, Becker T, Rietschel M, Scheef L, Block W, Schild HH, Maier W, Schwab SG. DNA sequence variants of the FKBP5 gene are associated with unipolar depression. *Int J Neuropsychopharmacol* 13(5), 649-60, 2010.
- Zou YF, Wang F, Feng XL, Li WF, Tao JH, Pan FM, Huang F, Su H. Meta-analysis of FKBP5 gene polymorphisms association with treatment response in patients with mood disorders. *Neurosci Lett* 484(1), 56-61, 2010.